Ecoulements granulaires

exemples de modélisations continues

Lagrée Pierre-Yves

CNRS Sorbonne-Université

Institut Jean Le Rond ∂'Alembert, Paris

Anaïs Abramian, Stéphanie Deboeuf, Stéphane Popinet, Lydie Staron (∂'Alembert)
Pascale Aussillous (IUSTI), Pierre Ruyer (IRSN)
Guillaume Saingier (∂'Alembert-SVI),
Yixian Zhou, Zhenhai Zou (IUSTI & IRSN)

SORBONNE UNIVERSITÉ
CRÉATEURS DE FUTURS DEPUIS 1257

cnrs

∂'Alembert
Institut Jean le Rond d'Alembert

motivation, facts

Jean Le Rond d'Alembert
1717 1783

- sand, granulates: $6\ 10^3$ kg/french/year
- 2nd most used "fluid" after water >> petroleum
  (water 1.0, granulates 0.1, petroleum 0.025)
- corn: 450 kg/french/year
- Food, Medicines
- Environmental flows (avalanches, mud flow….)

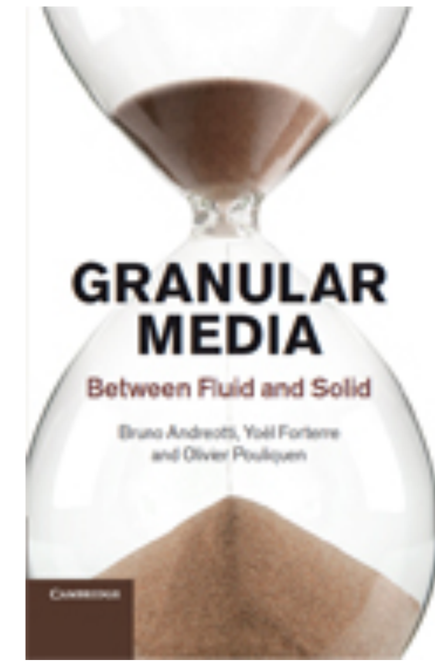

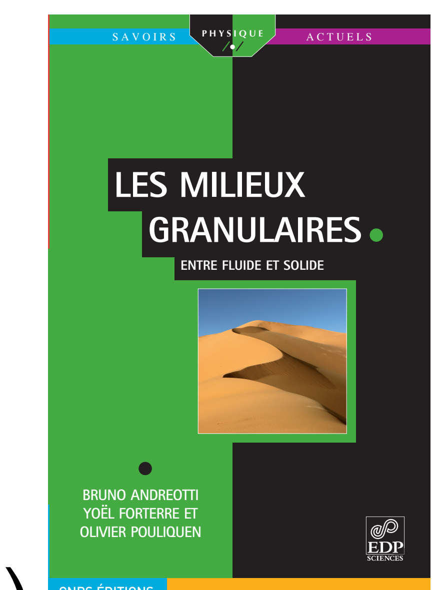

"useful" for industry and real live

motivation, facts

Méga Dune Maroc   (Dune "chantante")

motivation, facts

Val André le Pissot

PYL

motivation, facts

Rio de Janeiro,   Ipanema

motivation, facts

PYL

motivation, facts

IPGP

Paris, Univ. Pierre & Marie Curie, Sorbonne University, Jussieu

motivation, facts

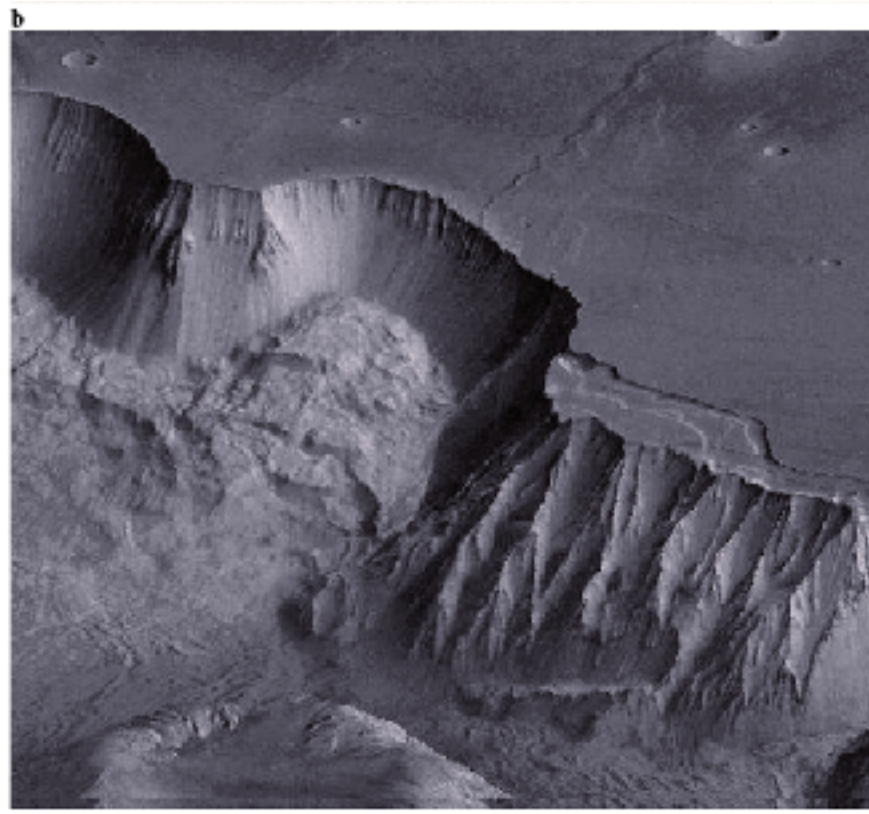

Mars

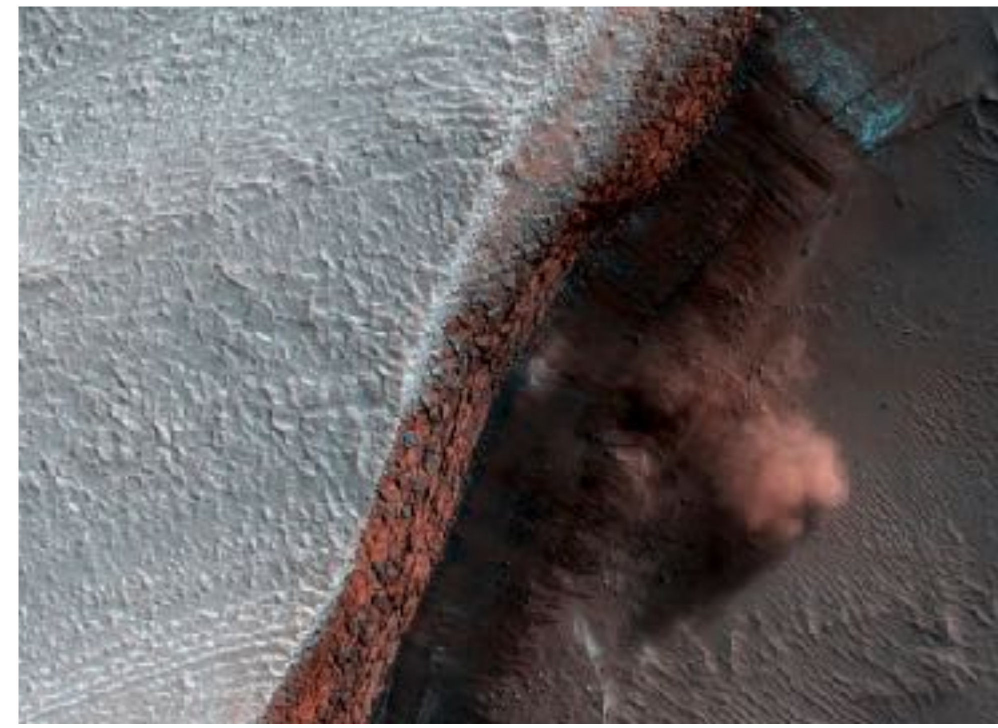

http://www.cieletespace.fr/image-du-jour/5126_la-saison-des-avalanches-sur-mars

NASA'S Mars Reconnaissance Orbiter (MRO)

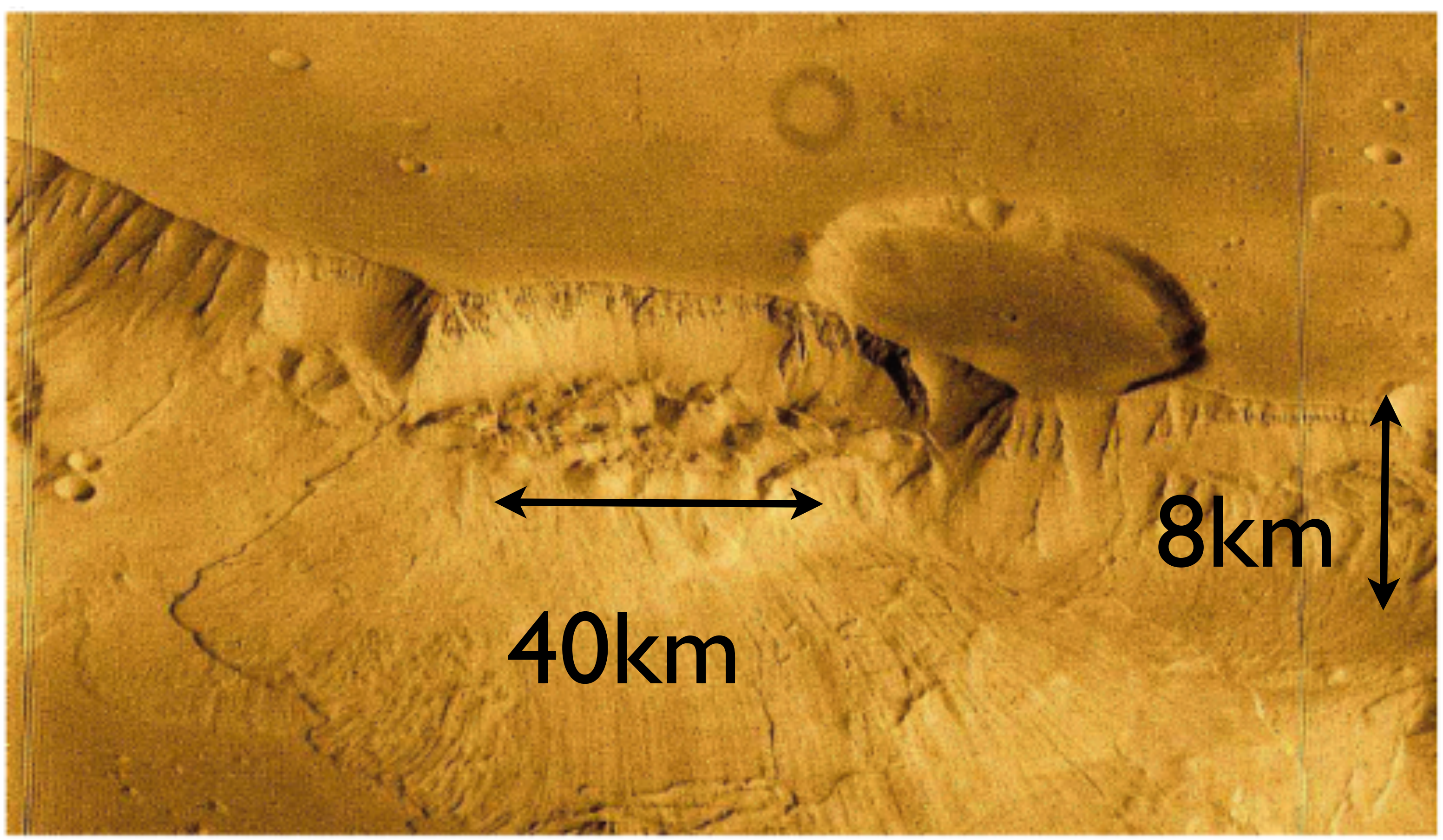

http://books.google.fr/books?id=HY6Z5od4-E4C&pg=PA49&dq=granular+flow&hl=fr&ei=lamtTaa_NYyVOoToldcL&sa=X&oi=book_result&ct=result&resnum=10&ved=0CFkQ6AEwCTgK#v=onepage&q&f=true

motivation, facts

PYL

motivation, facts

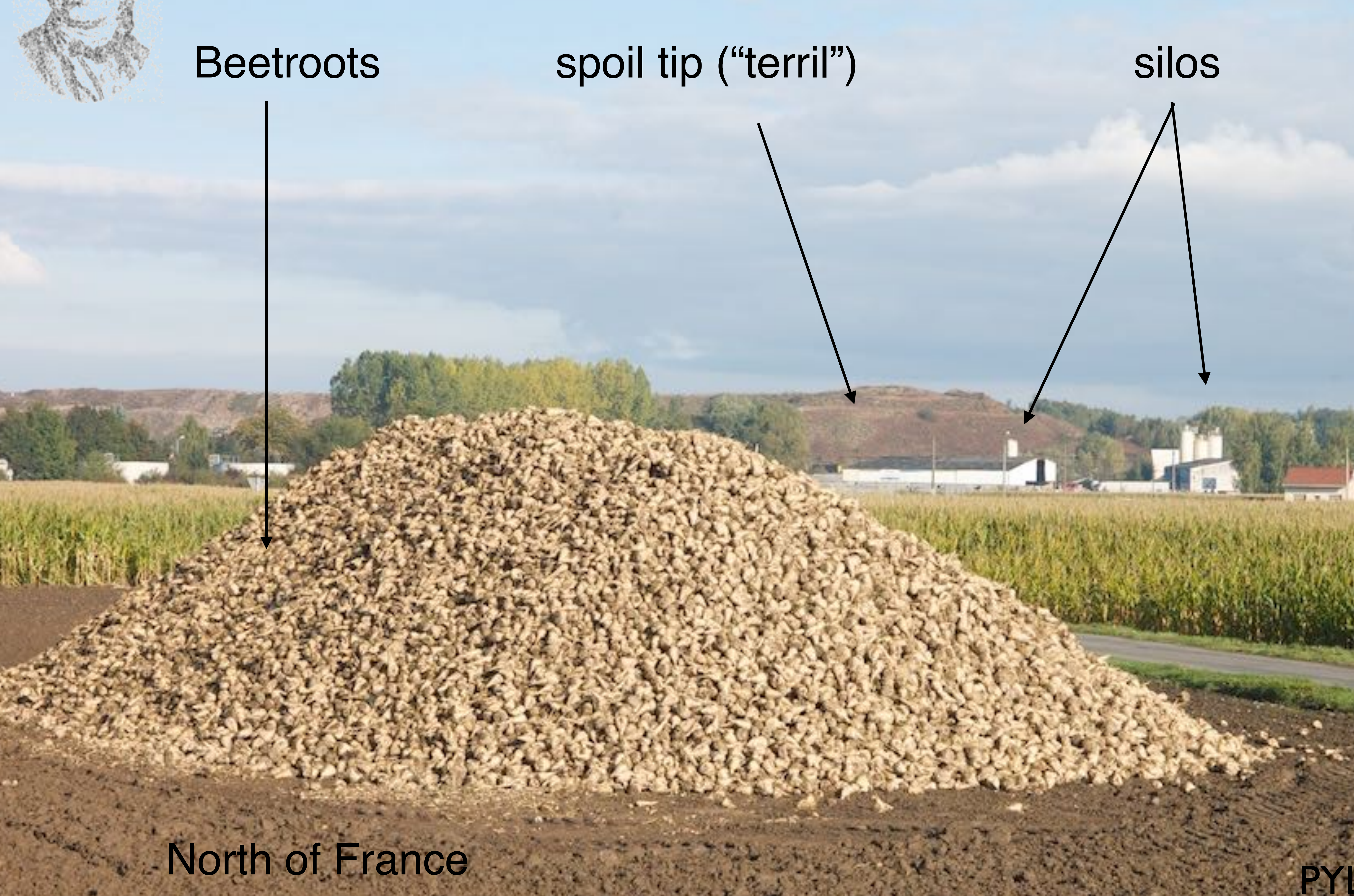

Jean Le Rond ∂'Alembert
1717 1783

- Solid - Liquid - Gas
- Looking for a continuum description for liquid phase
- Many experiments in simple configurations:
  shear/ inclined plane,
  with model material (glass beads, sand…)
- Simulations with discrete elements (disks, polygona, spheres)

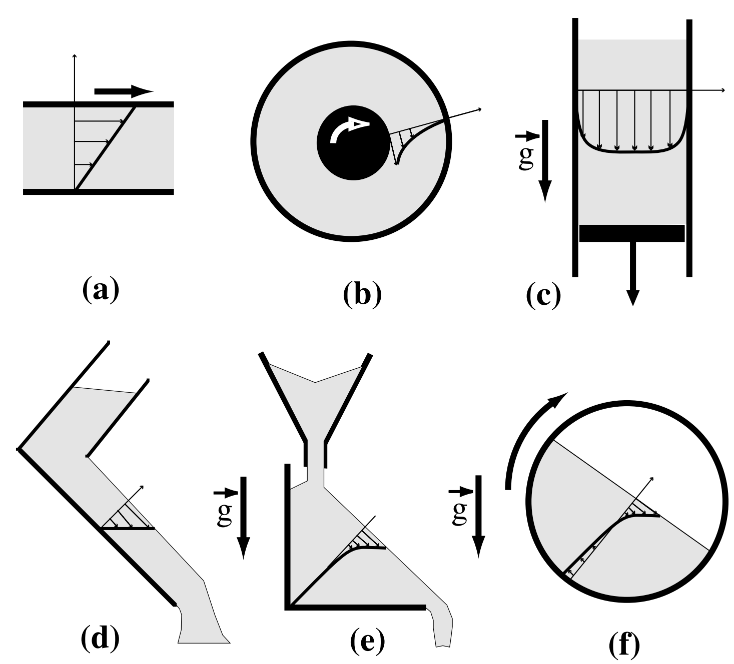

Fig. 1. The six configurations of granular flows: (a) plane shear, (b) annular shear, (c) vertical-chute flows, (d) inclined plane, (e) heap flow, (f) rotating drum.

Eur. Phys. J. E **14**, 341–365 (2004)
DOI 10.1140/epje/i2003-10153-0

THE EUROPEAN PHYSICAL JOURNAL E

On dense granular flows

GDR MiDi[a]

Jean Le Rond ∂'Alembert
1717 1783

- Solid - Liquid - Gas

- Looking for a continuum description for liquid phase

- Many experiments in simple configurations:
  shear/ inclined plane,
  with model material (glass beads, sand…)

- Simulations with discrete elements (disks, polygona, spheres)

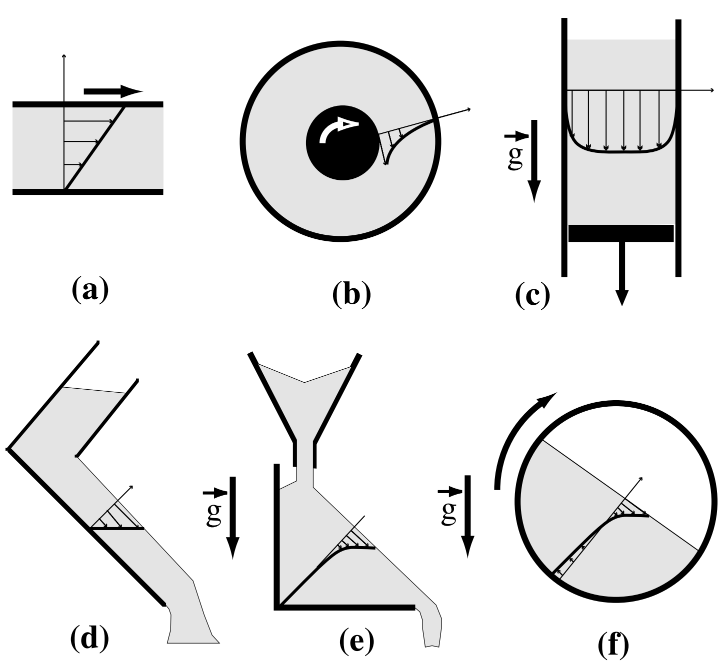

Fig. 1. The six configurations of granular flows: (a) plane shear, (b) annular shear, (c) vertical-chute flows, (d) inclined plane, (e) heap flow, (f) rotating drum.

Eur. Phys. J. E **14**, 341–365 (2004)
DOI 10.1140/epje/i2003-10153-0

THE EUROPEAN PHYSICAL JOURNAL E

On dense granular flows

GDR MiDi[a]

Utopian research paper with collective author name

The μ(I)-rheology

Charles-Augustin Coulomb
1736-1806

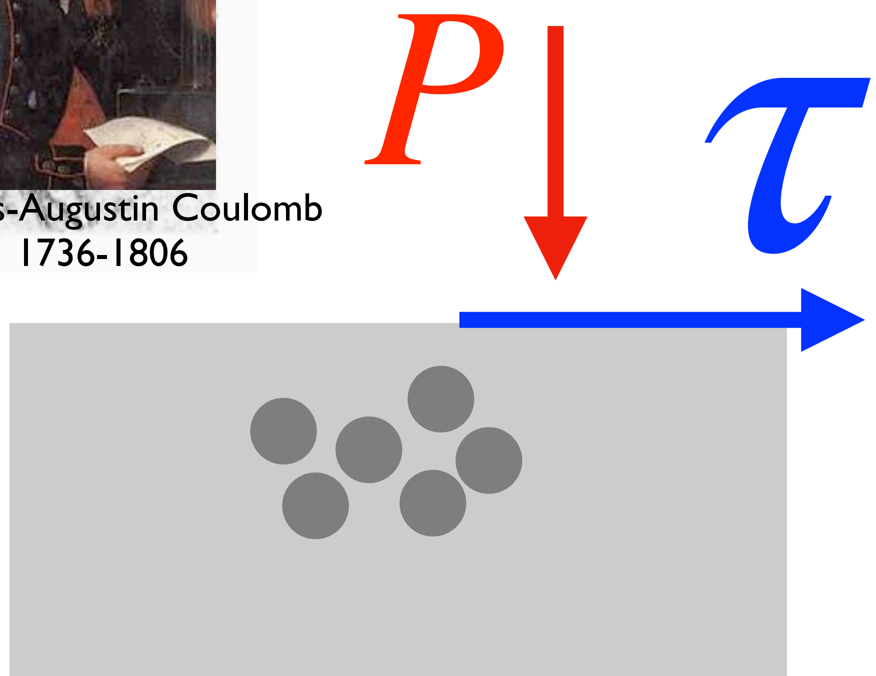

Coulomb friction law

$$\tau = \mu(I)P$$

The μ(I)-rheology

Charles-Augustin Coulomb
1736-1806

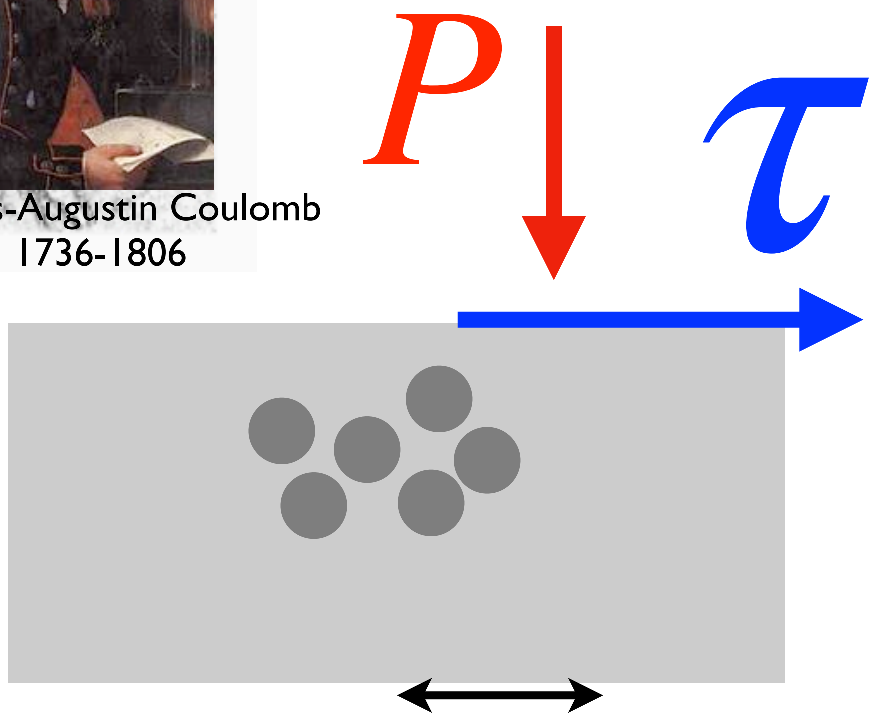

Coulomb friction law

$$\tau = \mu(I) P$$

$$I = \frac{d \frac{\partial u}{\partial y}}{\sqrt{P/\rho}}$$

$$\frac{\text{falling time}}{\text{displacement time}}$$

Charles-Augustin Coulomb
1736-1806

The μ(I)-rheology

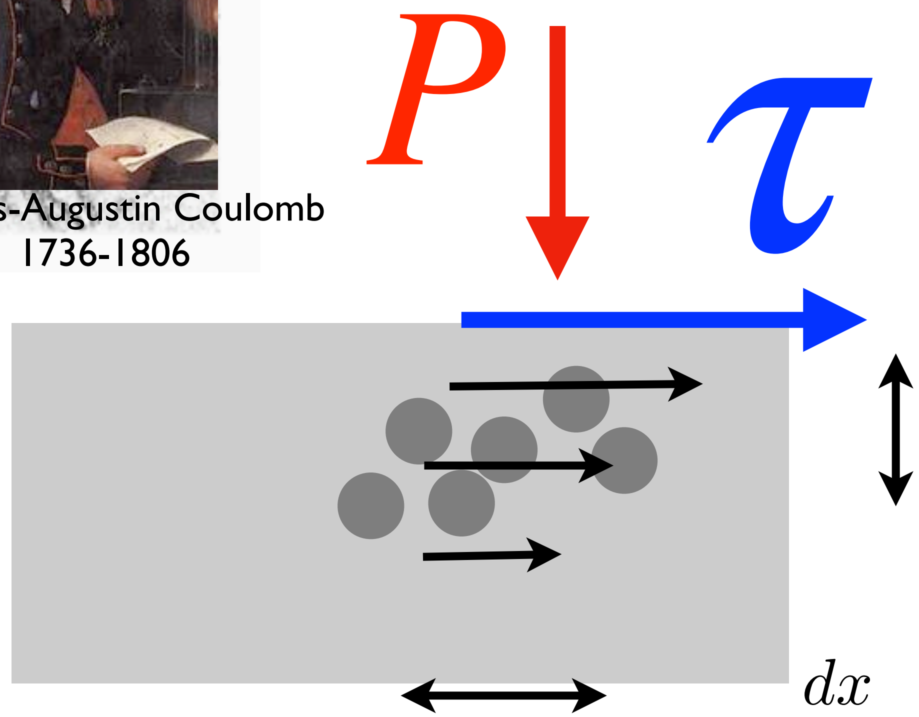

$$\frac{dx}{dt} = d\frac{\partial u}{\partial y}$$

Coulomb friction law

$$\tau = \mu(I)P$$

$$I = \frac{d\frac{\partial u}{\partial y}}{\sqrt{P/\rho}}$$

$$\frac{\text{falling time}}{\text{displacement time}}$$

The μ(I)-rheology

Charles-Augustin Coulomb
1736-1806

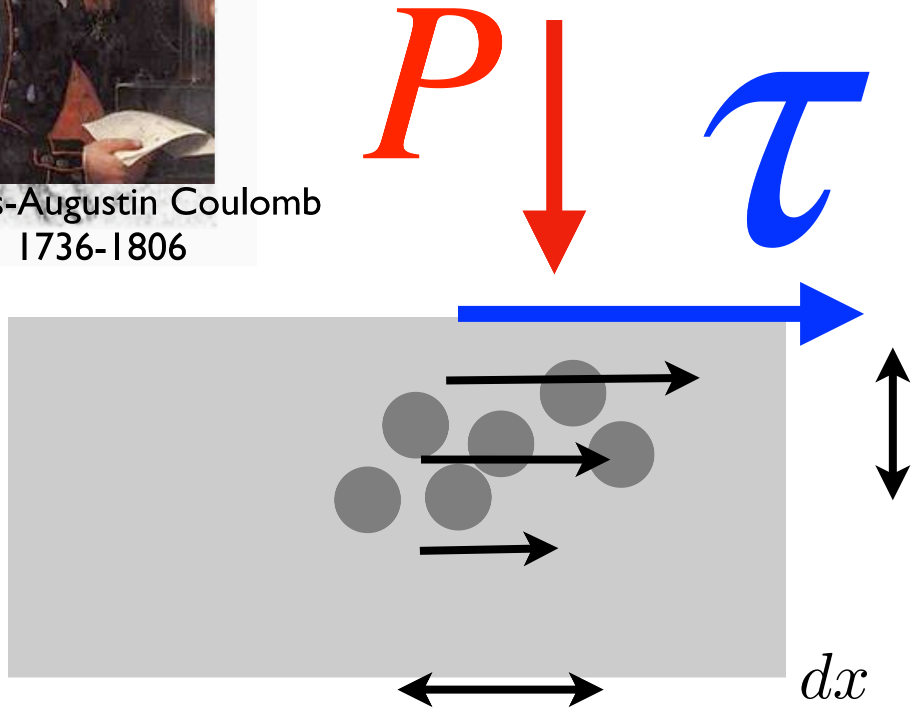

$$\frac{dx}{dt} = d\frac{\partial u}{\partial y} \qquad t = 1/\frac{\partial u}{\partial y}$$

Coulomb friction law

$$\tau = \mu(I)P$$

$$I = \frac{d\frac{\partial u}{\partial y}}{\sqrt{P/\rho}}$$

$$\frac{\text{falling time}}{\text{displacement time}}$$

The μ(I)-rheology

Charles-Augustin Coulomb
1736-1806

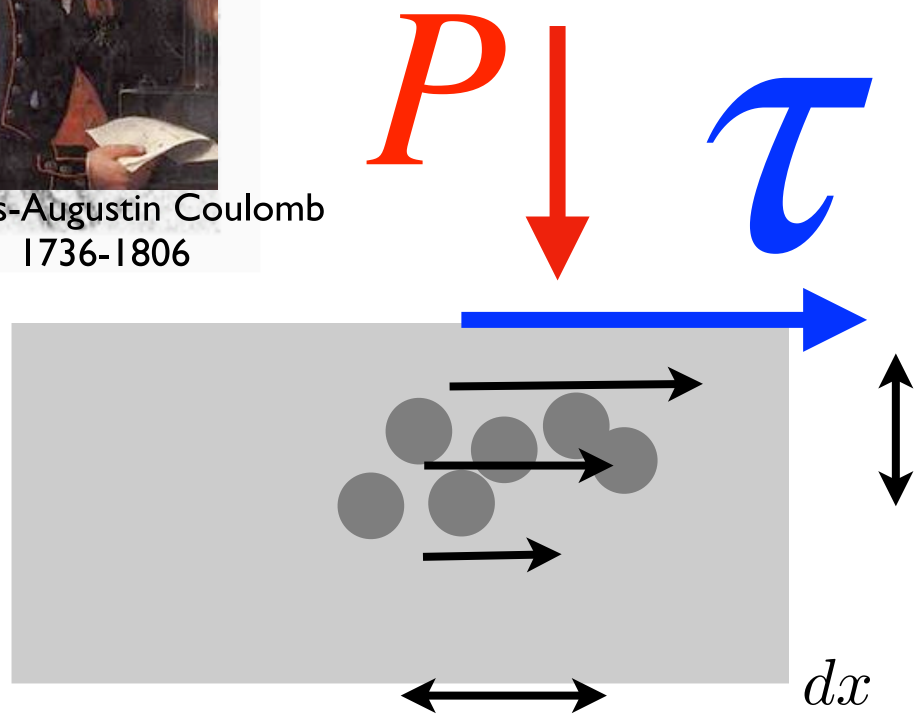

$$md^2y/dt^2 = Pd^2$$

$$t^2 = \rho d^2/(P)$$

$$\frac{dx}{dt} = d\frac{\partial u}{\partial y} \qquad t = 1/\frac{\partial u}{\partial y}$$

Coulomb friction law

$$\tau = \mu(I)P$$

$$I = \frac{d\frac{\partial u}{\partial y}}{\sqrt{P/\rho}} \qquad \frac{\text{falling time}}{\text{displacement time}}$$

The μ(I)-rheology

by grain dynamics

Charles-Augustin Coulomb
1736-1806

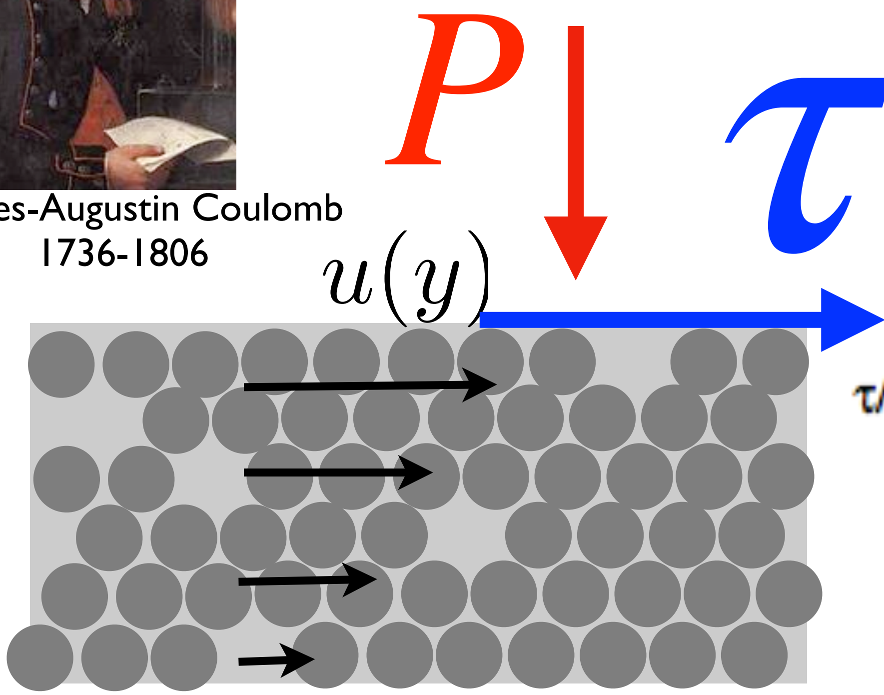

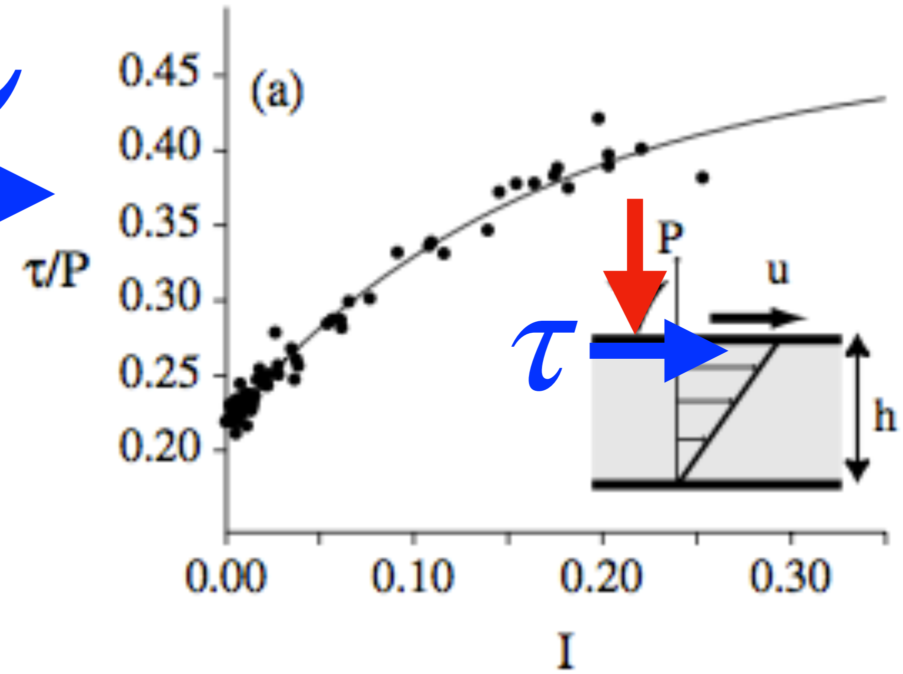

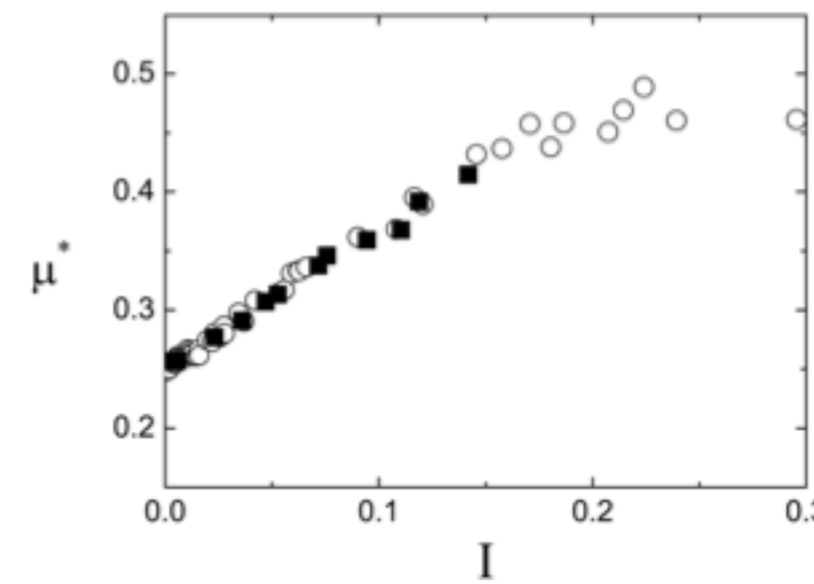

Da Cruz PRE 05

Coulomb friction law

«Drucker-Prager» plastic flow

$$\tau = \mu(I)P$$

«Inertial Number»

$$I = \frac{d\frac{\partial u}{\partial y}}{\sqrt{P/\rho}}$$

$$\frac{\text{falling time}}{\text{displacement time}}$$

non dimensional number: «Froude»
local «Inertial Number» (Da Cruz 04-05)
(Savage Number 89 / Ancey 00 I^2)

Pouliquen 99
Pouliquen Forterre JSM 06
Da Cruz 04-05
GDR MiDi 04

The μ(I)-rheology

Charles-Augustin Coulomb
1736-1806

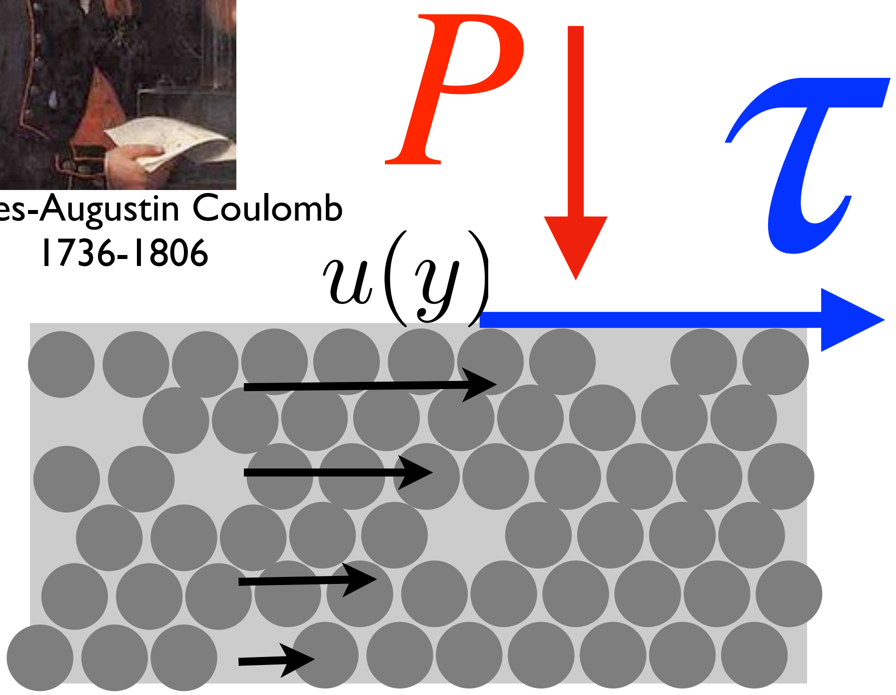

by grain dynamics

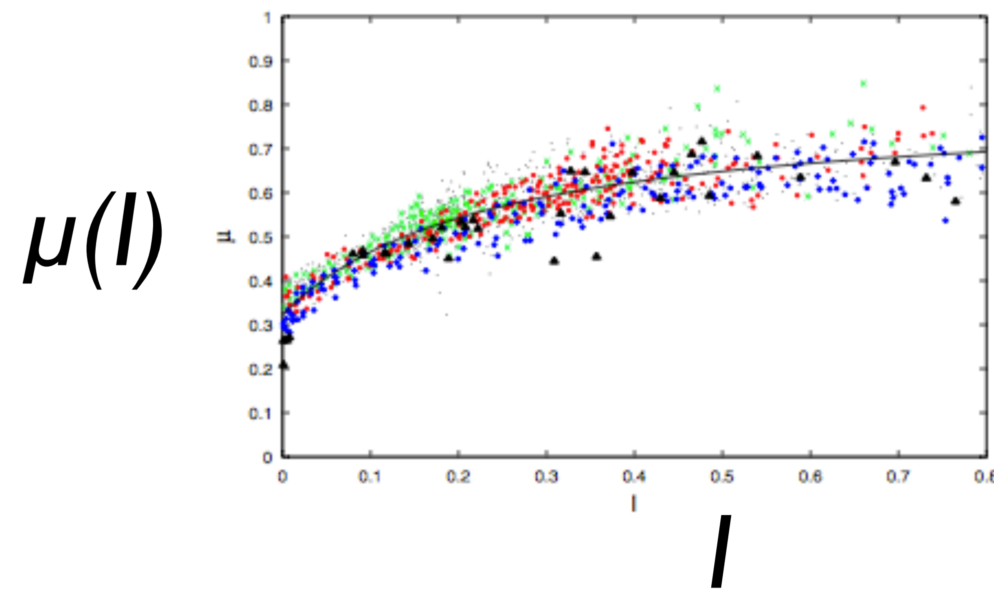

Lacaze Kerswell 09

Coulomb friction law

«Drucker-Prager» plastic flow

$$\tau = \mu(I)P$$

«Inertial Number»

$$I = \frac{d\frac{\partial u}{\partial y}}{\sqrt{P/\rho}}$$

$$\mu(I) = \mu_1 + \frac{\mu_2 - \mu_1}{I_0/I + 1}$$

$$\mu_1 \simeq 0.32 \quad (\mu_2 - \mu_1) \simeq 0.23 \quad I_0 \simeq 0.3$$

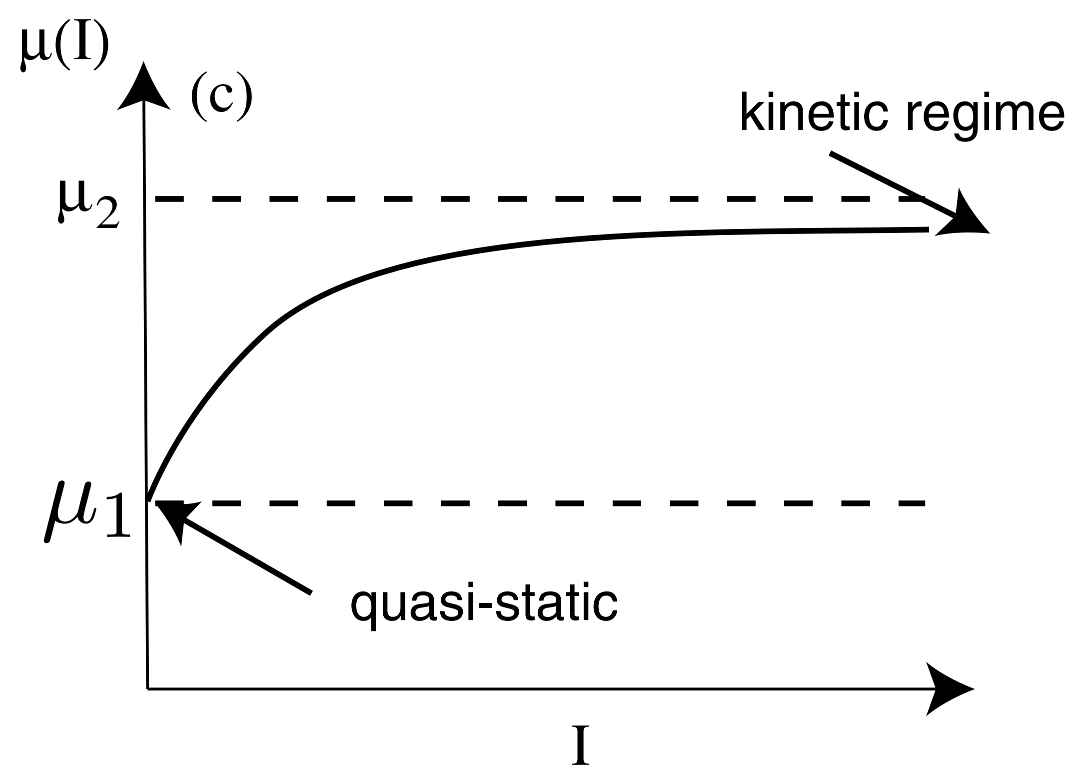

Jop Forterre Pouliquen 2005

The μ(I)-rheology

Charles-Augustin Coulomb
1736-1806

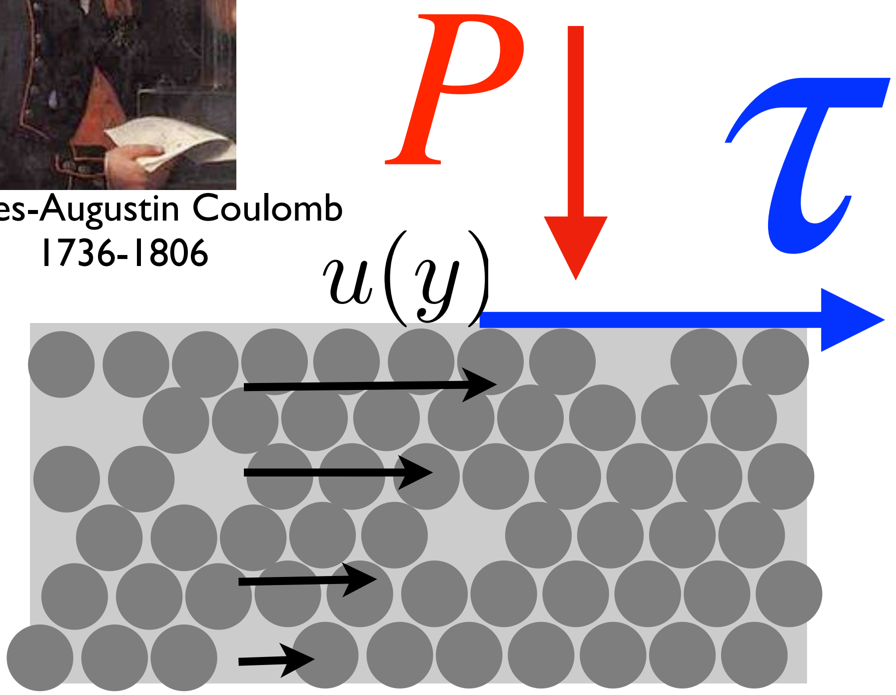

Cortet et al. 2009

This leads us to argue that the visco-plastic rheology proposed in [11] is extremely efficient to describe quasi- unidirectional flows as those investigated in [9–11] but remains unapplicable, when applied in its non-invariant form (eq. (1)), to highly multi-directional flows such as those observed in rotating drum.

Coulomb friction law

$$\tau = \mu(I)P$$

$$I = \frac{d\frac{\partial u}{\partial y}}{\sqrt{P/\rho}}$$

«Inertial Number»

$$\mu(I) = \mu_1 + \frac{\mu_2 - \mu_1}{I_0/I + 1}$$

$$\mu_1 \simeq 0.32 \quad (\mu_2 - \mu_1) \simeq 0.23 \quad I_0 \simeq 0.3$$

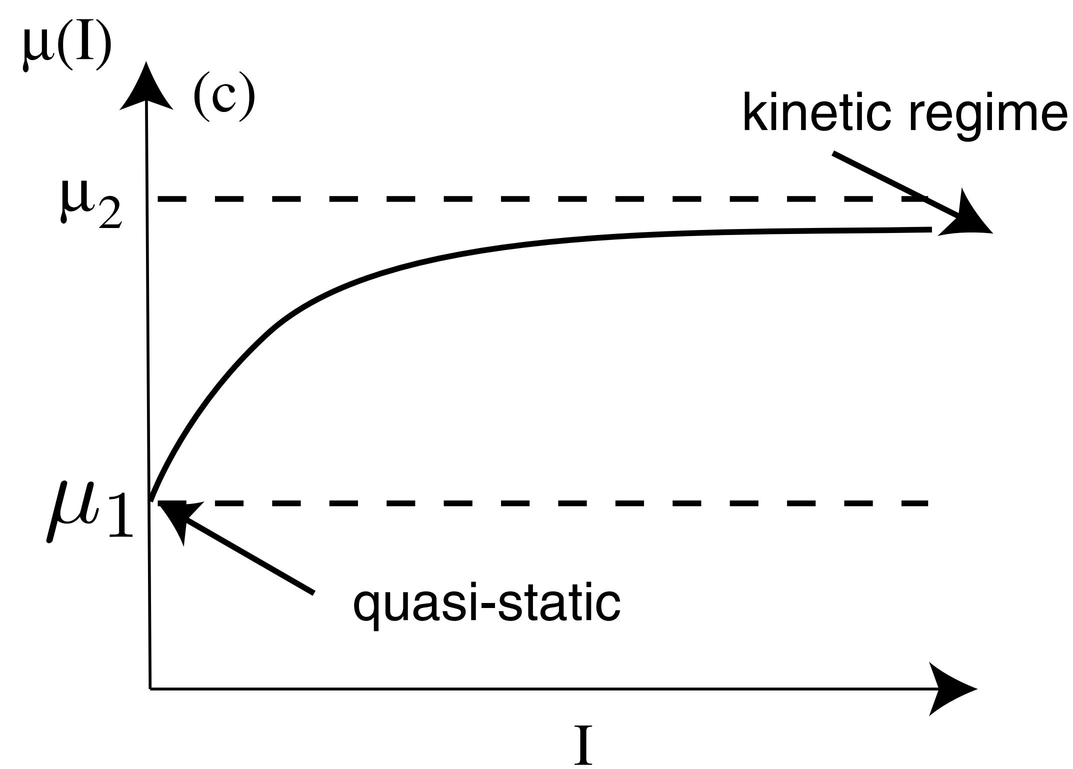

Jop Forterre Pouliquen 2005

The μ(I)-rheology

Charles-Augustin Coulomb
1736-1806

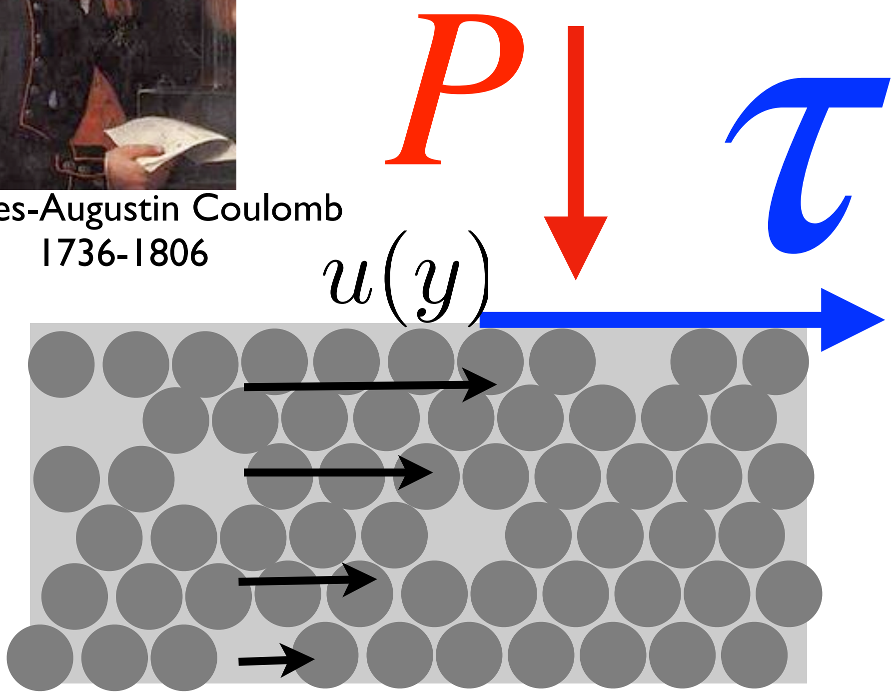

Shaeffer 87

Even if the initial value problem for (2.1) is well posed, solutions of this equation will probably behave erratically. In particular, it seems likely to us that as time evolves, some of the assumptions in the derivation of (2.1) may cease to hold.

<u>ill posed</u>

Barker Shaeffer Bohorquez & Gray 2015

Coulomb friction law

$$\tau = \mu(I)P$$

«Inertial Number»

$$I = \frac{d\frac{\partial u}{\partial y}}{\sqrt{P/\rho}}$$

$$\mu(I) = \mu_1 + \frac{\mu_2 - \mu_1}{I_0/I + 1}$$

$$\mu_1 \simeq 0.32 \quad (\mu_2 - \mu_1) \simeq 0.23 \quad I_0 \simeq 0.3$$

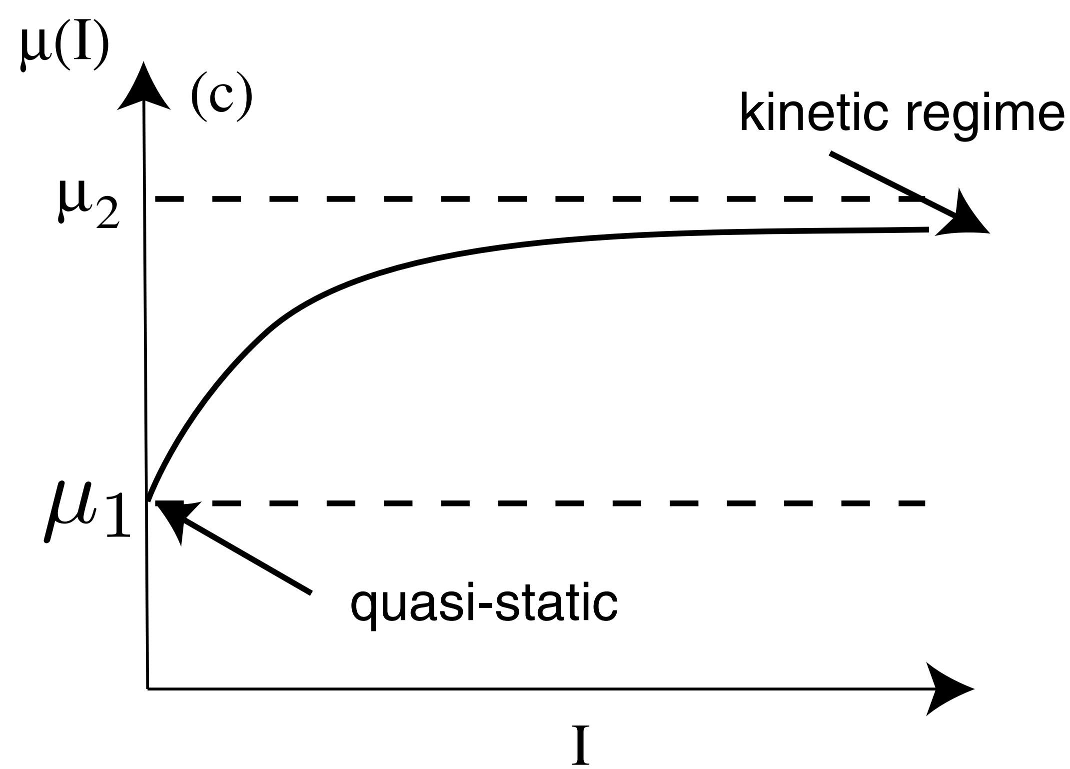

Jop Forterre Pouliquen 2005

Jean Le Rond ∂'Alembert
1717 1783

Outline

- Introduction
- presentation of μ(I) rheology
- Simplification with shallow water (depth average) 1D continuum model

- use of contact dynamics (simulation all grains, discrete, here 2D)
- implementation of μ(I) in a continuum Navier Stokes 2D code
- applications to archetypal flows: collapse of columns - hourglass

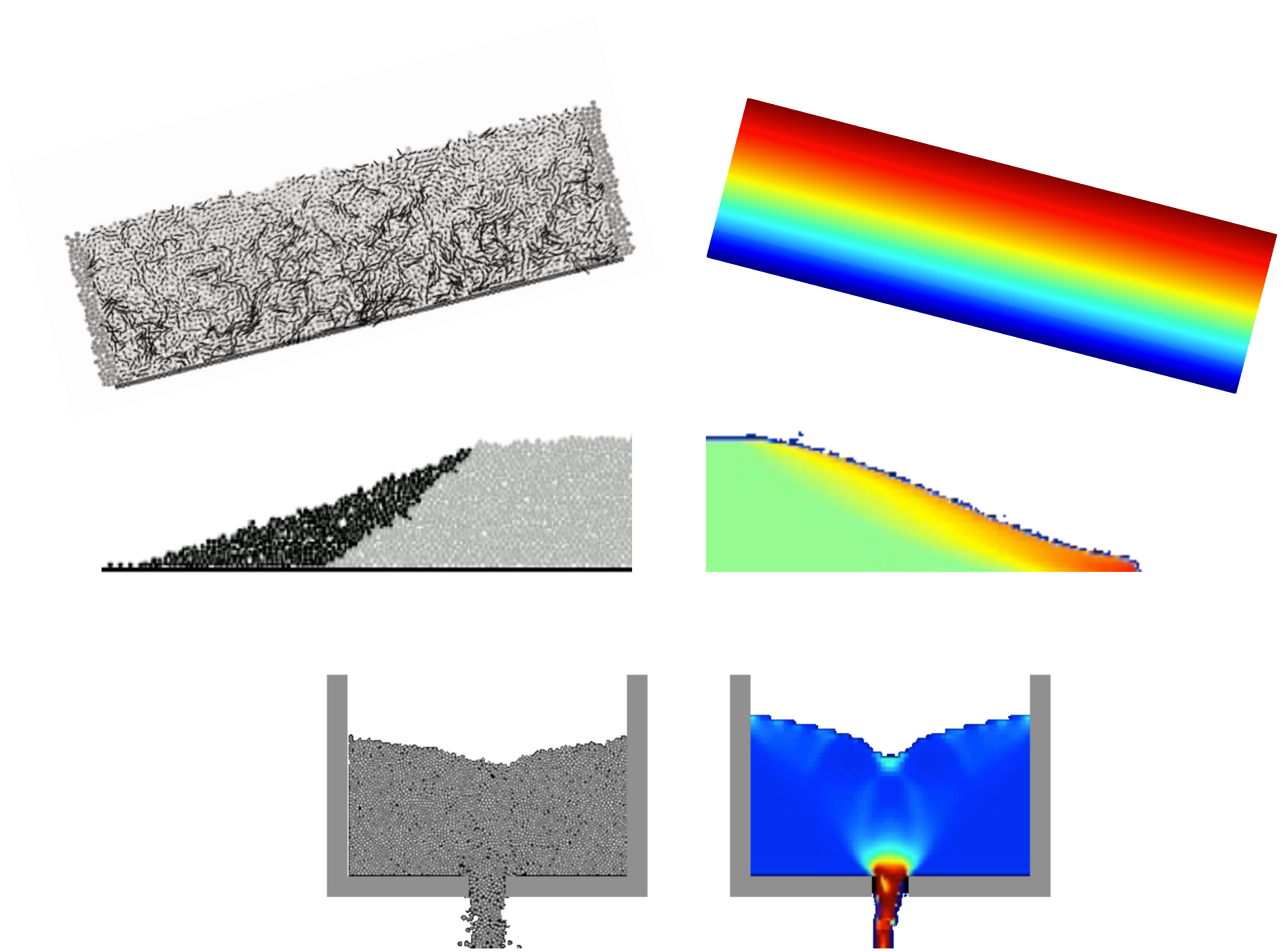


ST VENANT

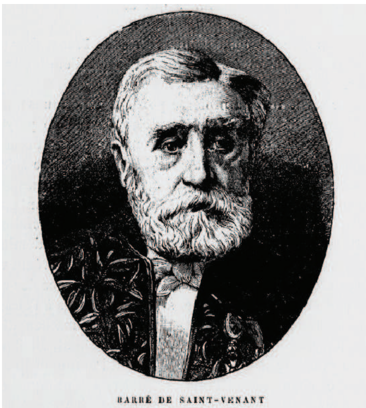

Adhémar Barré de Saint-Venant
1797-1886

Saint-Venant Savage Hutter Shallow water/ depth averaged

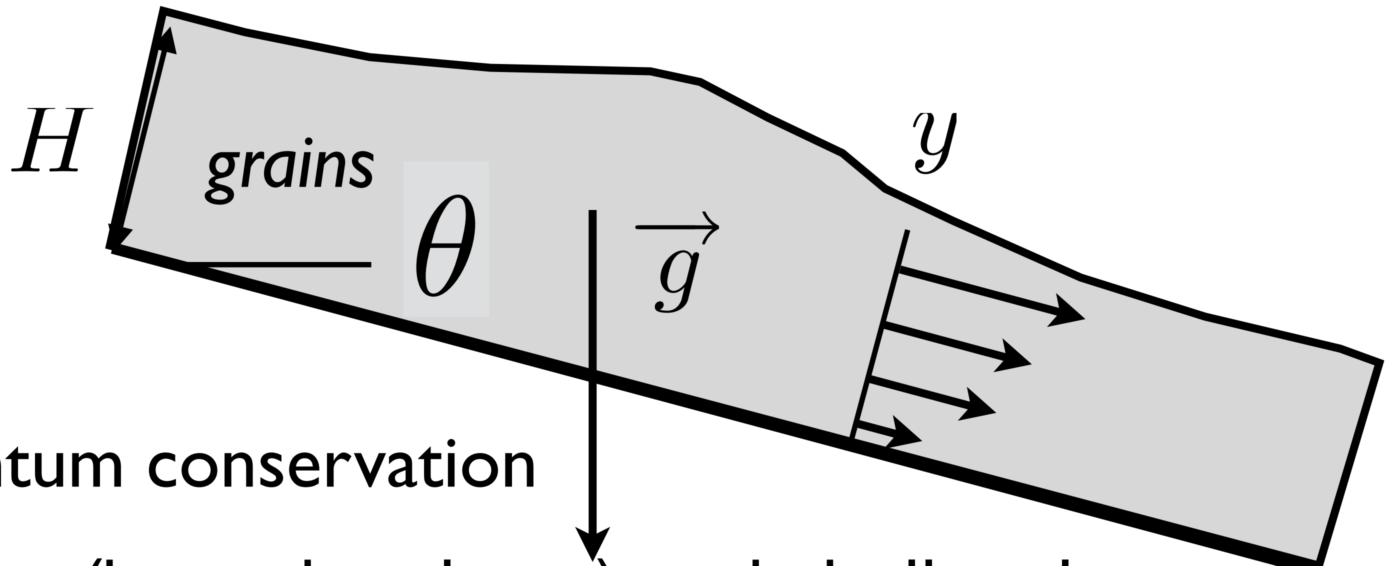

Mass and Momentum conservation

Write thin layer (boundary layer) and shallow layer equations,
test the most simple implementation of μ(I) in shallow water

$$
\left\{
\begin{aligned}
\frac{\partial u}{\partial x} + \frac{\partial v}{\partial y} &= 0 \\
\rho\left(\frac{\partial u}{\partial t} + \frac{\partial u^2}{\partial x} + \frac{\partial uv}{\partial y}\right) &= -\rho g \tan\theta - \frac{\partial p}{\partial x} + \frac{\partial \tau_{xy}}{\partial y} + \frac{\partial \tau_{xx}}{\partial x} \\
\rho\left(\frac{\partial v}{\partial t} + \frac{\partial uv}{\partial x} + \frac{\partial v^2}{\partial y}\right) &= -\rho g - \frac{\partial p}{\partial y} + \frac{\partial \tau_{xy}}{\partial x} + \frac{\partial \tau_{yy}}{\partial y}
\end{aligned}
\right.
$$

Dominant terms in the shallow layer / thin layer (boundary layer equations)

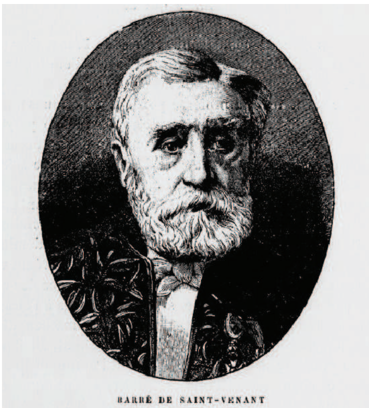

Adhémar Barré de Saint-Venant
1797-1886

Saint-Venant Savage Hutter Shallow water/ depth averaged

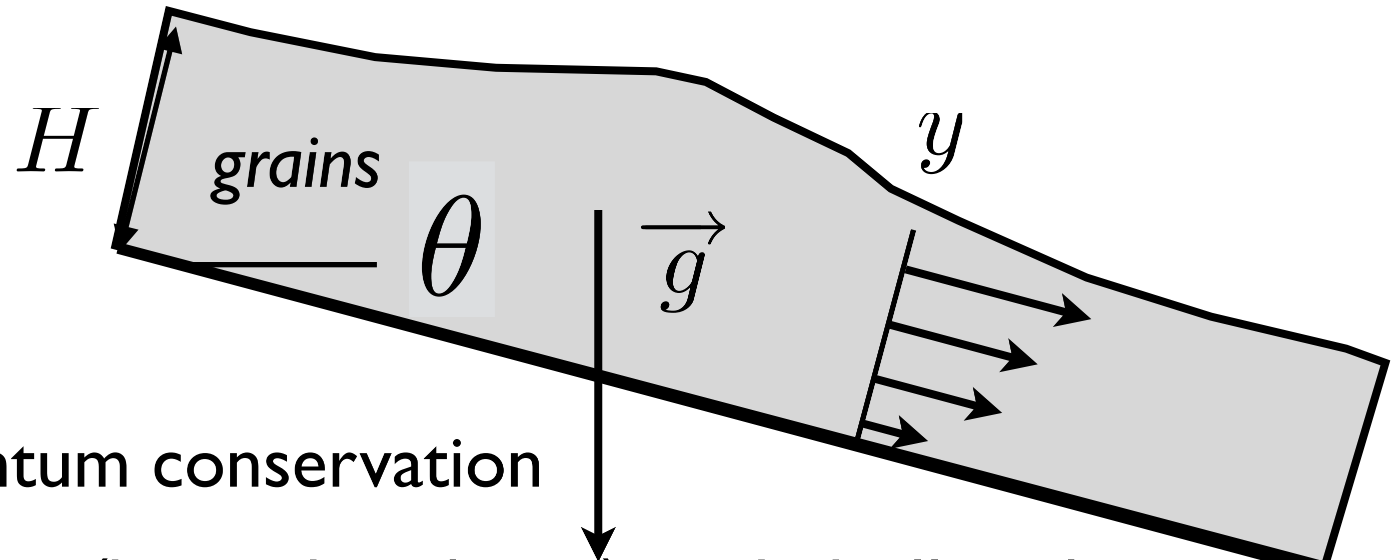

Mass and Momentum conservation

Write thin layer (boundary layer) and shallow layer equations, test the most simple implementation of μ(I) in shallow water

$$
\begin{cases}
\dfrac{\partial u}{\partial x} + \dfrac{\partial v}{\partial y} = 0 \\
\rho\left(\dfrac{\partial u}{\partial t} + \dfrac{\partial u^2}{\partial x} + \dfrac{\partial uv}{\partial y}\right) = -\rho g \tan\theta - \dfrac{\partial p}{\partial x} + \dfrac{\partial \tau}{\partial y} \\
0 = -\rho g - \dfrac{\partial p}{\partial y} \qquad \tau = \mu(I) p
\end{cases}
$$

Dominant terms in the shallow layer / thin layer (boundary layer equations)

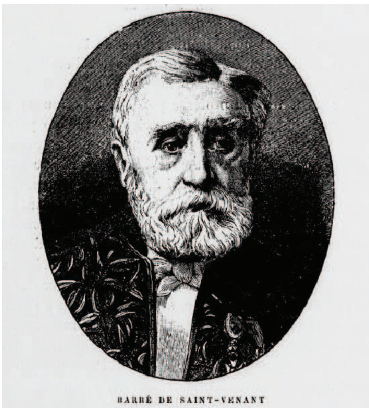
Adhémar Barré de Saint-Venant
1797-1886

Saint-Venant Savage Hutter Shallow water/ depth averaged

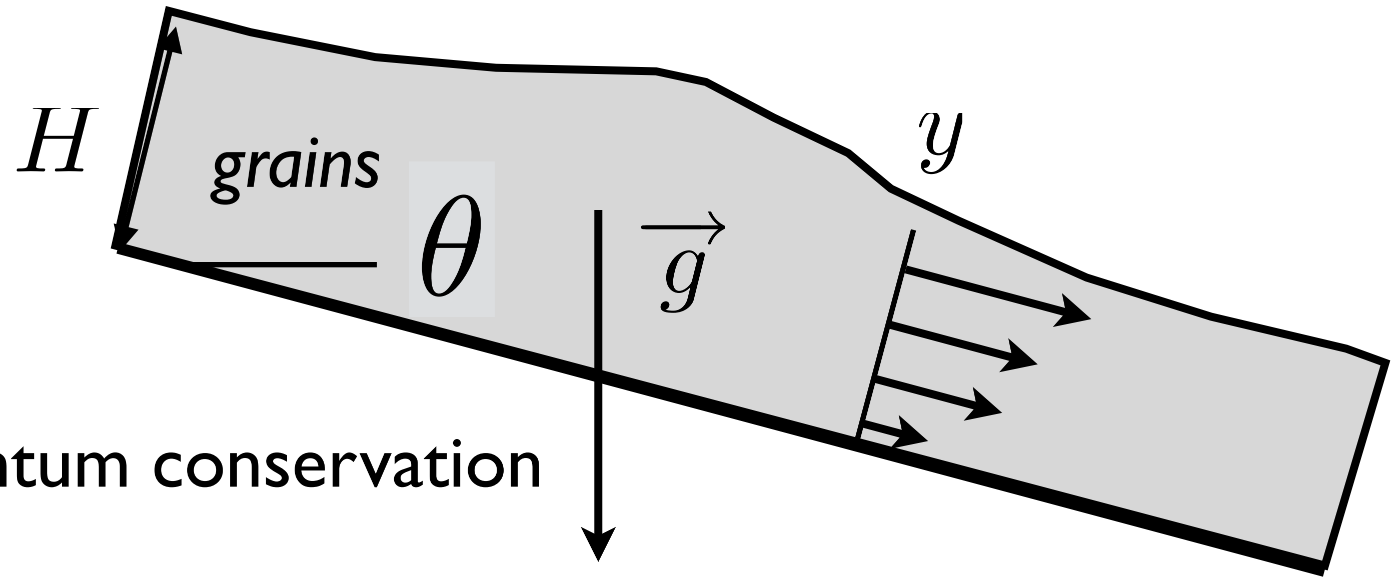

$$Q = h\overline{u}$$

Mass and Momentum conservation

Integrate across the layer

$$\frac{\partial h}{\partial t} + \frac{\partial}{\partial x}(h\overline{u}) = 0$$

$$\frac{\partial}{\partial t}(h\overline{u}) + \alpha\frac{\partial}{\partial x}(h\overline{u}^2) = hg(\tan\theta - \frac{\partial h}{\partial x} - \mu(\bar{I}))$$

Closure (here use Bagnold profile, next slide), if flat profile α=1, if half Poiseuille α=6/5

$$\alpha = \frac{\frac{1}{h}\int_0^h u^2(z)dz}{\left(\frac{1}{h}\int_0^h u(z)dz\right)^2} \qquad \alpha = \frac{5}{4} \qquad \bar{I} = \frac{5}{2}\frac{\overline{u}d_g}{h\sqrt{gh}}, \qquad \mu(\bar{I}) = \mu_0 + \frac{\Delta\mu}{I_0/\bar{I}+1},$$

Ralph Bagnold
1896-1990

«Bagnold» avalanche

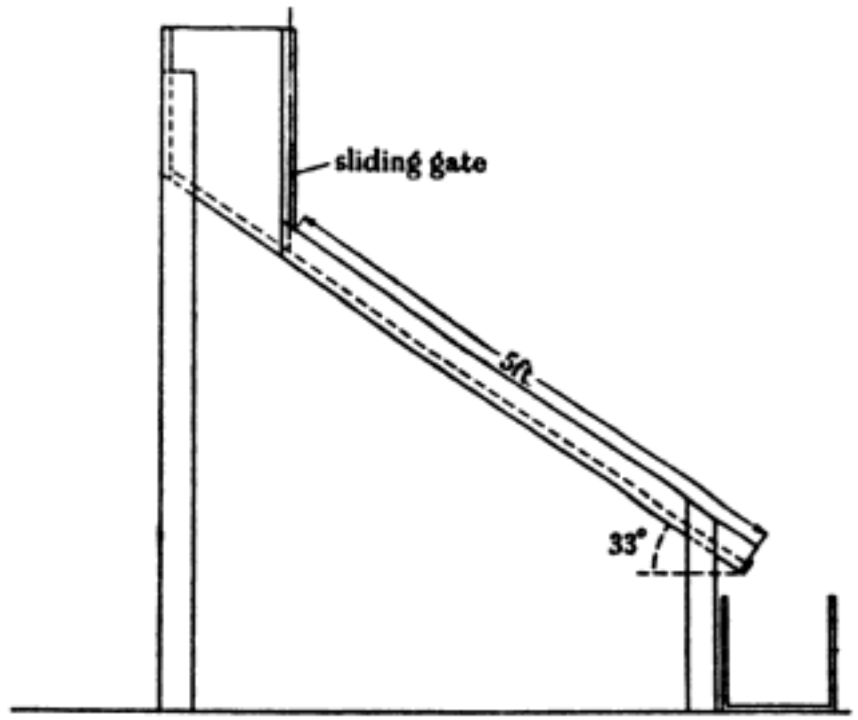

kind of Nusselt solution

$$T \propto \sigma(\lambda D)^2 \, (dU/dy)^2$$

$$U = \frac{2}{3} \times 0.165 \, (g \sin \beta)^{1/2} \, \frac{y'^{3/2}}{D} \, ,$$

TABLE 1.

flow height Y (cm)	measured speed (cm/sec)	speed, from (9) (cm/sec)	ratio
0.5	17.2	26.4	1.53
0.65	27.5	38.8	1.41
0.75	30.0	48.0	1.6
0.9	39.0	63.0	1.61

Bagnold 1954

- explored Lybian desert in 30'
- low pressure in tires when driving on sand
- waffle-boards (*tôle de désensablement*)
- commando in desert WW2 (Long Range Desert Group)
- field observations (The Physics of Blown Sand & Desert Dunes, 1941)

Ralph Bagnold
1896-1990

«Bagnold» avalanche

An analytical solution of the μ(I) rheology for an infinite layer on an inclined plane analog of Nusselt flow (or half-Poiseuille) in Newtonian fluids

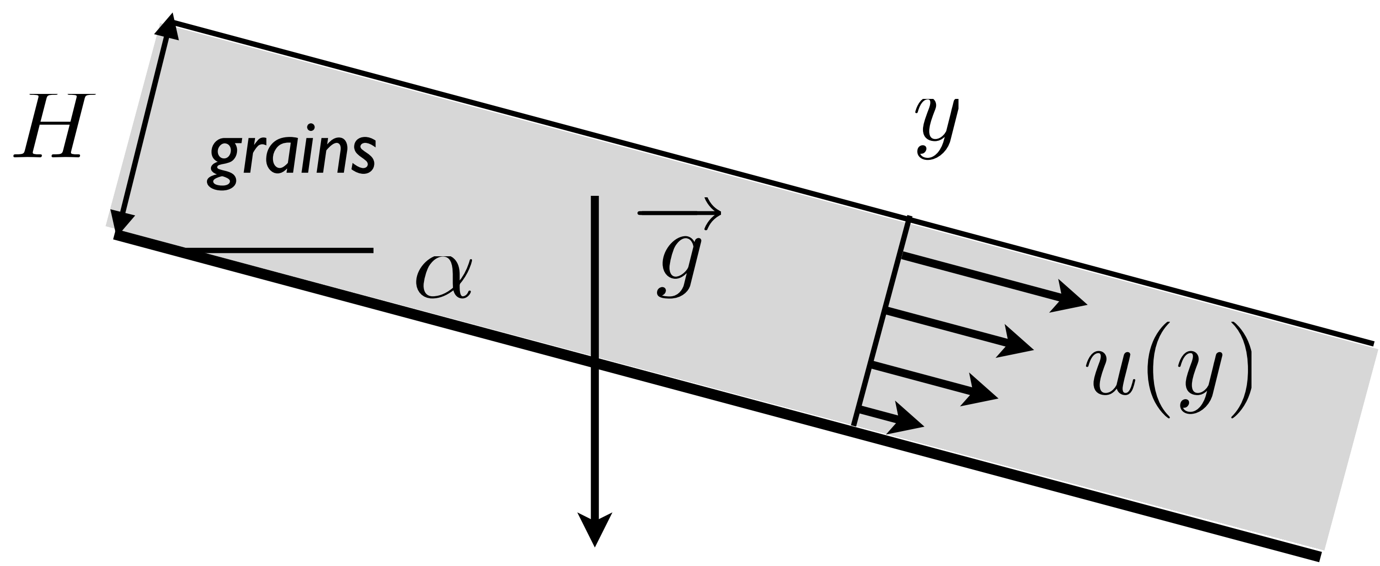

$$\mu(I) = \tan\alpha$$

$$u = \frac{2}{3} I_\alpha \sqrt{gd\cos\alpha \frac{H^3}{d^3}} \left(1 - \left(1 - \frac{y}{H}\right)^{3/2}\right),$$

Bagnold velocity profile

$$v = 0, \quad p = \rho g H \left(1 - \frac{y}{H}\right)\cos\alpha.$$

$$\alpha = \frac{\frac{1}{h}\int_0^h u^2(z)dz}{\left(\frac{1}{h}\int_0^h u(z)dz\right)^2}$$

$$\alpha = \frac{5}{4}$$

Front in Savage Hutter St Venant

Experimental set up:
Pouliquen 99 & 99

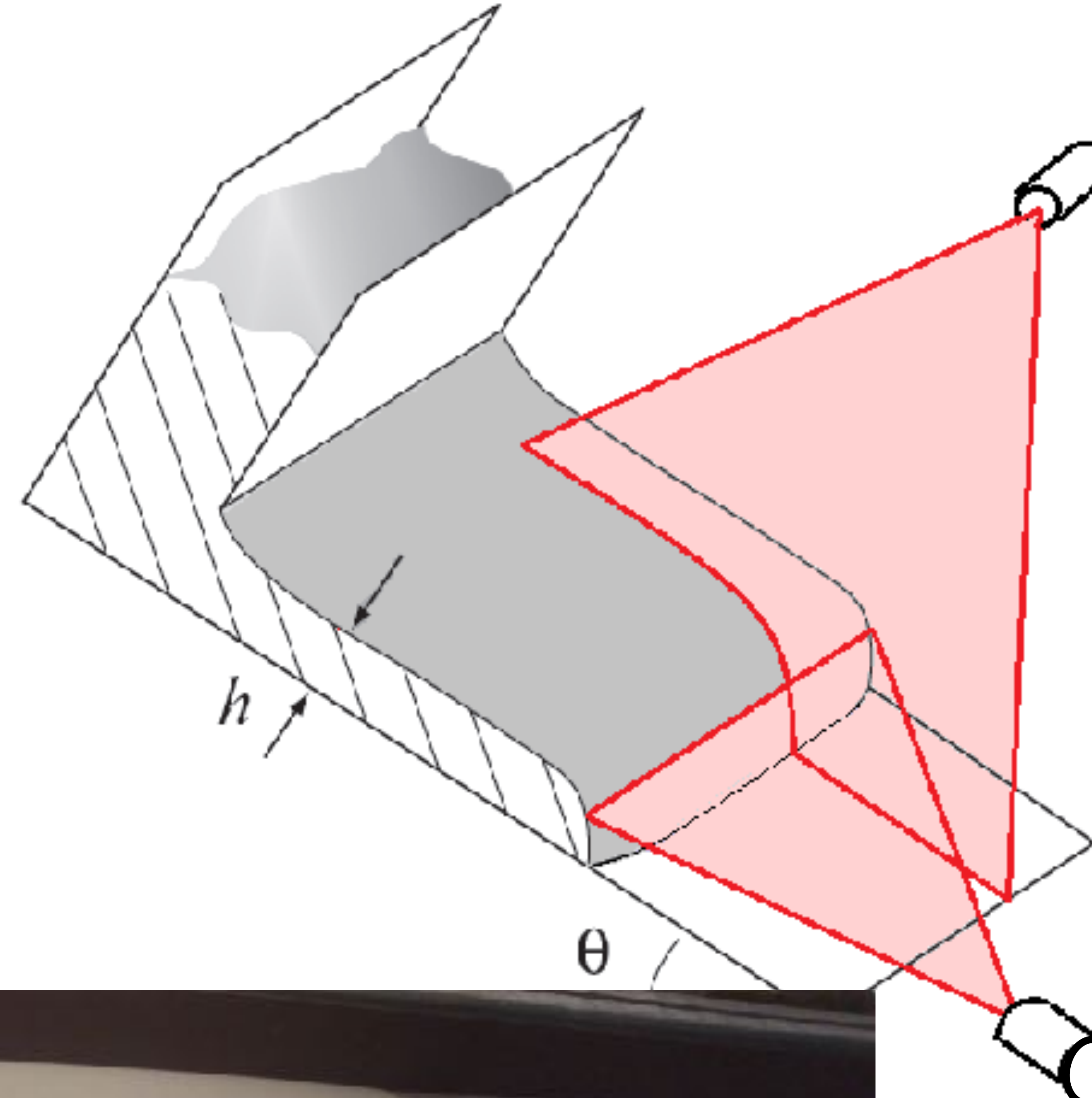

With Stéphanie Deboeuf and Guillaume Saingier

Front in Savage Hutter St Venant

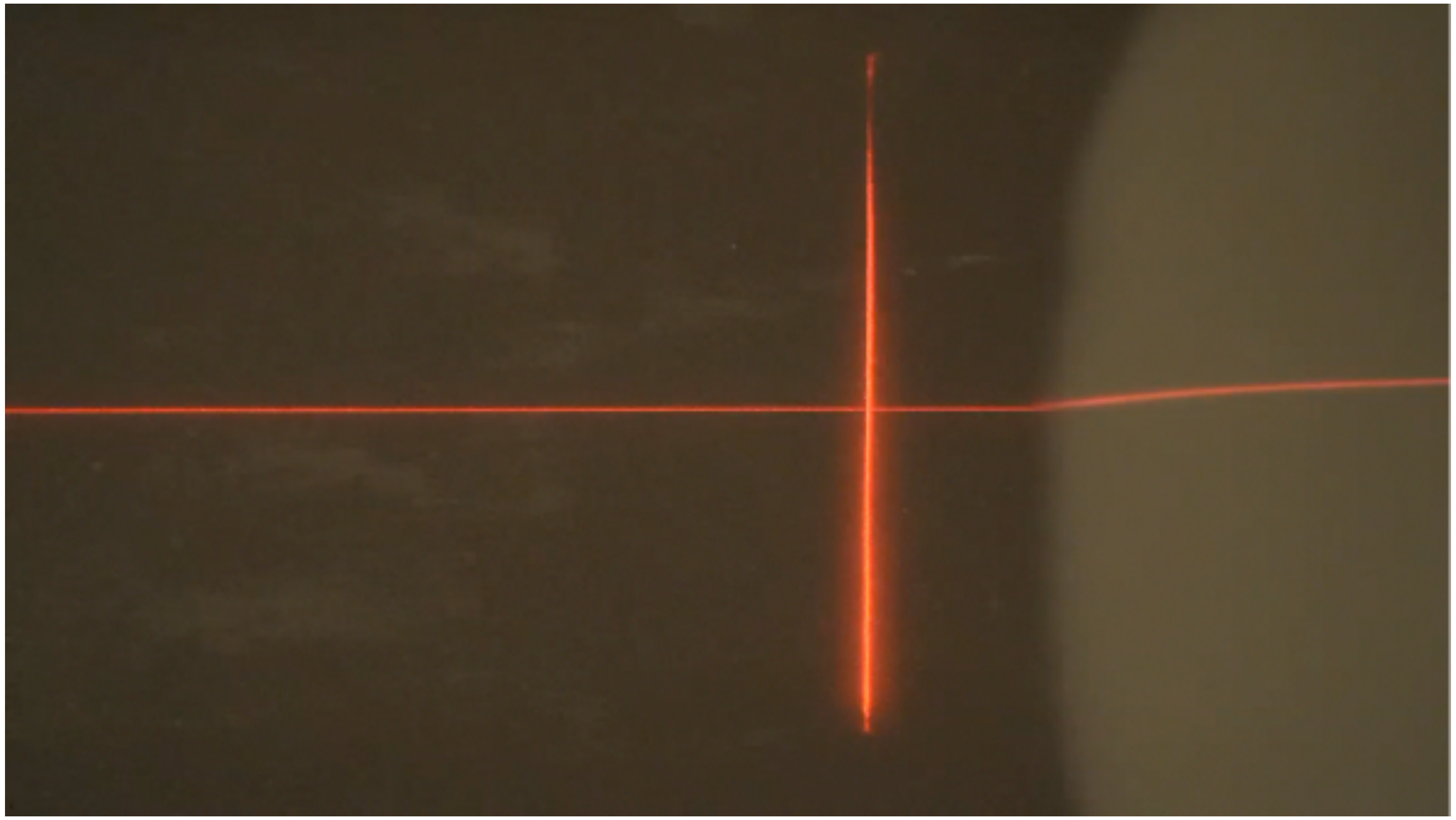

glass bead 400μm

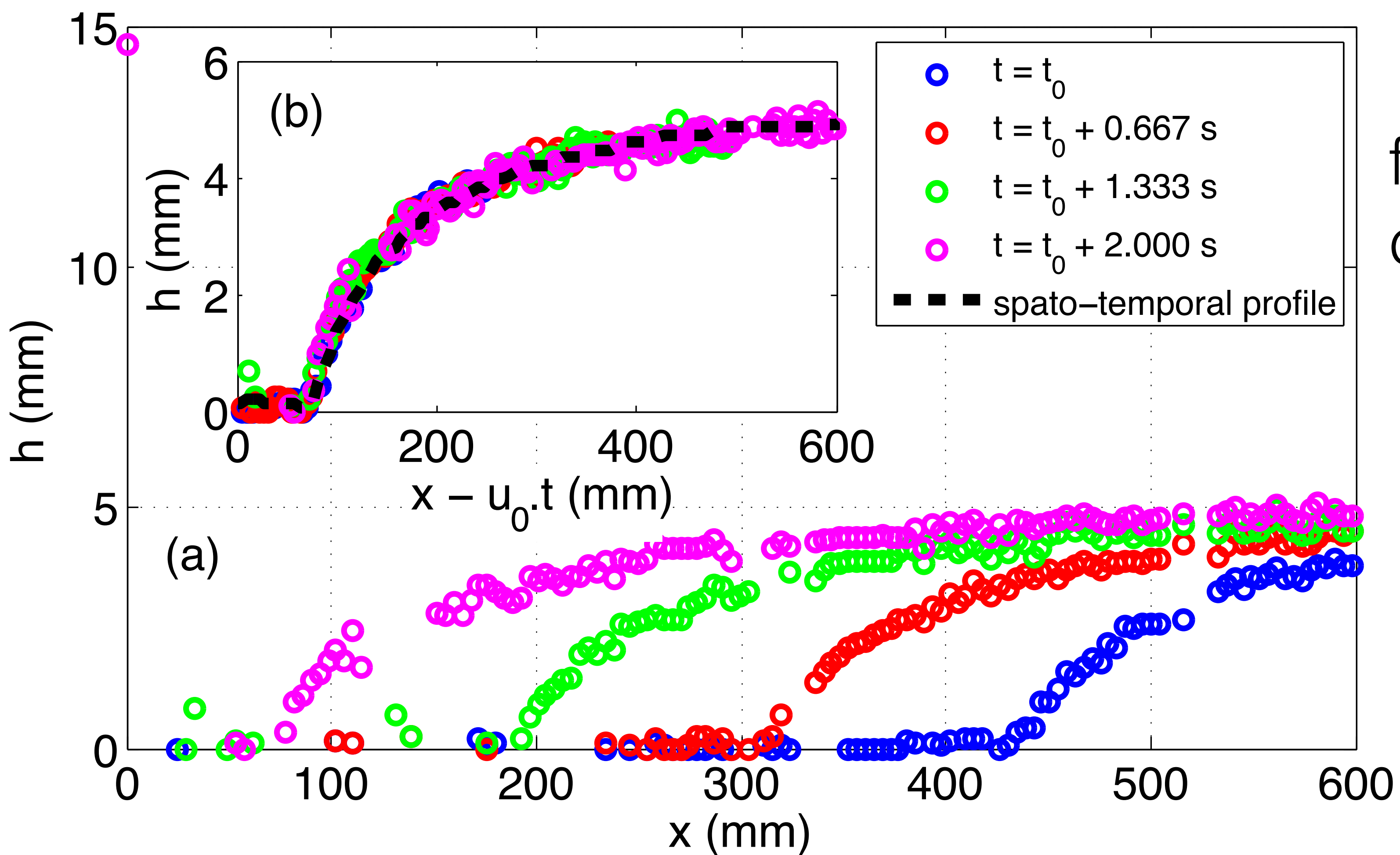

front moving at constant velocity u_0

Front in Savage Hutter St Venant

In a moving framework

$$((\alpha-1)Fr^2\frac{h_\infty}{h}+1)\frac{dh}{d\xi}=\tan\theta-\mu(I).$$

$$\xi = x - u_0 t$$

analytical implicit solution: $X=\frac{\xi(\tan\theta-\mu_0)}{h_\infty},\quad H=\frac{h}{h_\infty},\quad d=\frac{\mu_0-\tan\theta}{\Delta\mu},$

$$\boxed{X(H)=X_0-\frac{1}{3(-1+d)}(3H(d-1)-2\sqrt{3}\tan^{-1}(\frac{1+2\sqrt{H}}{\sqrt{3}})-2\log(1-\sqrt{H})+3d(1-\alpha)Fr^2\log(H)+\log(1+\sqrt{H}+H)-2(1-\alpha)Fr^2\log(1-H^{3/2})),}$$

superposed on Pouliquen 99 (who supposed α =1)

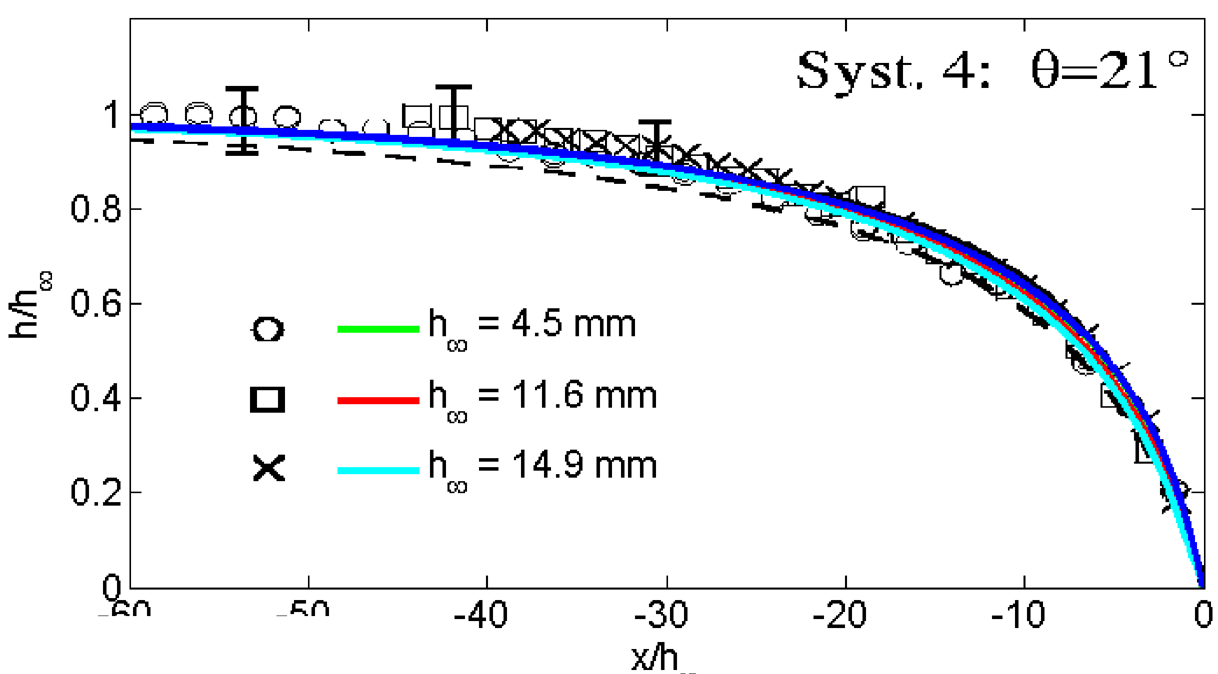

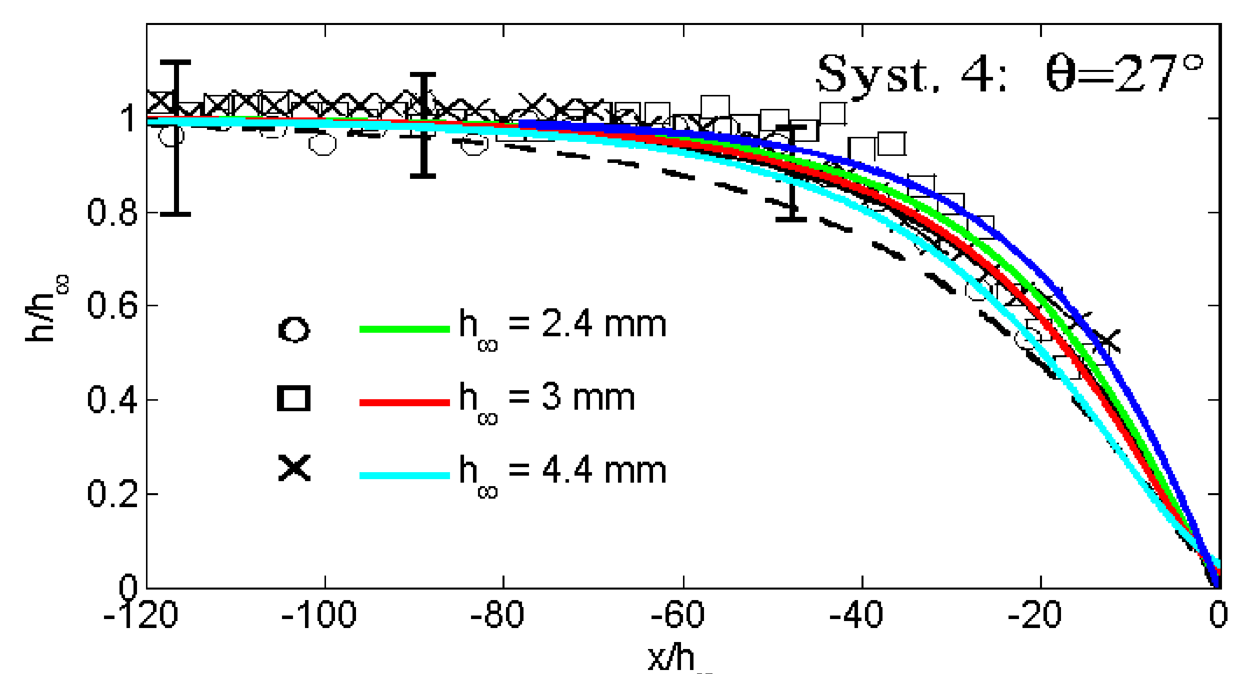

Front in Savage Hutter St Venant

with our inclined plane

$$((\alpha-1)Fr^2\frac{h_\infty}{h}+1)\frac{dh}{d\xi}=\tan\theta-\mu(I).$$

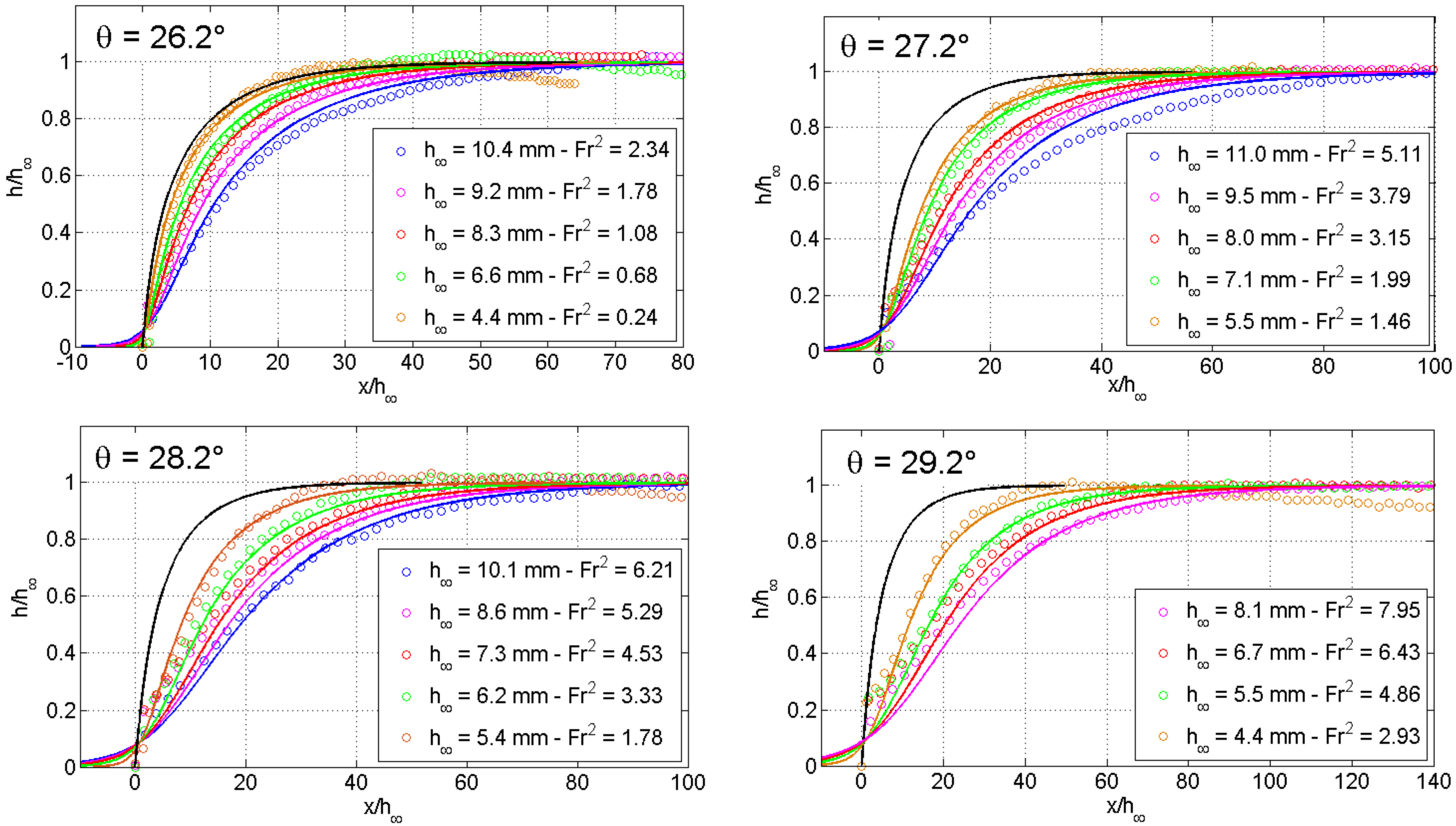

Rescaled granular profiles: comparison between experiments and analytical predictions for different inclinations and different thicknesses h_∞. Analytical solutions (colored lines) are calculated by using the thickness h_∞ and the front velocity u_0 measured for each experimental front (colored circles) with a shape factor $\alpha = 5/4$. The analytical solution evaluated for $\alpha = 1$ is plotted in black line.

importance of the up to now neglected inertial effects

Front in Savage Hutter St Venant

with our inclined plane

$$((\alpha-1)Fr^2\frac{h_\infty}{h}+1)\frac{dh}{d\xi}=\tan\theta-\mu(I).$$

unphysical exponential

precursor

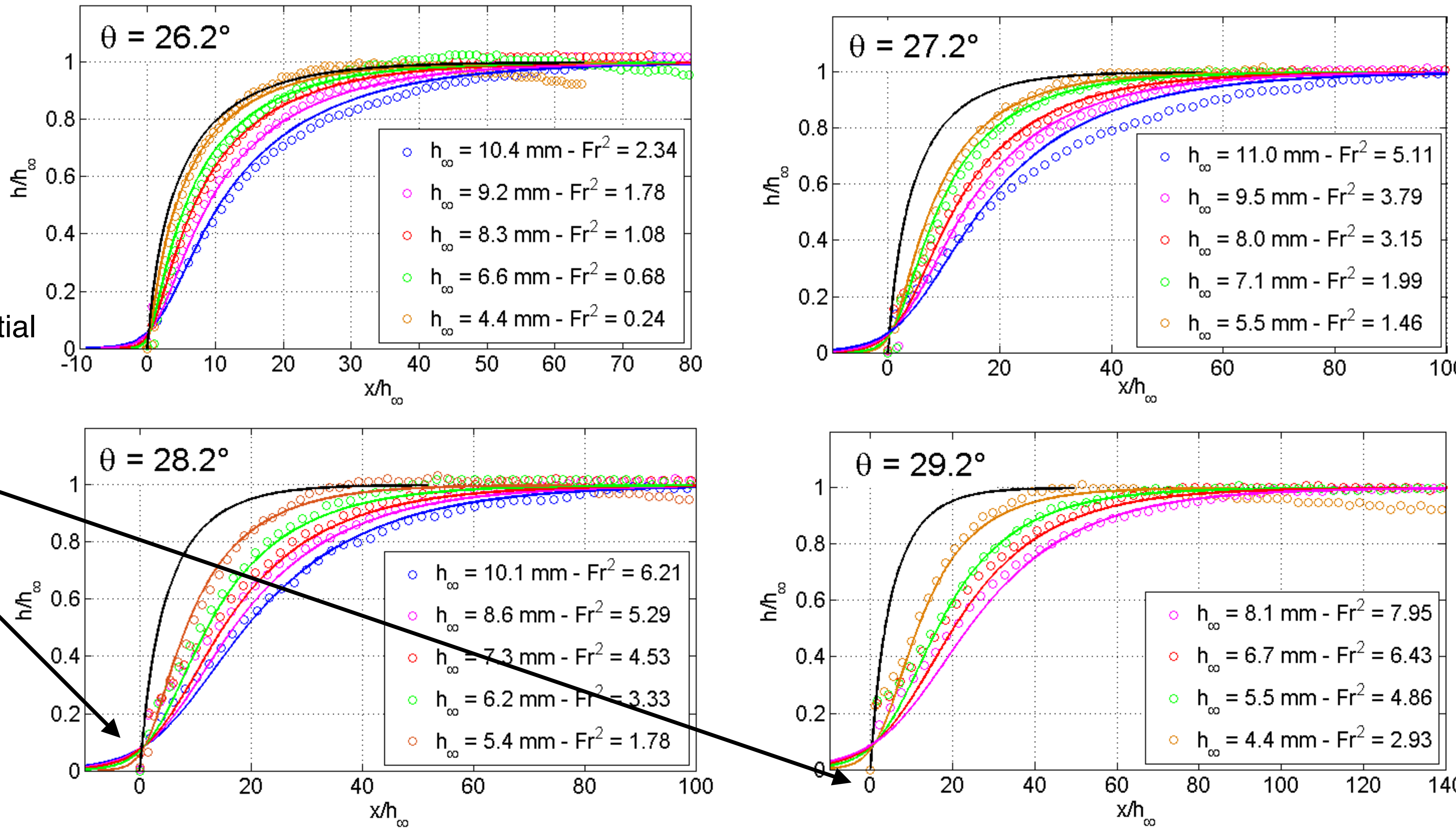

Rescaled granular profiles: comparison between experiments and analytical predictions for different inclinations and different thicknesses h_∞. Analytical solutions (colored lines) are calculated by using the thickness h_∞ and the front velocity u_0 measured for each experimental front (colored circles) with a shape factor $\alpha = 5/4$. The analytical solution evaluated for $\alpha = 1$ is plotted in black line.

importance of the up to now neglected inertial effects

Front in Savage Hutter St Venant

$$\frac{\partial u}{\partial x}+\frac{\partial v}{\partial y}=0$$

$$\frac{\partial u}{\partial t}+\frac{\partial u^2}{\partial x}+\frac{\partial uv}{\partial y}=-g\tan\theta-\frac{\partial p}{\rho\partial x}+\frac{\partial \tau}{\partial y}$$

$$0=-\frac{\partial p}{\rho\partial y}-g$$

numerical resolution of the

full system before averaging

RNSP (Reduced NS Prandtl)

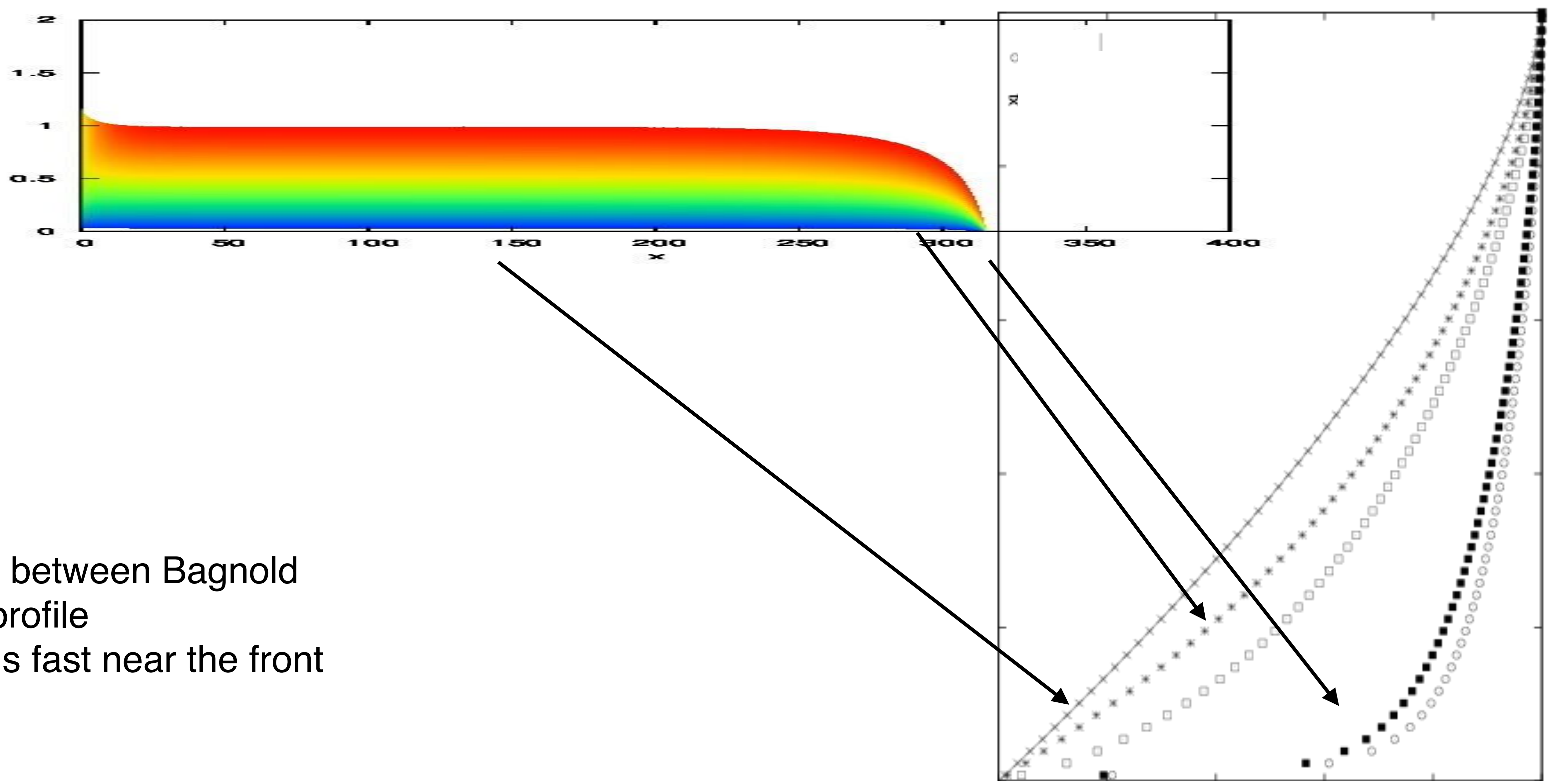

the profile is between Bagnold
and a “flat” profile
the change is fast near the front

Front in Savage Hutter St Venant

$$\frac{\partial u}{\partial x} + \frac{\partial v}{\partial y} = 0$$

$$\frac{\partial u}{\partial t} + \frac{\partial u^2}{\partial x} + \frac{\partial uv}{\partial y} = -g\tan\theta - \frac{\partial p}{\rho \partial x} + \frac{\partial \tau}{\partial y}$$

$$0 = -\frac{\partial p}{\rho \partial y} - g$$

numerical resolution of the

full system before averaging

RNSP (Reduced NS Prandtl)

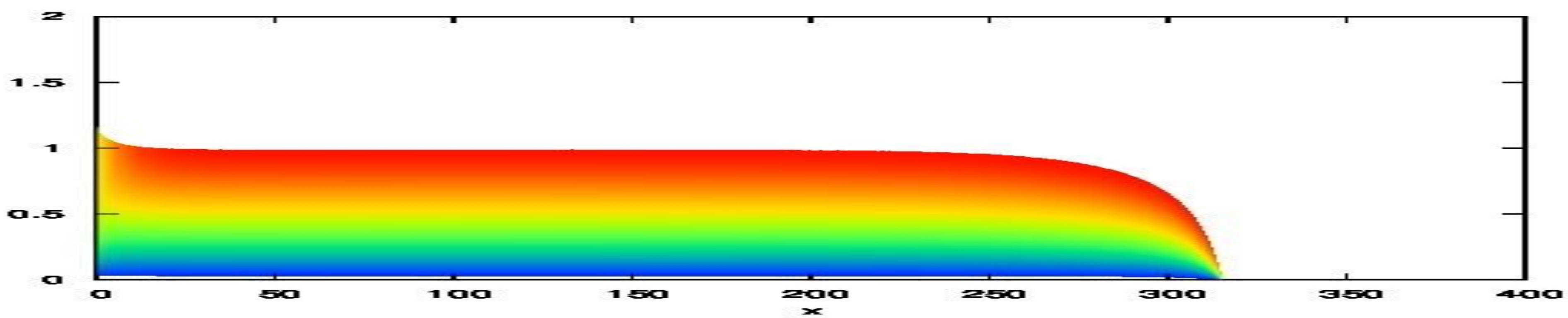

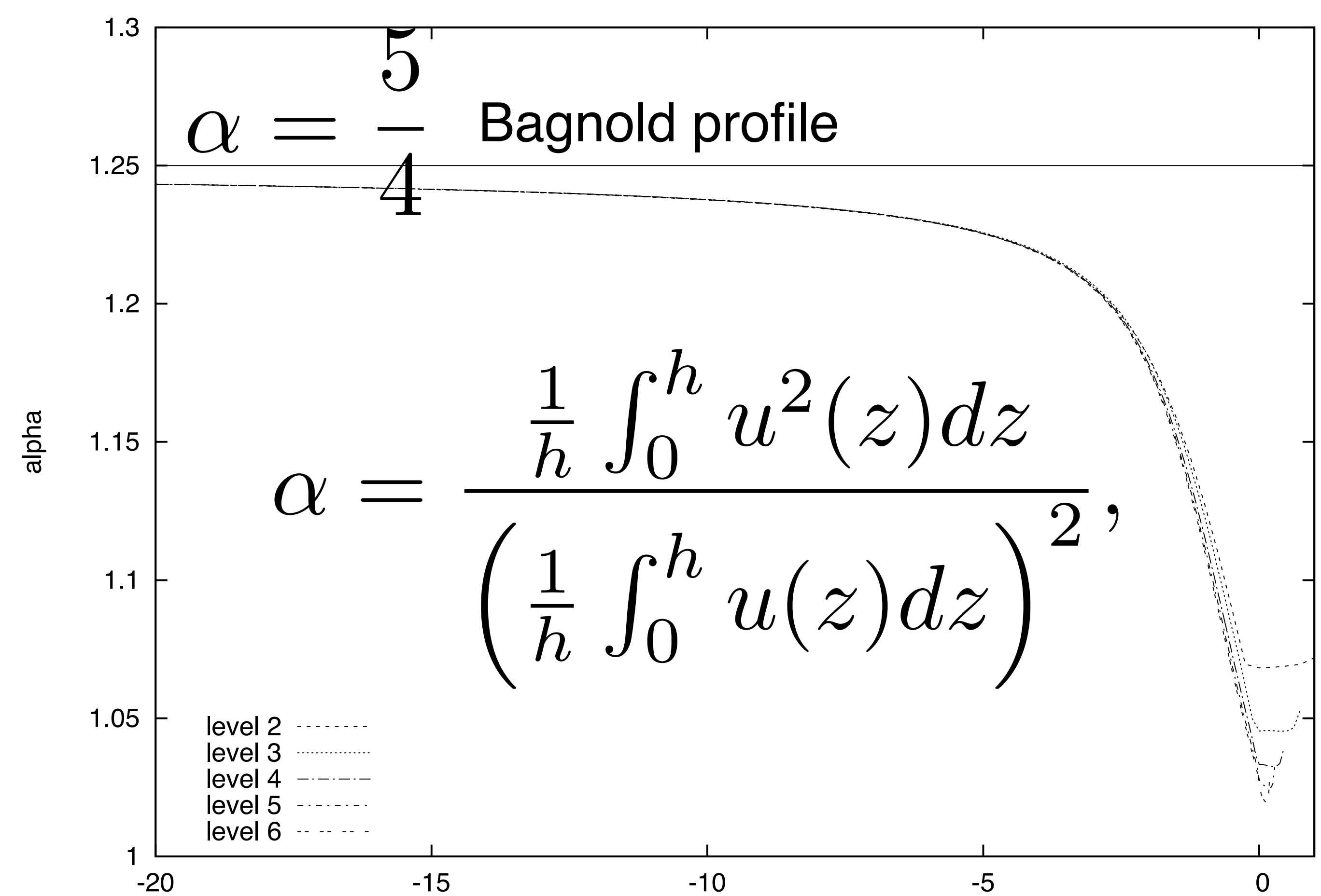

$$\alpha = \frac{5}{4}$$ Bagnold profile

$$\alpha = \frac{\frac{1}{h}\int_0^h u^2(z)dz}{\left(\frac{1}{h}\int_0^h u(z)dz\right)^2},$$

$$\alpha = 1$$

compute the shape factor:

the profile is between Bagnold
and a “flat” profile
the change is fast near the front

Front in Savage Hutter St Venant

$$\frac{\partial u}{\partial x} + \frac{\partial v}{\partial y} = 0$$

$$\frac{\partial u}{\partial t} + \frac{\partial u^2}{\partial x} + \frac{\partial uv}{\partial y} = -g\tan\theta - \frac{\partial p}{\rho \partial x} + \frac{\partial \tau}{\partial y}$$

$$0 = -\frac{\partial p}{\rho \partial y} - g$$

numerical resolution of the

full system before averaging

RNSP (Reduced NS Prandtl)

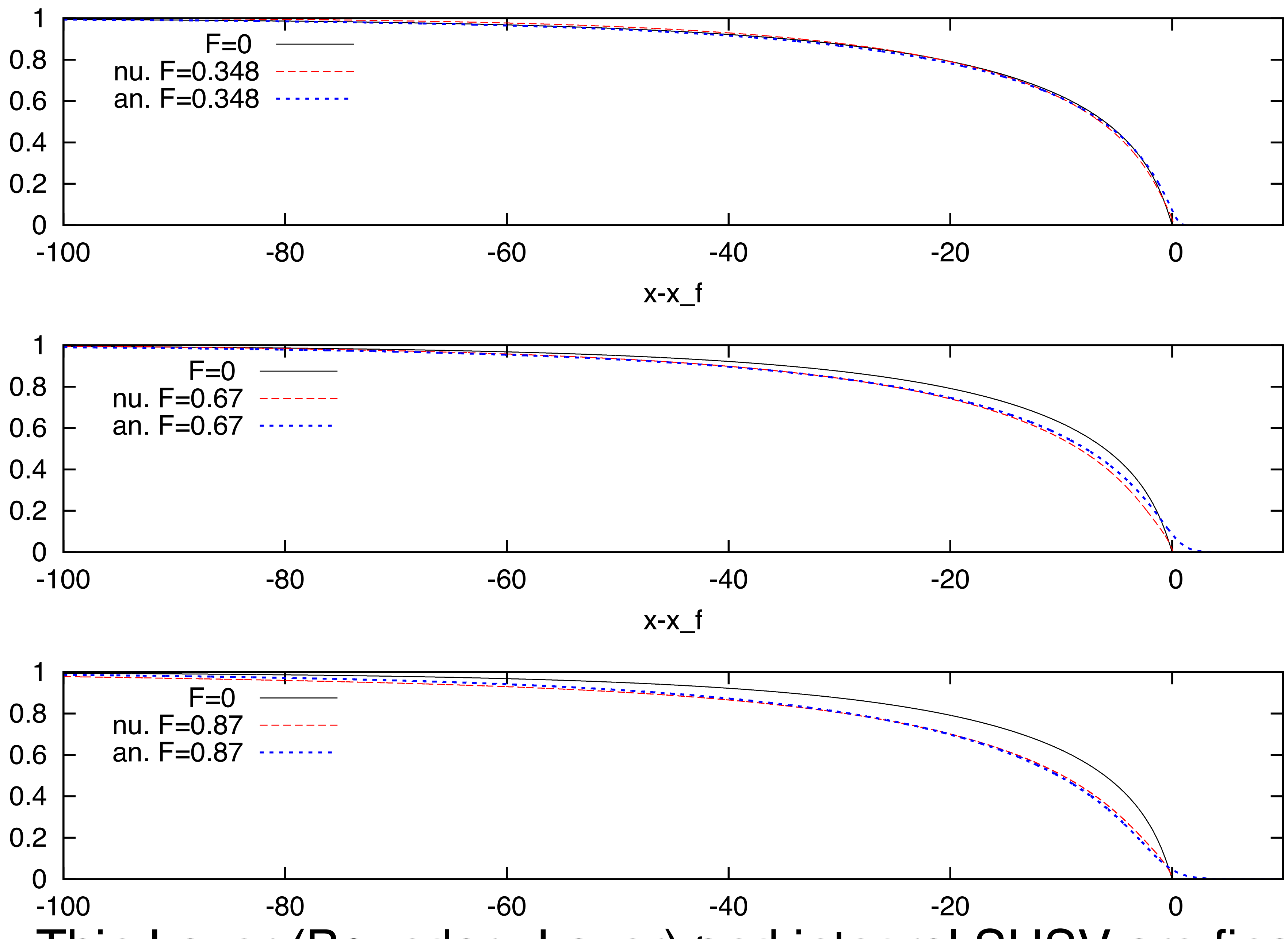

compared

with F=0/α=1 (SHSV)
with the analytical solution F/α=5/4

Thin Layer (Boundary Layer) and integral SHSV are finally very close
there is a noticeable effect of inertia

Front in Savage Hutter St Venant

$$\frac{\partial u}{\partial x} + \frac{\partial v}{\partial y} = 0$$

$$\frac{\partial u}{\partial t} + \frac{\partial u^2}{\partial x} + \frac{\partial uv}{\partial y} = -g\tan\theta - \frac{\partial p}{\rho \partial x} + \frac{\partial \tau}{\partial y}$$

$$0 = -\frac{\partial p}{\rho \partial y} - g$$

numerical resolution of the

full system before averaging

RNSP (Reduced NS Prandtl)

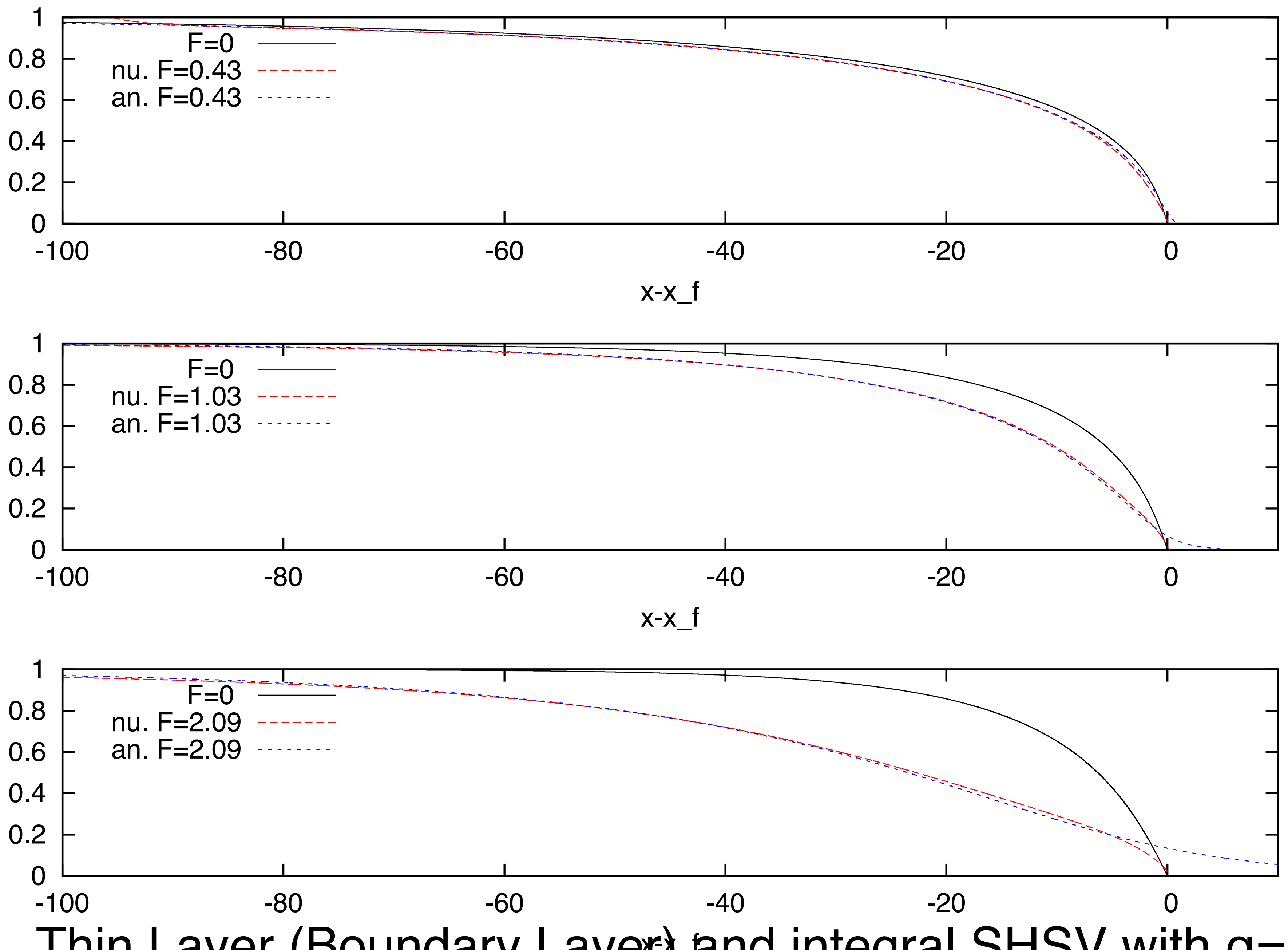

compared

with F=0/α=1 (SHSV)
with the analytical solution F/α=5/4

Thin Layer (Boundary Layer) and integral SHSV with α=5/4 are finally very close
there is a noticeable effect of inertia

Front in Savage Hutter St Venant

- implementing the $\mu(I)$ friction law in Shallow Water (SVSH)
  - friction is only at the bottom
  - pay attention to the shape factor: should be $\alpha=5/4$
  - but: $\alpha=1$ in the SVSH for Galilean invariance and entropy

- Widely used in geophysics with $\alpha=1$

- 1 D model

Go now to grains (contact dynamics) vs full Navier Stokes

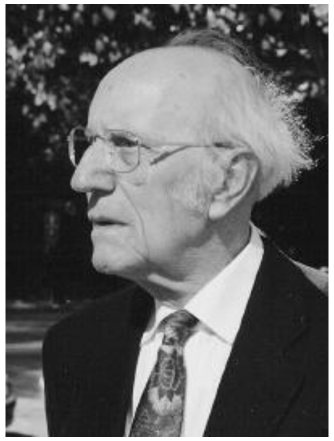

Jean-Jacques Moreau
1923-2014

Contact Dynamics 1988

- Direct simulation of movement of thousands of grains

take the form of an equality between the change of momentum and the average impulse during δt.

Newton's law

$$m(\overrightarrow{U}^+ - \overrightarrow{U}^-) = \overrightarrow{F}\delta t$$

written for each grain at the contact

u_n, u_t

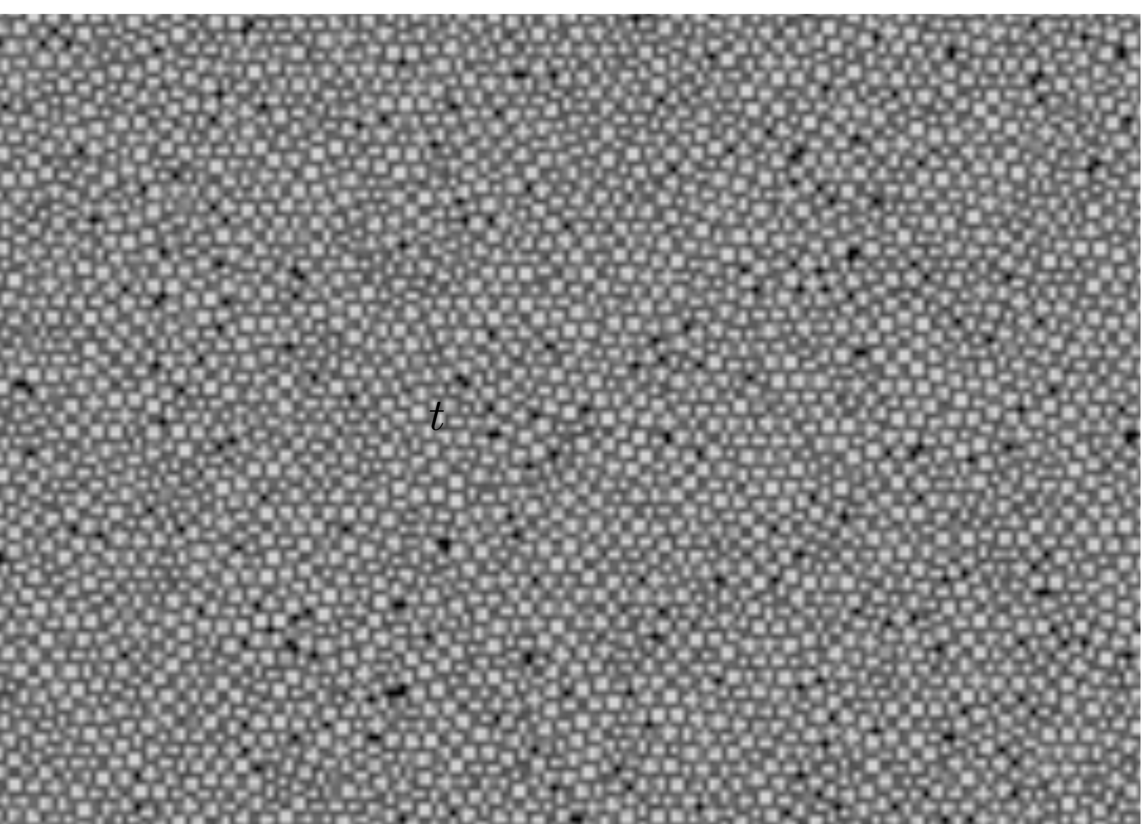

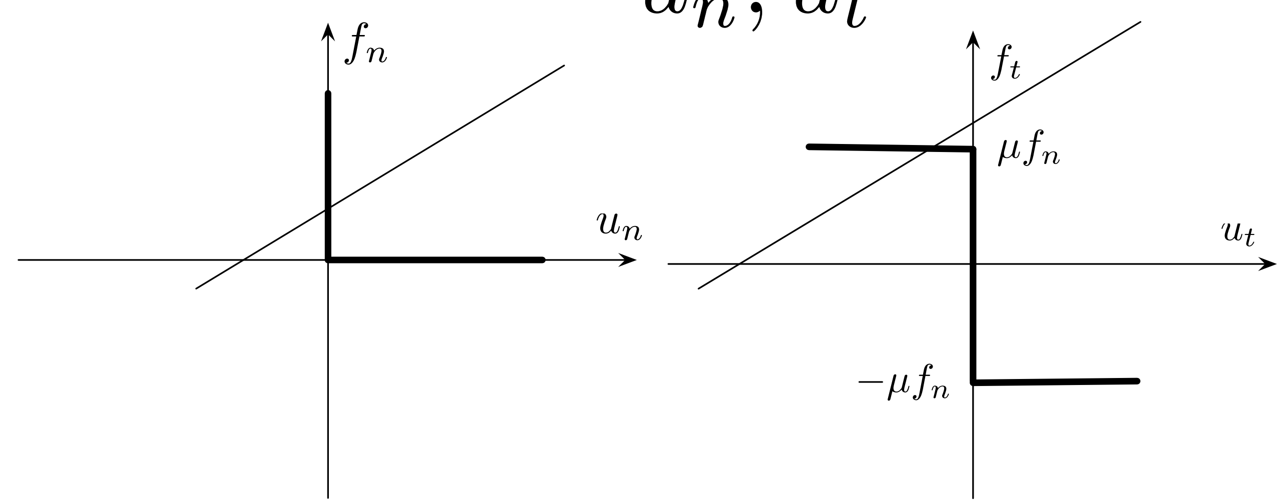

With Lydie Staron

General formulation

Non newtonian flows:
local constitutive law

(Stokesian or Reiner Rivlin)

$$\sigma_{ij} = f(D_{ij})$$

With strain rate tensor

$$D_{ij} = \frac{u_{i,j} + u_{j,i}}{2}$$

second invariant of strain rate tensor

$$D_2 = \sqrt{D_{ij} D_{ij}}$$

first order fluids
(linear Stokesian or linear Reiner Rivlin)

$$\sigma_{ij} = -p\delta_{ij} + 2\eta(D_2)D_{ij}$$

tensorial formulation

$$\tau_{ij} = 2(\eta(D_2))D_{ij}$$

simple form $\dot{\gamma} = \frac{\partial u}{\partial y}$

$$\tau = \left(\eta(\frac{\partial u}{\partial y})\right)\frac{\partial u}{\partial y}$$

General formulation

classic formulation

$$\tau = \mu p$$

practical formulation

$$\tau = \left(\frac{\mu p}{\frac{\partial u}{\partial y}} \right) \frac{\partial u}{\partial y}$$

$$\tau = \left(\eta(\frac{\partial u}{\partial y}) \right) \frac{\partial u}{\partial y}$$

$$\sigma_{ij} = f(D_{ij})$$

With strain rate tensor

$$D_{ij} = \frac{u_{i,j} + u_{j,i}}{2}$$

second invariant of strain rate tensor

$$D_2 = \sqrt{D_{ij} D_{ij}}$$

$$\sigma_{ij} = -p\delta_{ij} + 2\eta(D_2) D_{ij}$$

tensorial formulation

$$\tau_{ij} = 2(\eta(D_2)) D_{ij}$$

$$\eta = \left(\frac{\mu(I)}{\sqrt{2} D_2} p \right)$$

$$\mu(I) = \mu_1 + \frac{\mu_2 - \mu_1}{I_0/I + 1}$$

$\mu_1 \simeq 0.32 \quad (\mu_2 - \mu_1) \simeq 0.23 \quad I_0 \simeq 0.3$

$$I = d\sqrt{2} D_2 / \sqrt{(|p|/\rho)}.$$

Implementation in *Basilisk* flow solver?

$$\sigma_{ij} = -p\delta_{ij} + 2\eta(D_2)D_{ij}$$

$$D_2 = \sqrt{D_{ij}D_{ij}} \qquad D_{ij} = \frac{u_{i,j} + u_{j,i}}{2} \qquad \eta = \left(\frac{\mu(I)}{\sqrt{2}D_2}p\right)$$

construction of a viscosity based on the D_2 invariant and redefinition of I

$$\eta = \min(\eta_{max}, \max\left(\eta(D_2)\ ,\ 0\right)) \qquad I = d\sqrt{2}D_2/\sqrt{(|p|/\rho)}.$$

- the «min» limits viscosity to a large constant value
- always flow, even slowl

Boundary Conditions: no slip and *p=0* at the interface for μ(I)

Implementation in *Basilisk* flow solver?

$$\sigma_{ij} = -p\delta_{ij} + 2\eta(D_2)D_{ij}$$

$$D_2 = \sqrt{D_{ij}D_{ij}} \qquad D_{ij} = \frac{u_{i,j} + u_{j,i}}{2} \qquad \eta = \left(\frac{\mu(I)}{\sqrt{2}D_2}p\right)$$

construction of a viscosity based on the D_2 invariant and redefinition of I

$$\eta = \min(\eta_{max}, \max\left(\eta(D_2)\ ,\ 0\right)) \qquad I = d\sqrt{2}D_2/\sqrt{(|p|/\rho)}.$$

- the «min» limits viscosity to a large constant value
- always flow, even slowl

Boundary Conditions: no slip and $p=0$ at the interface for μ(I)

Implementation in *Basilisk* flow solver?

$$\sigma_{ij} = -p\delta_{ij} + 2\eta(D_2)D_{ij}$$

$$D_2 = \sqrt{D_{ij}D_{ij}} \qquad D_{ij} = \frac{u_{i,j} + u_{j,i}}{2} \qquad \eta = \left(\frac{\mu(I)}{\sqrt{2}D_2}p\right)$$

construction of a viscosity based on the D_2 invariant and redefinition of I

$$\eta = \min(\eta_{max}, \max\left(\eta(D_2)\ ,\ 0\right)) \qquad I = d\sqrt{2}D_2/\sqrt{(|p|/\rho)}.$$

Volume Of Fluids, projection method, finite volumes

$$\nabla\cdot\mathbf{u} = 0, \;\; \rho\left(\frac{\partial\mathbf{u}}{\partial t} + \mathbf{u}\cdot\nabla\mathbf{u}\right) = -\nabla p + \nabla\cdot(2\eta\mathbf{D}) + \rho g,$$

$$\frac{\partial c}{\partial t} + \nabla\cdot(c\mathbf{u}) = 0, \;\; \rho = c\rho_1 + (1-c)\rho_2, \;\; \eta = c\eta_1 + (1-c)\eta_2$$

The granular fluid is covered by a passive light fluid (it allows for a zero pressure boundary condition at the surface, bypassing an up to now difficulty which was to impose this condition on a unknown moving boundary).

Boundary Conditions: no slip and $p=0$ at the interface for μ(I)

Implementation in *Basilisk* flow solver?

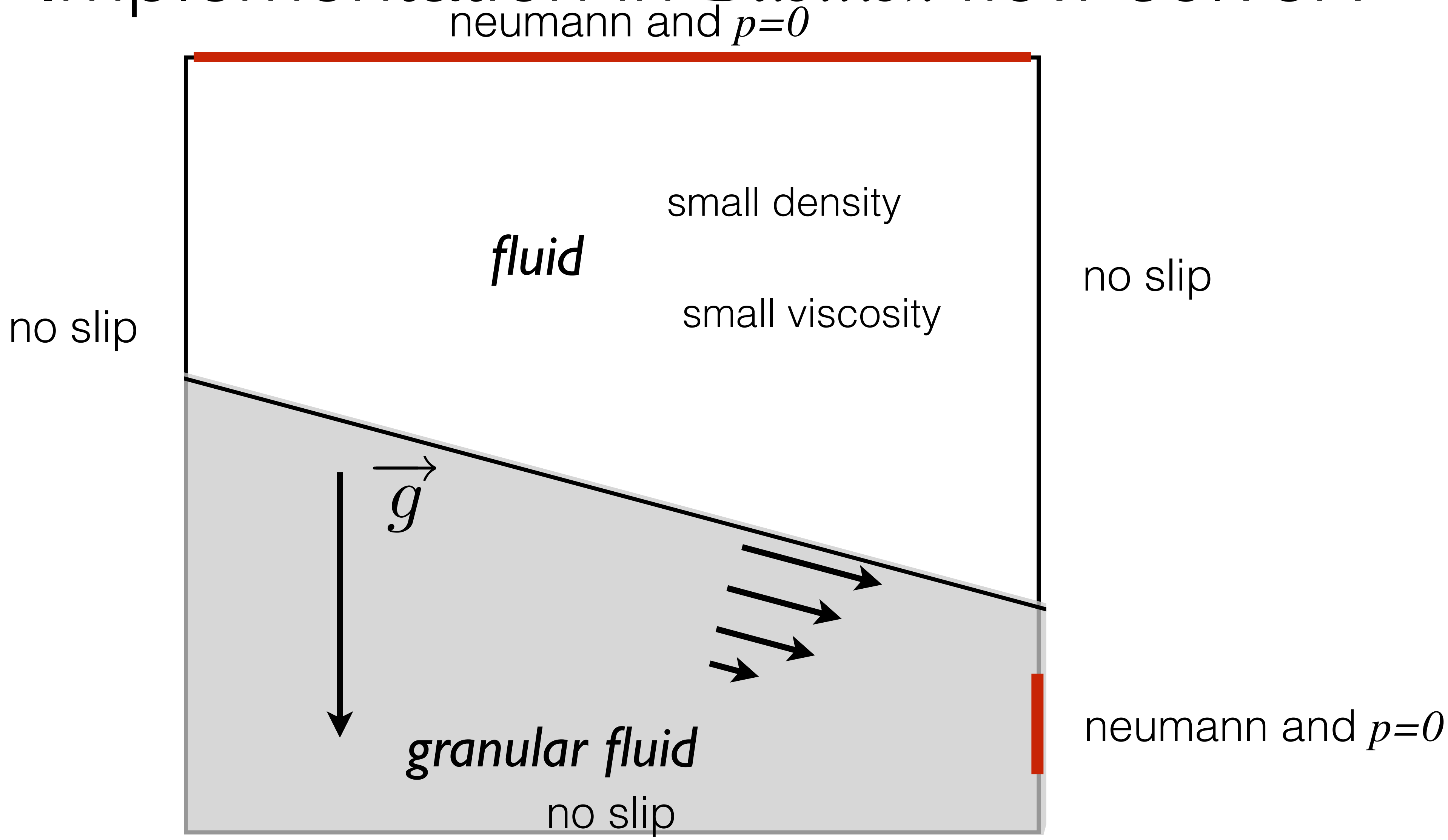

Volume Of Fluids, projection method, finite volumes

$$\nabla \cdot \mathbf{u} = 0, \quad \rho \left(\frac{\partial \mathbf{u}}{\partial t} + \mathbf{u} \cdot \nabla \mathbf{u} \right) = -\nabla p + \nabla \cdot (2\eta \mathbf{D}) + \rho g,$$

$$\frac{\partial c}{\partial t} + \nabla \cdot (c\mathbf{u}) = 0, \quad \rho = c\rho_1 + (1-c)\rho_2, \quad \eta = c\eta_1 + (1-c)\eta_2$$

The granular fluid is covered by a passive light fluid (it allows for a zero pressure boundary condition at the surface, bypassing an up to now difficulty which was to impose this condition on a unknown moving boundary).

Boundary Conditions: no slip and $p=0$ at the interface for μ(I)

Implementations of NS-μ(I)

$$\tau = \left(\frac{\mu p}{\frac{\partial u}{\partial y}}\right)\frac{\partial u}{\partial y}$$

- Lagrée Staron Popinet 2011
- Mangeney, Ionescu, Bouchut, Lusso 2016
- Krabbenhoft 2014
- Dunatunga & Kamrin 2015
- Barker Shaeffer Bohorquez & Gray 2015
- Daviet & Bertails-Descoubes 2016

Implementations of Bingham

$$\tau = \left(\frac{\tau_0}{\frac{\partial u}{\partial y}} + \eta\right)\frac{\partial u}{\partial y}$$

- Liu, Balmforth, Hormozi, Hewitt, 2016,
- Dufour and Pijaudier-Cabotz 2005
- Vinay Wachs, Agassant 2005
- Vola, Babik, Latché 2004

Test of the code: «Bagnold» avalanche

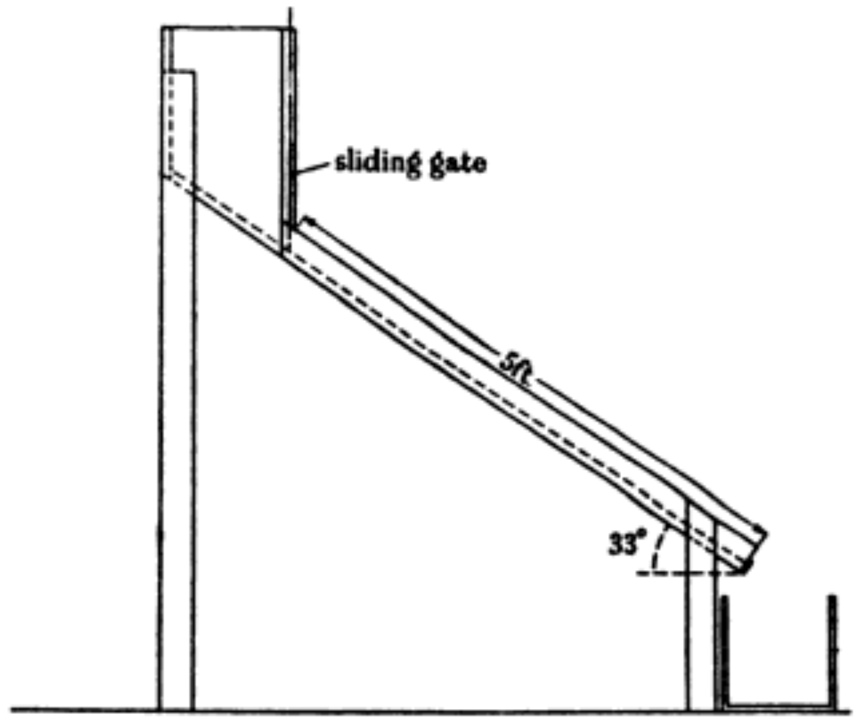

kind of Nuβelt solution

$$T \propto \sigma(\lambda D)^2 \; (dU/dy)^2$$

$$U = \frac{2}{3} \times 0.165 \; (g \sin \beta)^{1/2} \; \frac{y'^{3/2}}{D} \; ,$$

TABLE 1.

flow height Y (cm)	measured speed (cm/sec)	speed, from (9) (cm/sec)	ratio
0.5	17.2	26.4	1.53
0.65	27.5	38.8	1.41
0.75	30.0	48.0	1.6
0.9	39.0	63.0	1.61

Bagnold 1954

http://www.boker.org.il/meida/negev/desert_biking/bagnold/tsoar_paper.htm

Test of the code: «Bagnold» avalanche

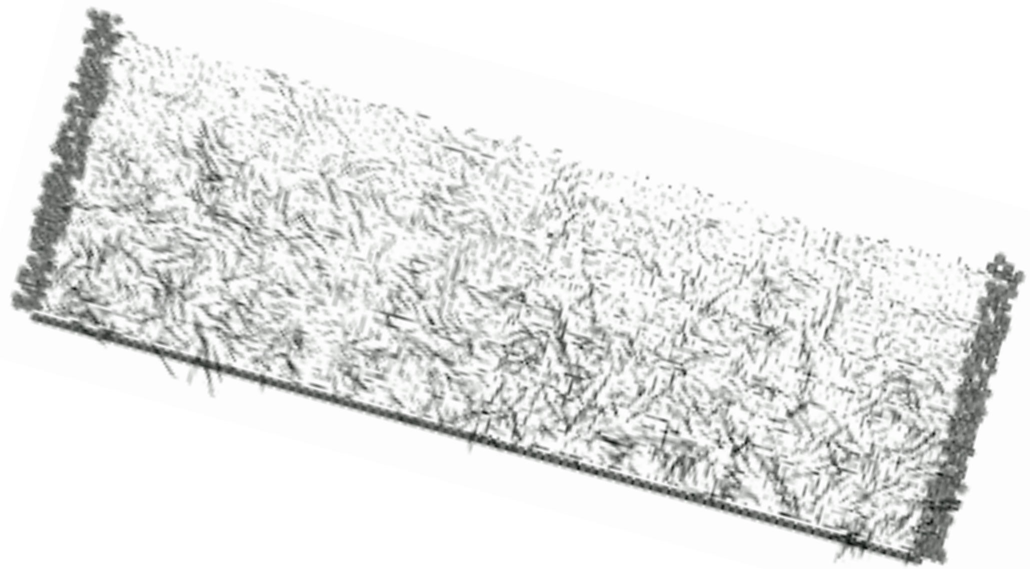

kind of Nusselt film solution
“Half Poiseuille”

Contact Dynamic simulation

Test of the code: «Bagnold» avalanche

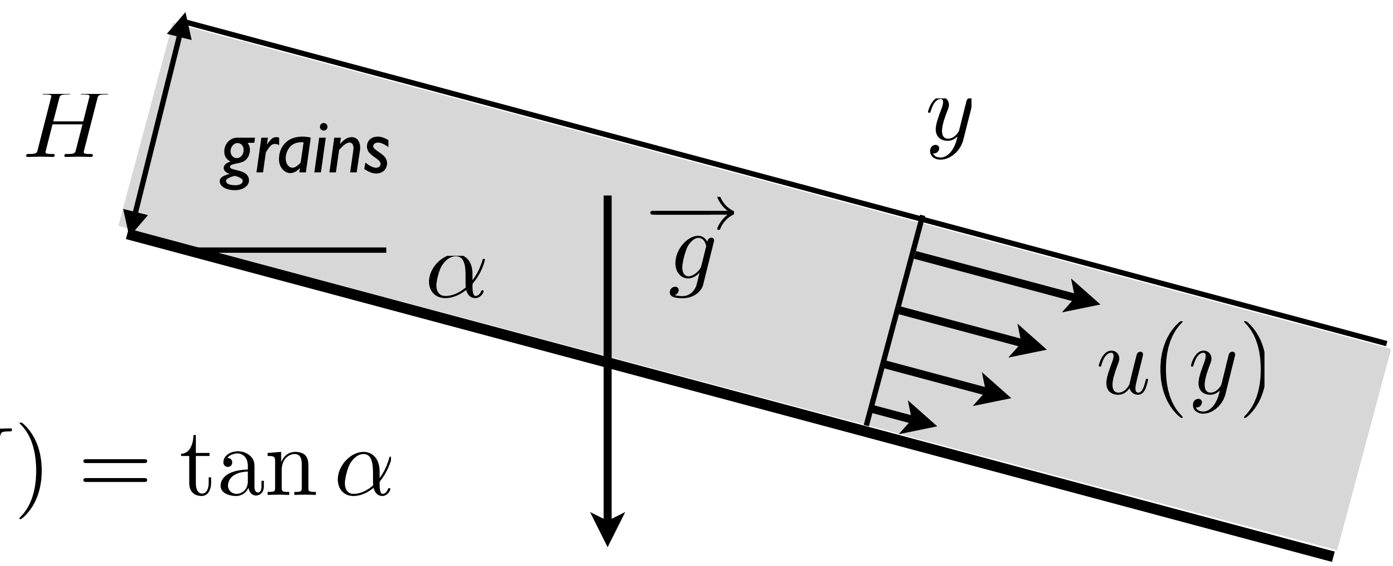

$$\mu(I) = \tan\alpha$$

$$u = \frac{2}{3} I_\alpha \sqrt{g d \cos\alpha \frac{H^3}{d^3}} \left(1 - \left(1 - \frac{y}{H}\right)^{3/2}\right),$$

$$v = 0, \quad p = \rho g H \left(1 - \frac{y}{H}\right)\cos\alpha.$$

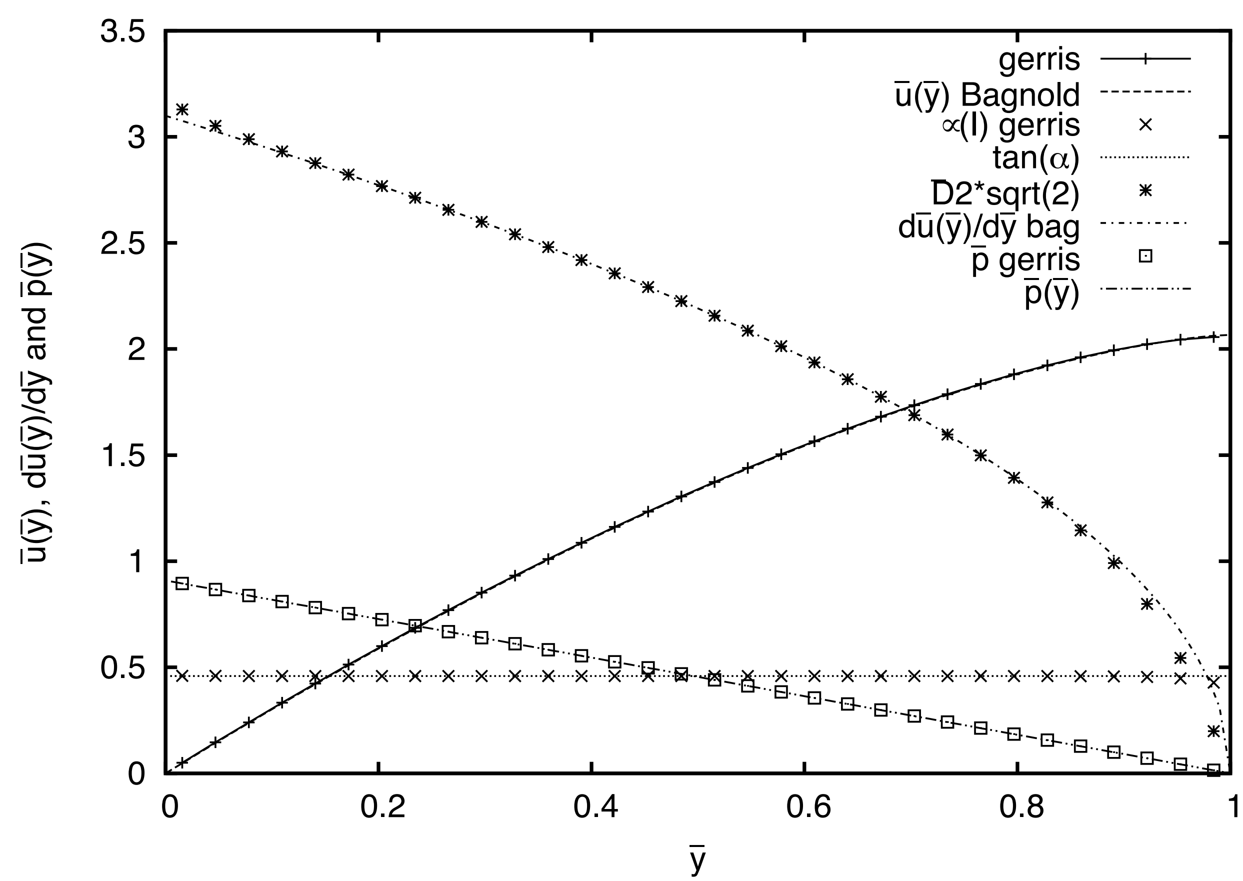

Test of the code: «Bagnold» avalanche

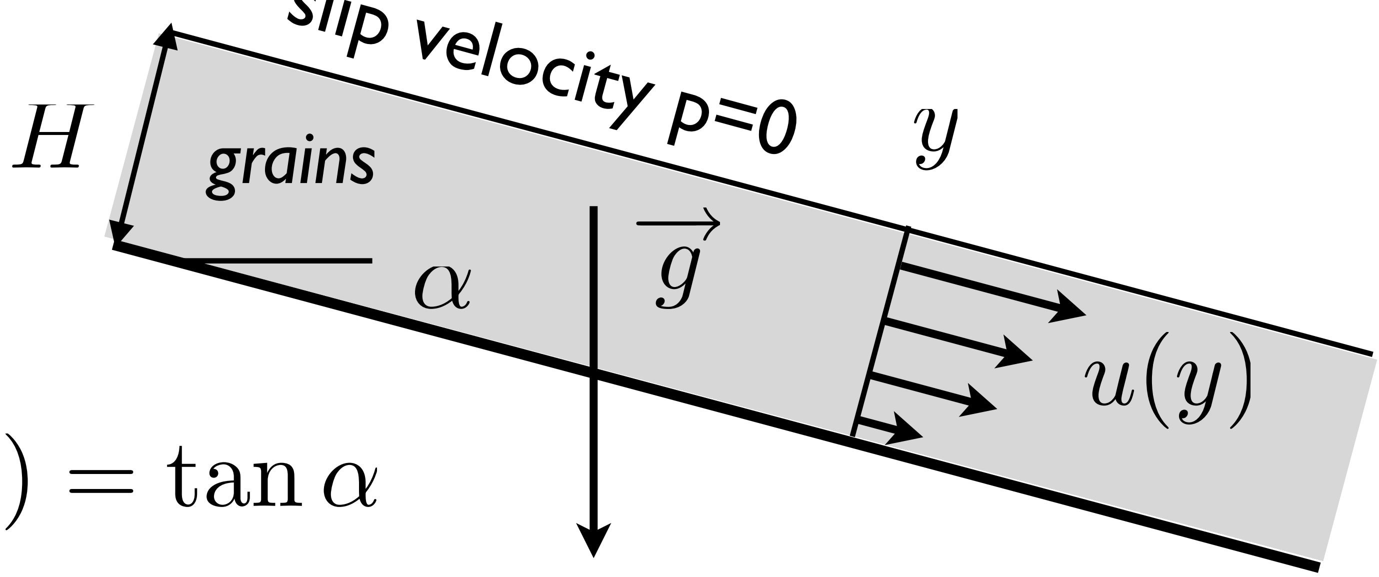

$$\mu(I) = \tan\alpha$$

$$u = \frac{2}{3} I_\alpha \sqrt{gd\cos\alpha \frac{H^3}{d^3}} \left(1 - \left(1 - \frac{y}{H}\right)^{3/2}\right),$$

$$v = 0, \;\; p = \rho g H \left(1 - \frac{y}{H}\right) \cos\alpha.$$

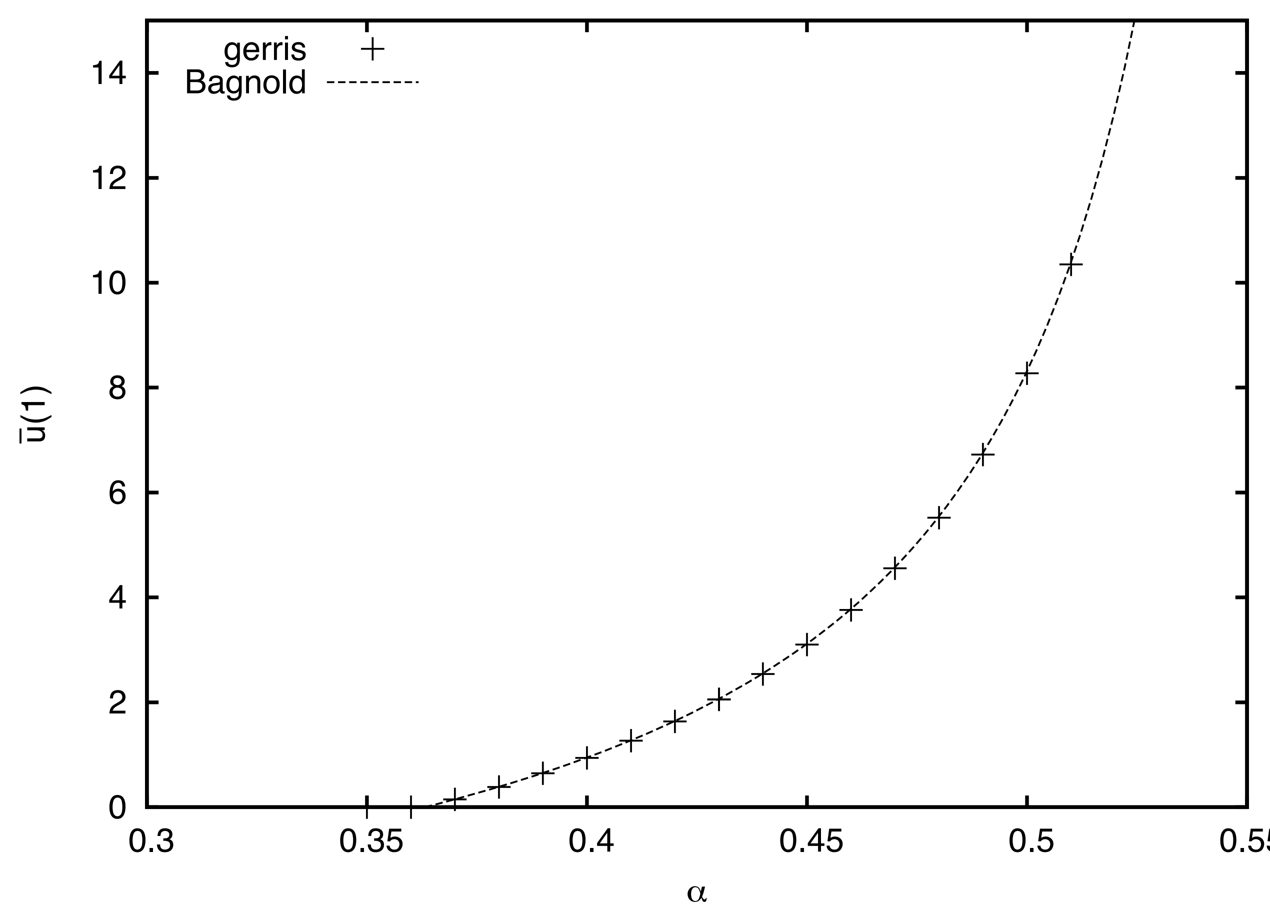

granulars are fluids and solids

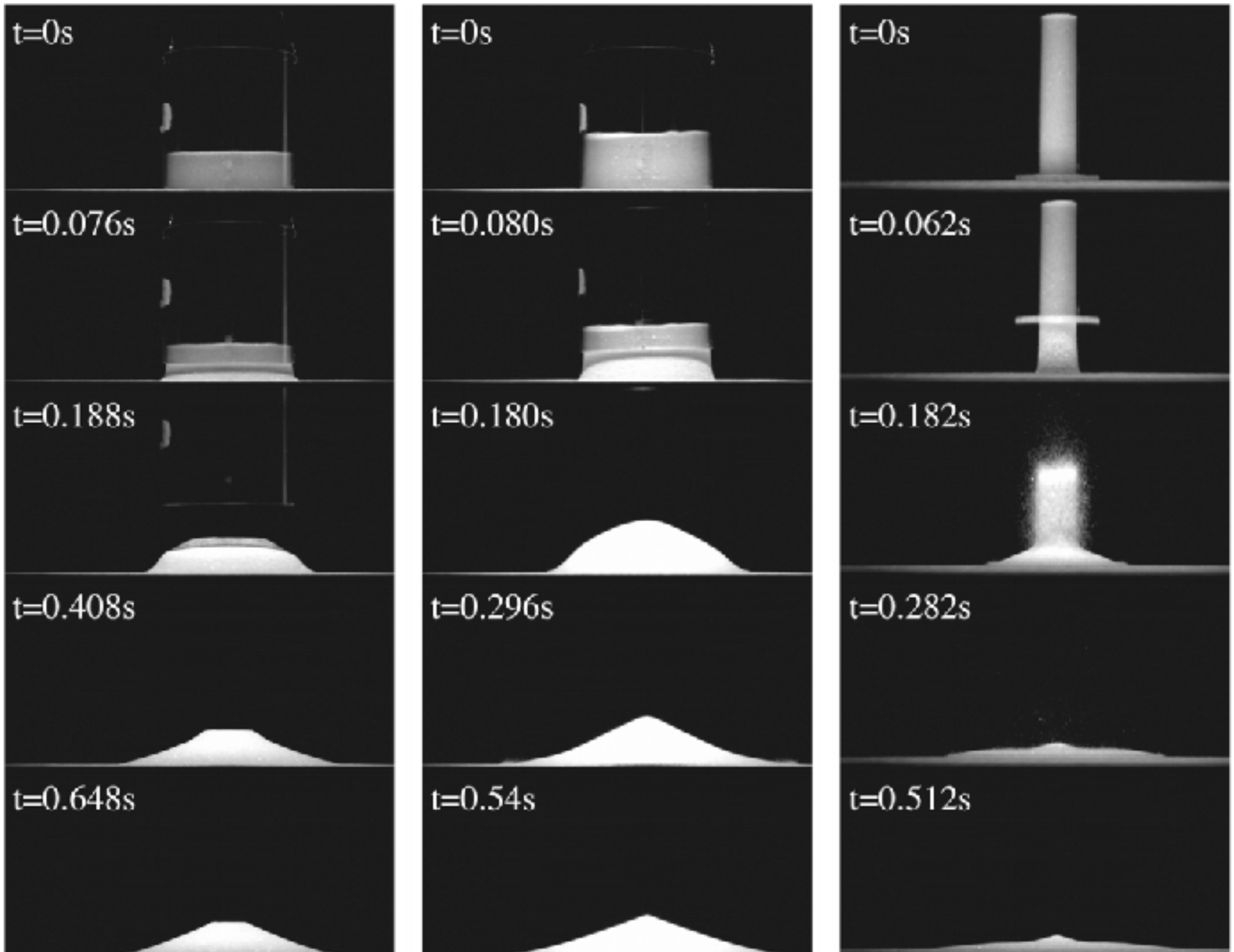

E. Lajeunesse A. Mangeney-Castelnau and J.-P. Vilotte PoF 2005

Granular Column Collapse

aspect ratio $a = H_0/R_0 = H_0/L_0$

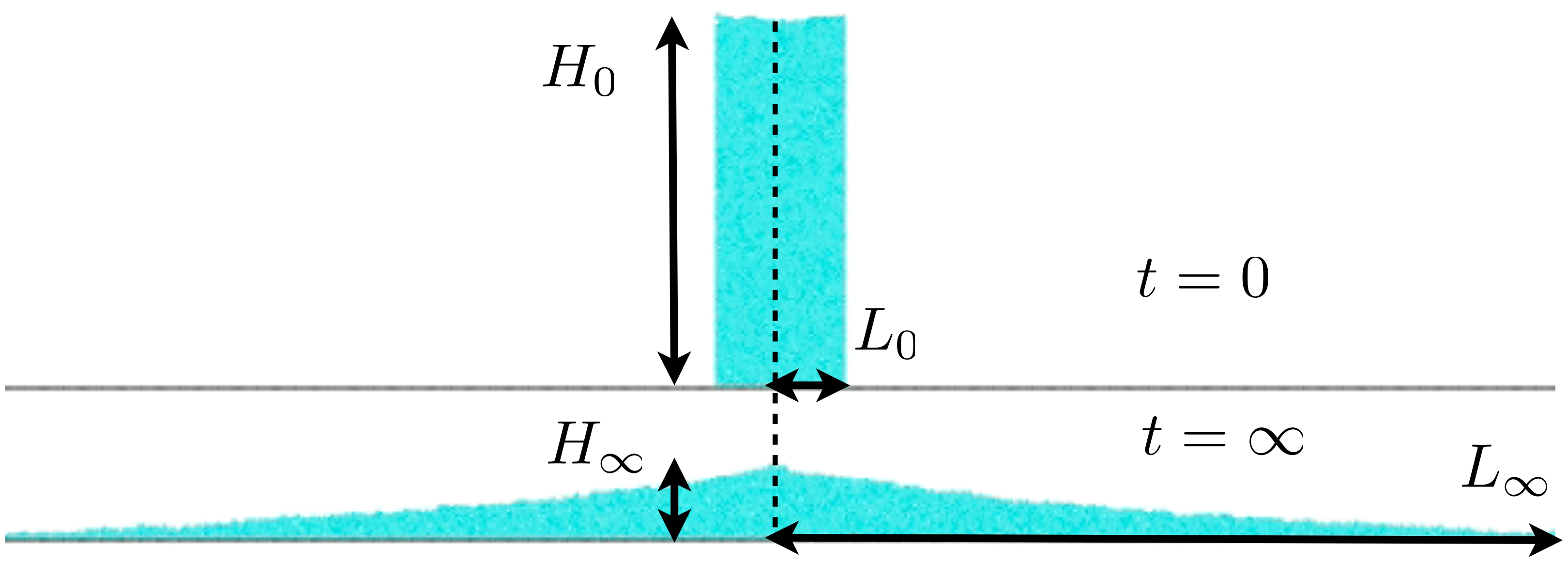

The sand pit problem: quickly remove the bucket of sand

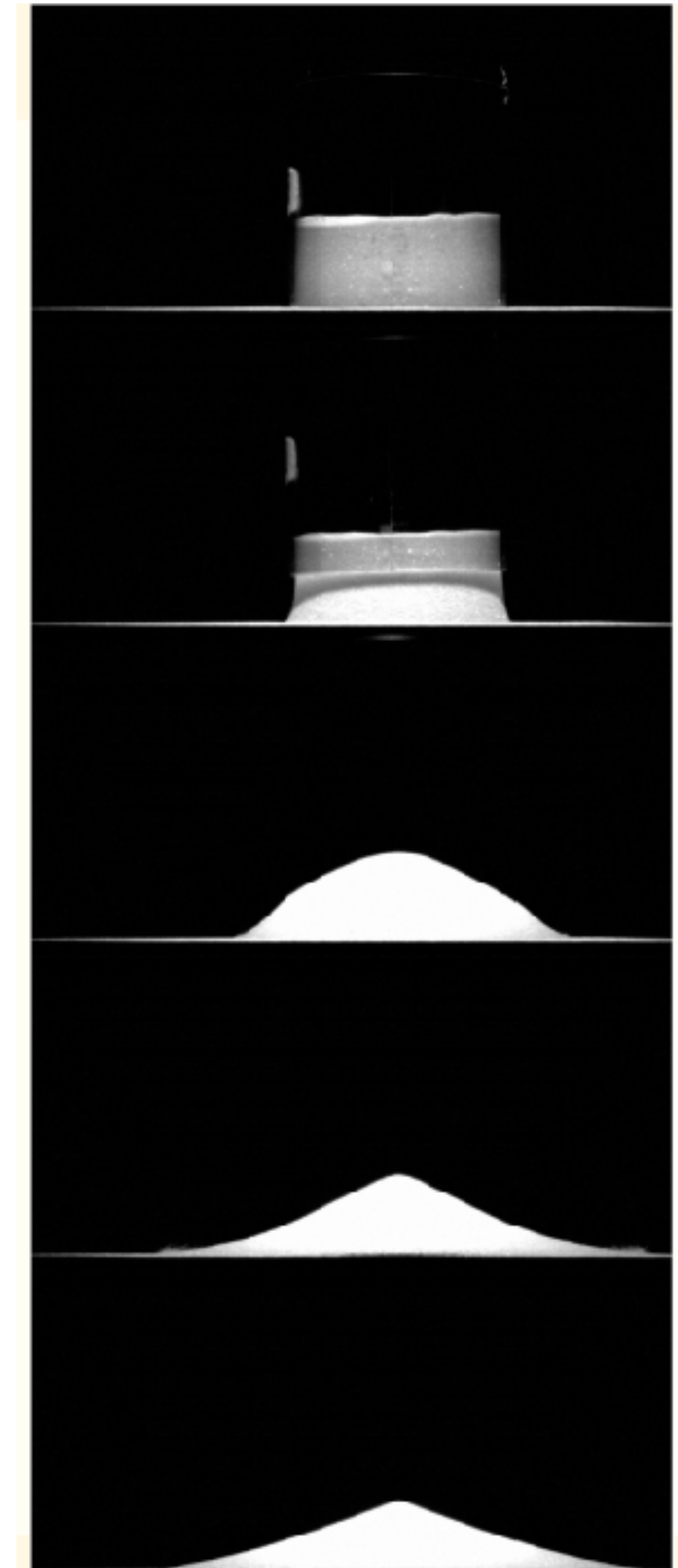

Lajeunesse et al., 2004

Collapse of columns simulation *Basilisk* $\mu(I)$

reproduce Lagrée Staron Popinet 2011

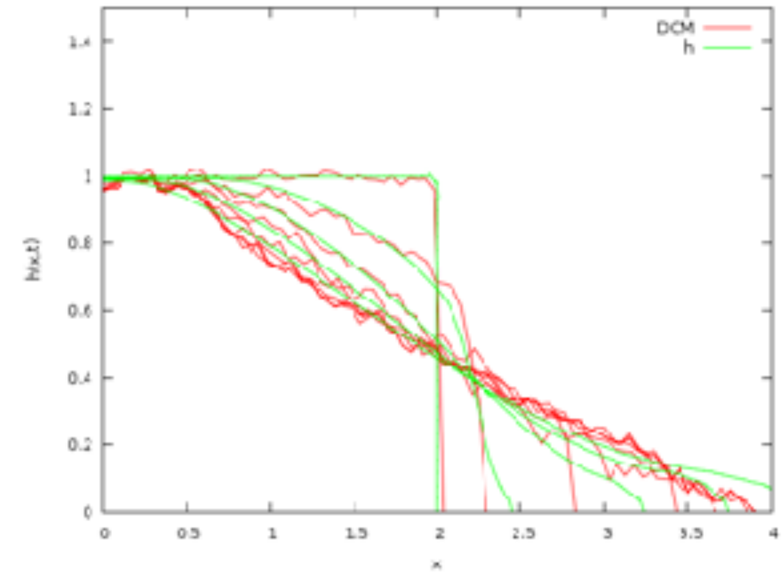

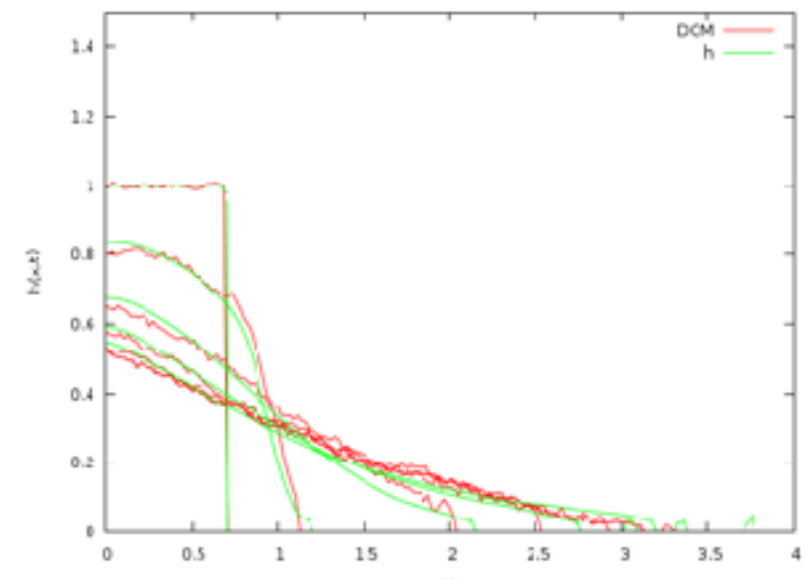

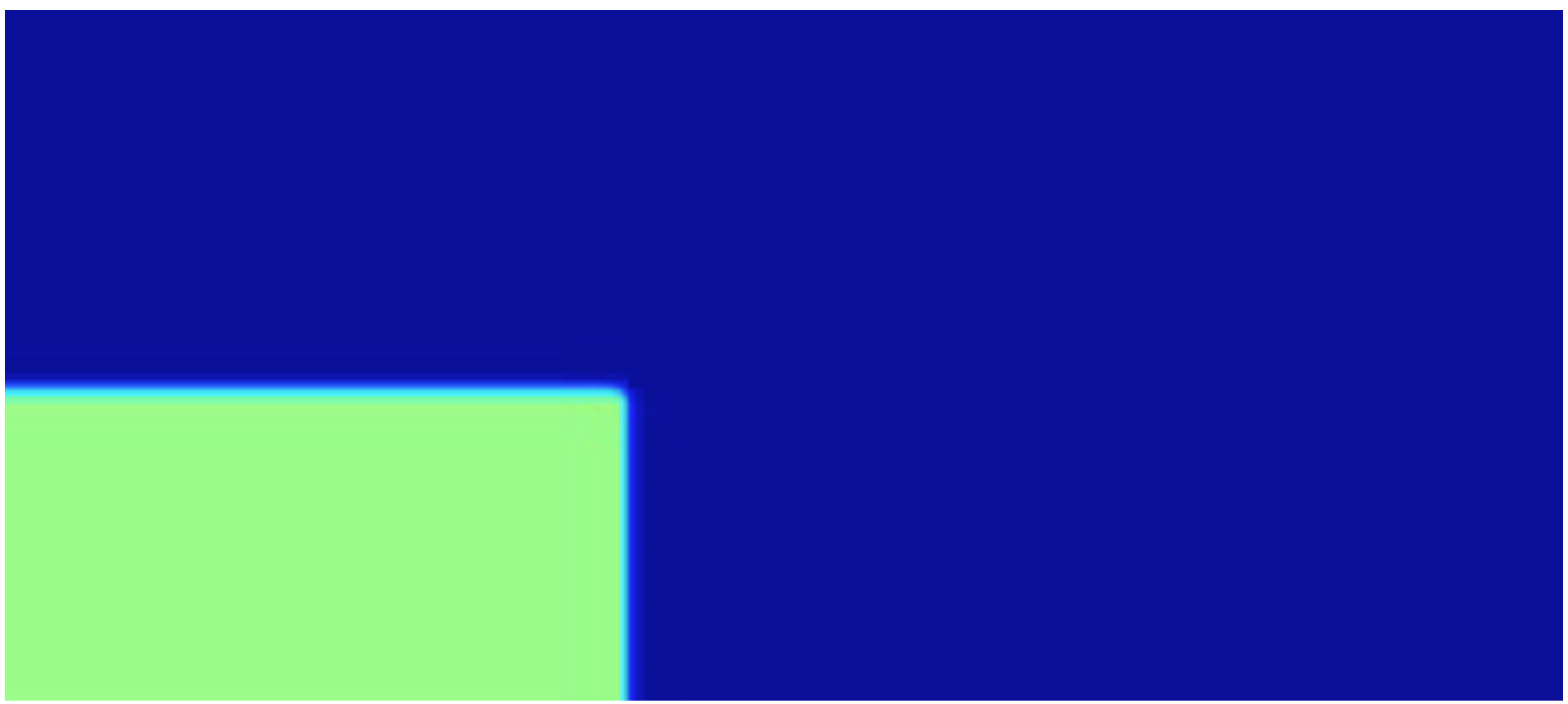

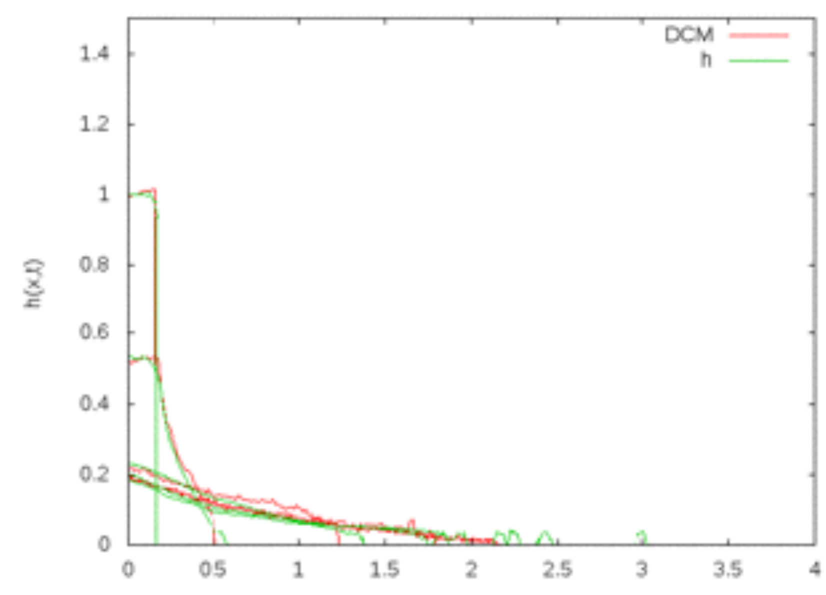

http://basilisk.fr/sandbox/M1EMN/Exemples/granular_column.c

Collapse of columns simulation *Gerris μ(I)*

optimisation

$$\mu(I) = \mu_s + \frac{\Delta\mu}{\frac{I_0}{I} + 1}$$

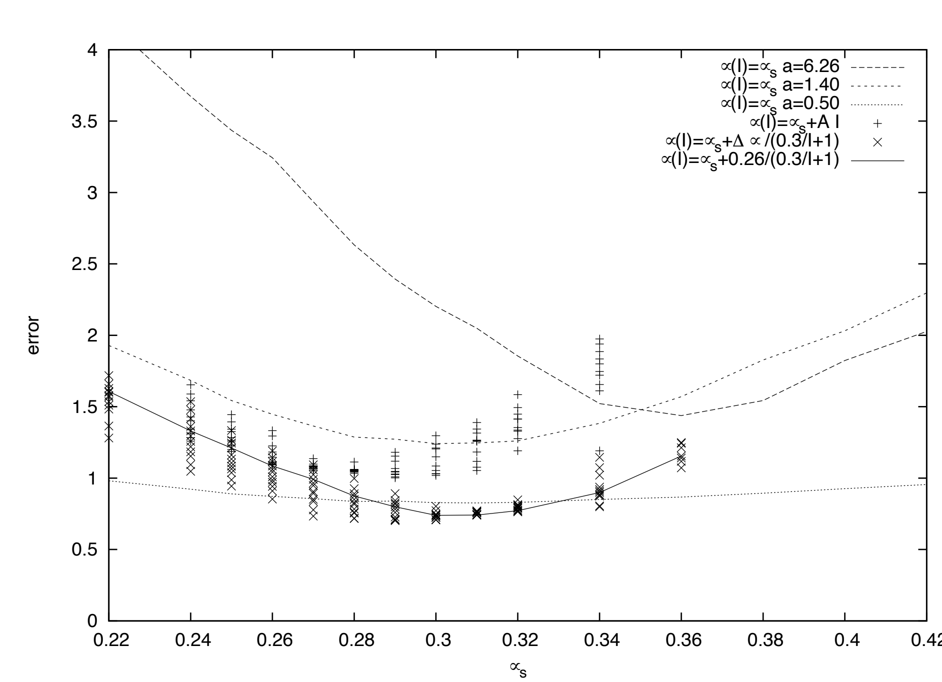

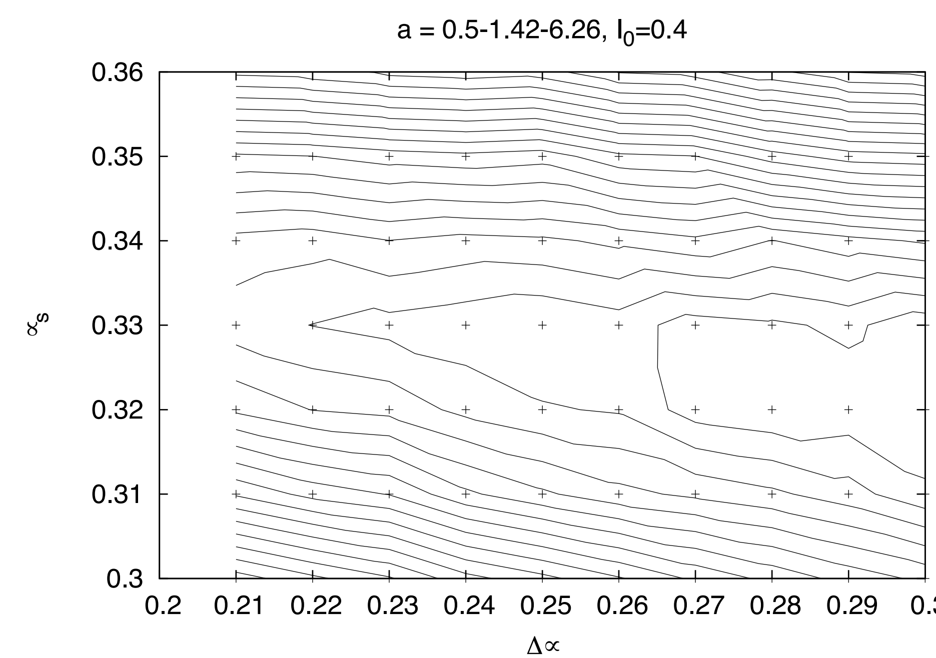

final values

$$\mu_s = 0.32 \ \Delta\mu = 0.28 \ I_0 = 0.4$$

Collapse of columns

$a = 0.5$ DCM vs *μ(I)*

Collapse of columns

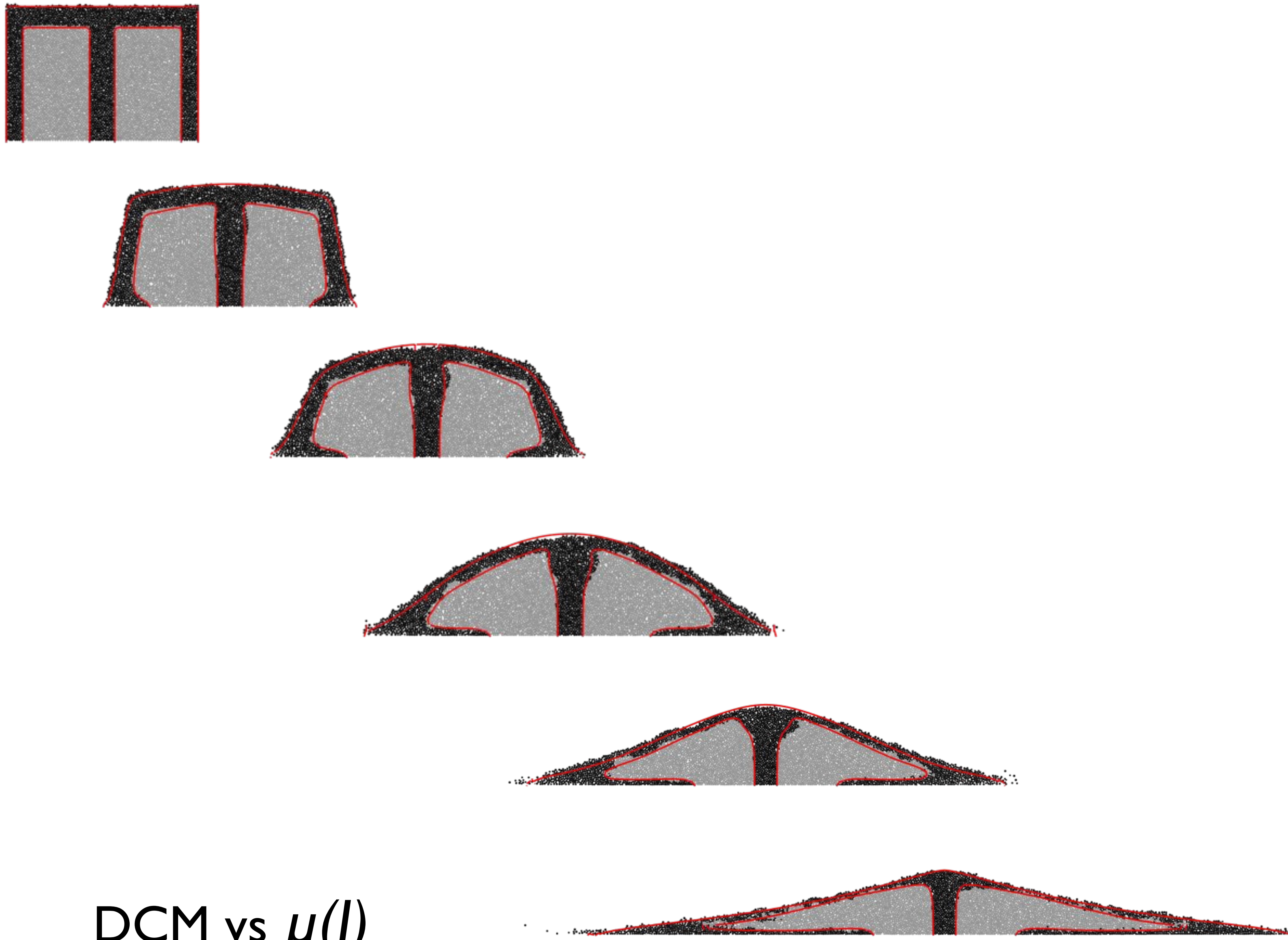

$a = 1.42$ DCM vs *μ(I)*

Collapse of columns

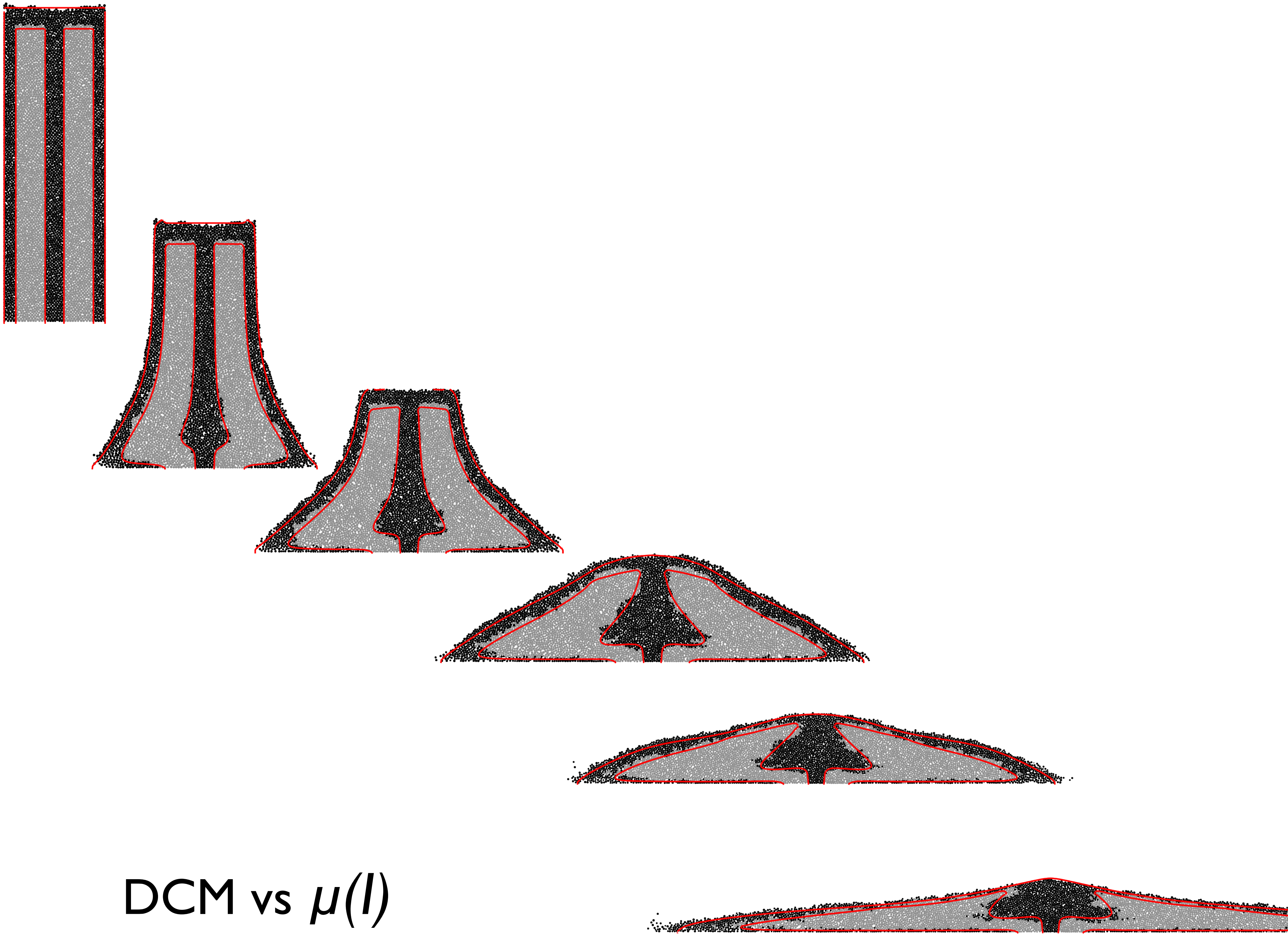

$a = 6.6$

DCM vs *μ(I)*

Collapse of columns

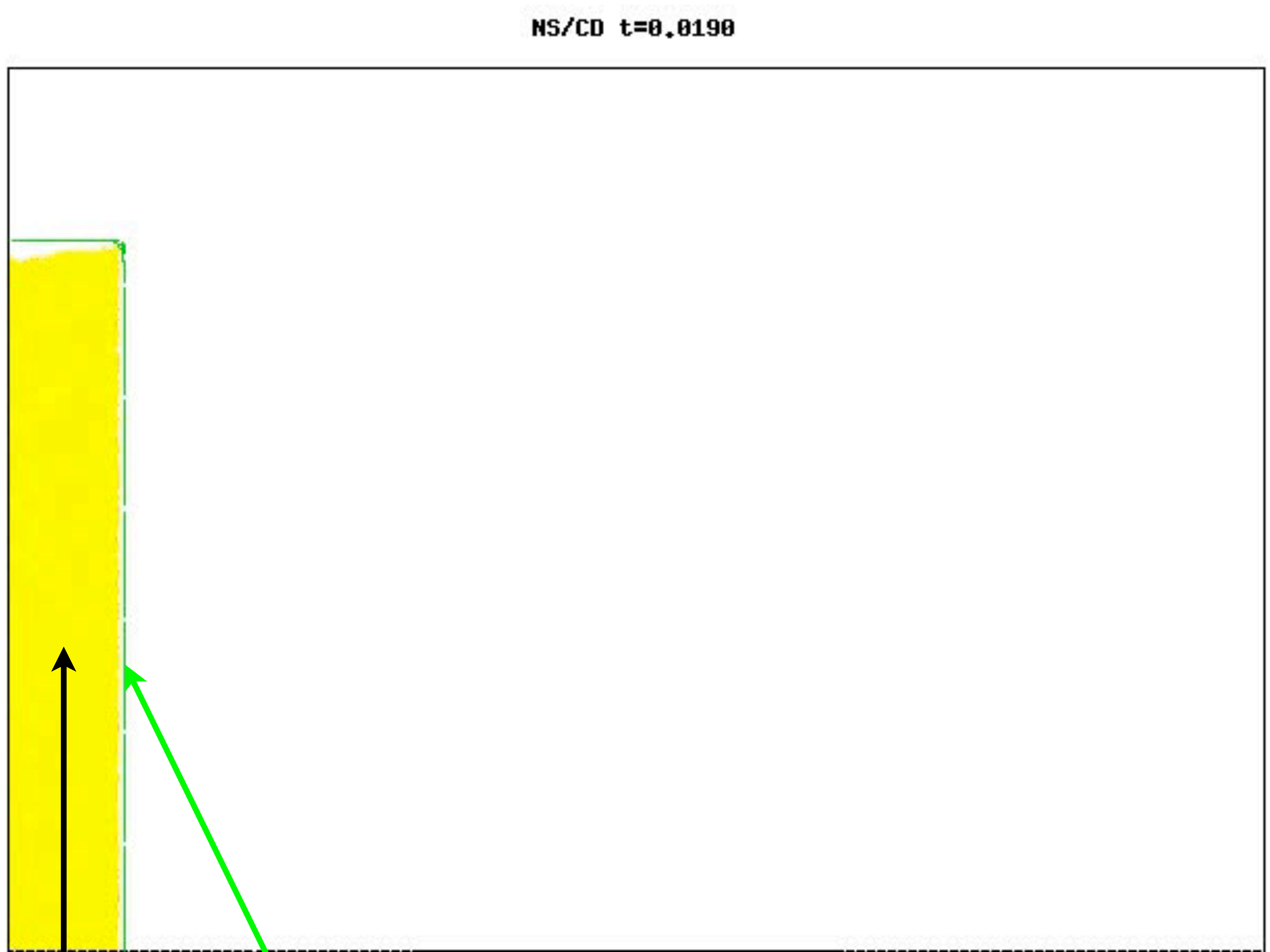

DCM vs Navier Stokes $\mu(I)$

Collapse of columns

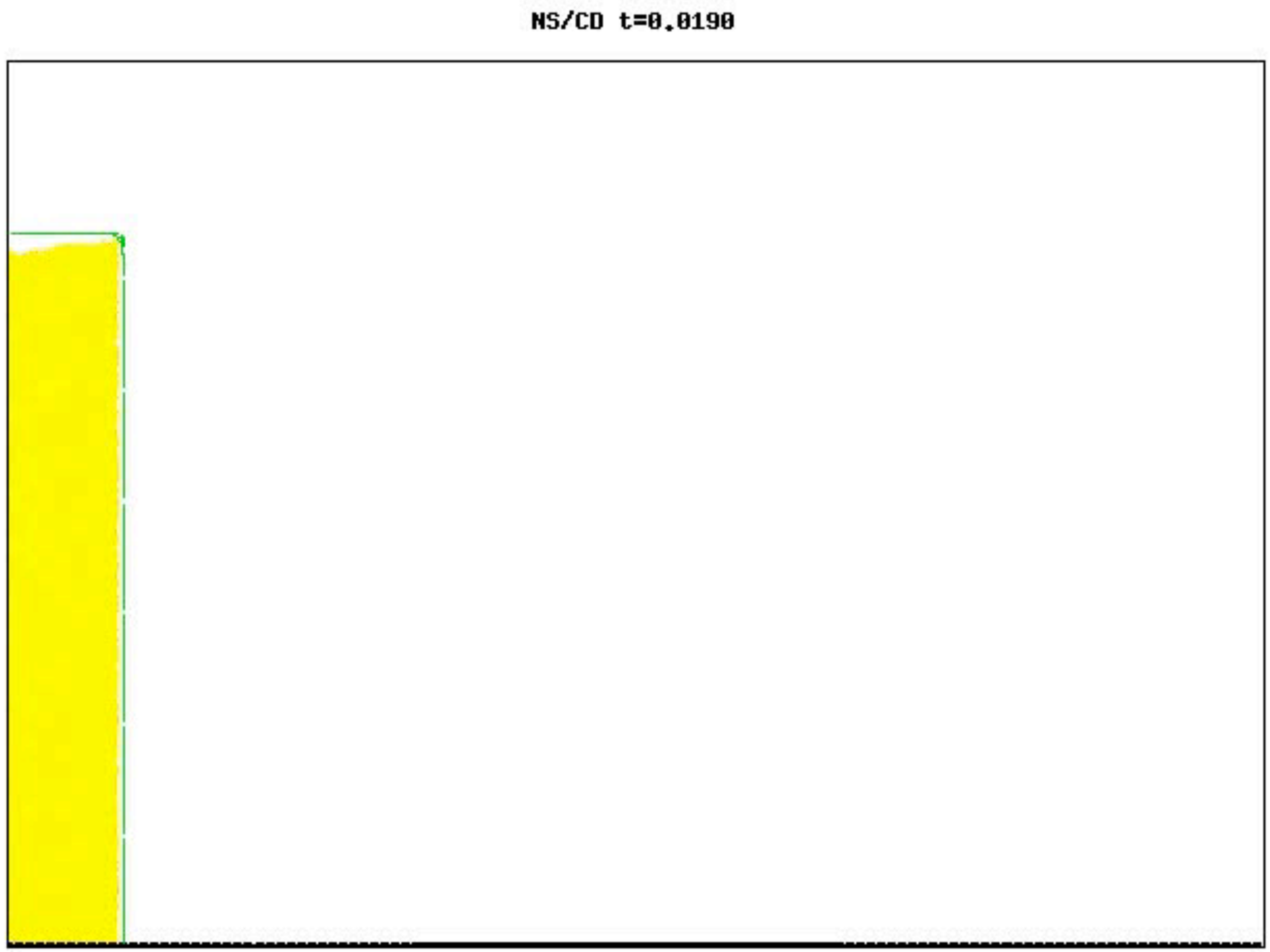

DCM vs Navier Stokes $\mu(I)$

Collapse of columns

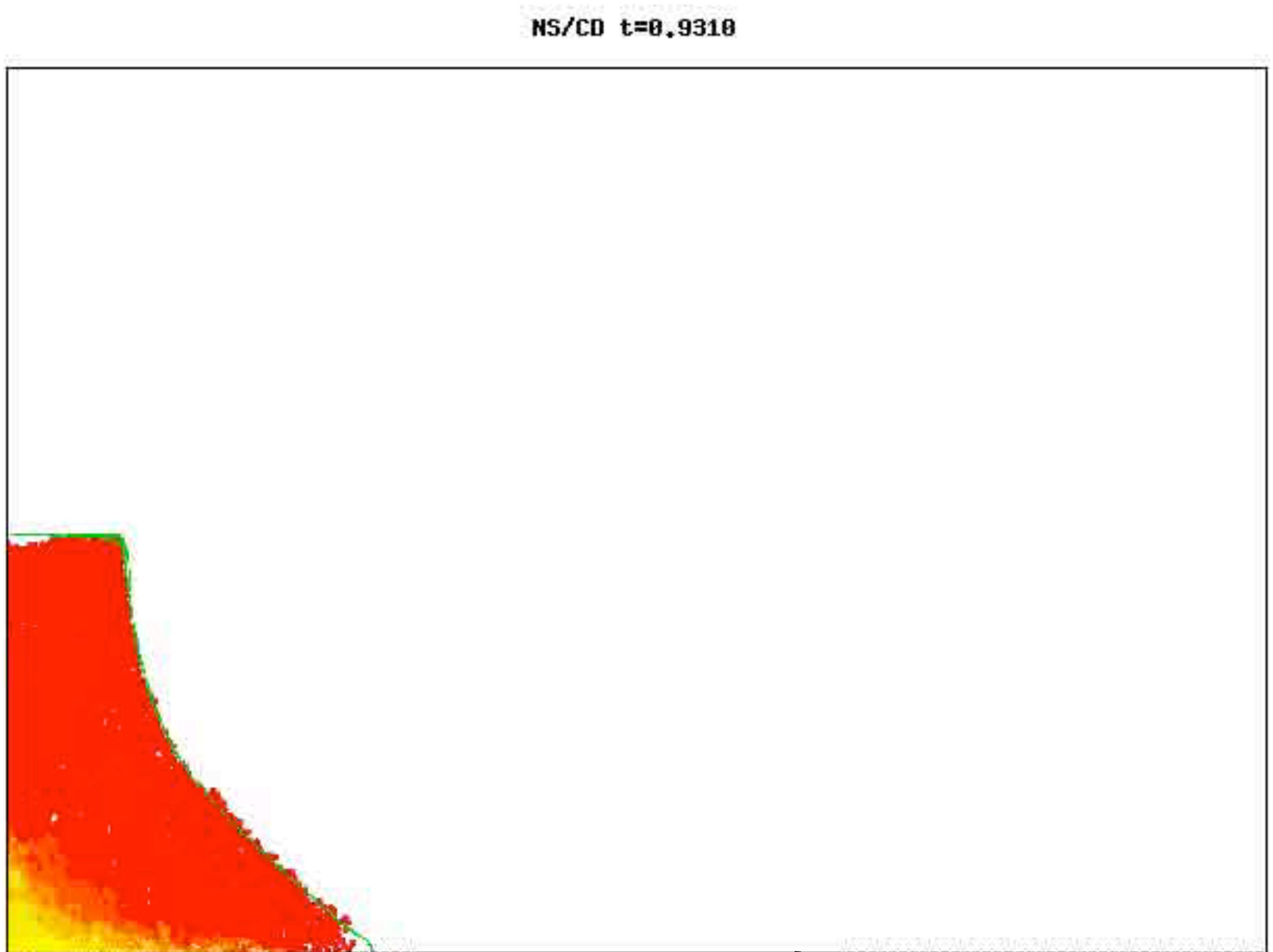

at the tip, a=6.6 t=1.33 2 2.66

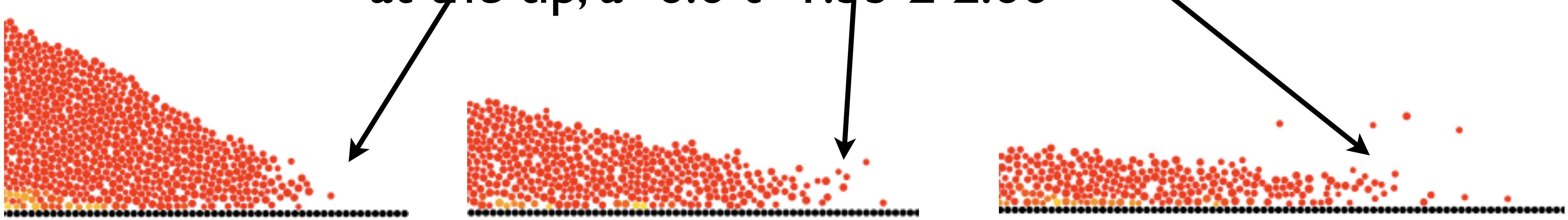

DCM vs Navier Stokes $\mu(I)$

Collapse of columns

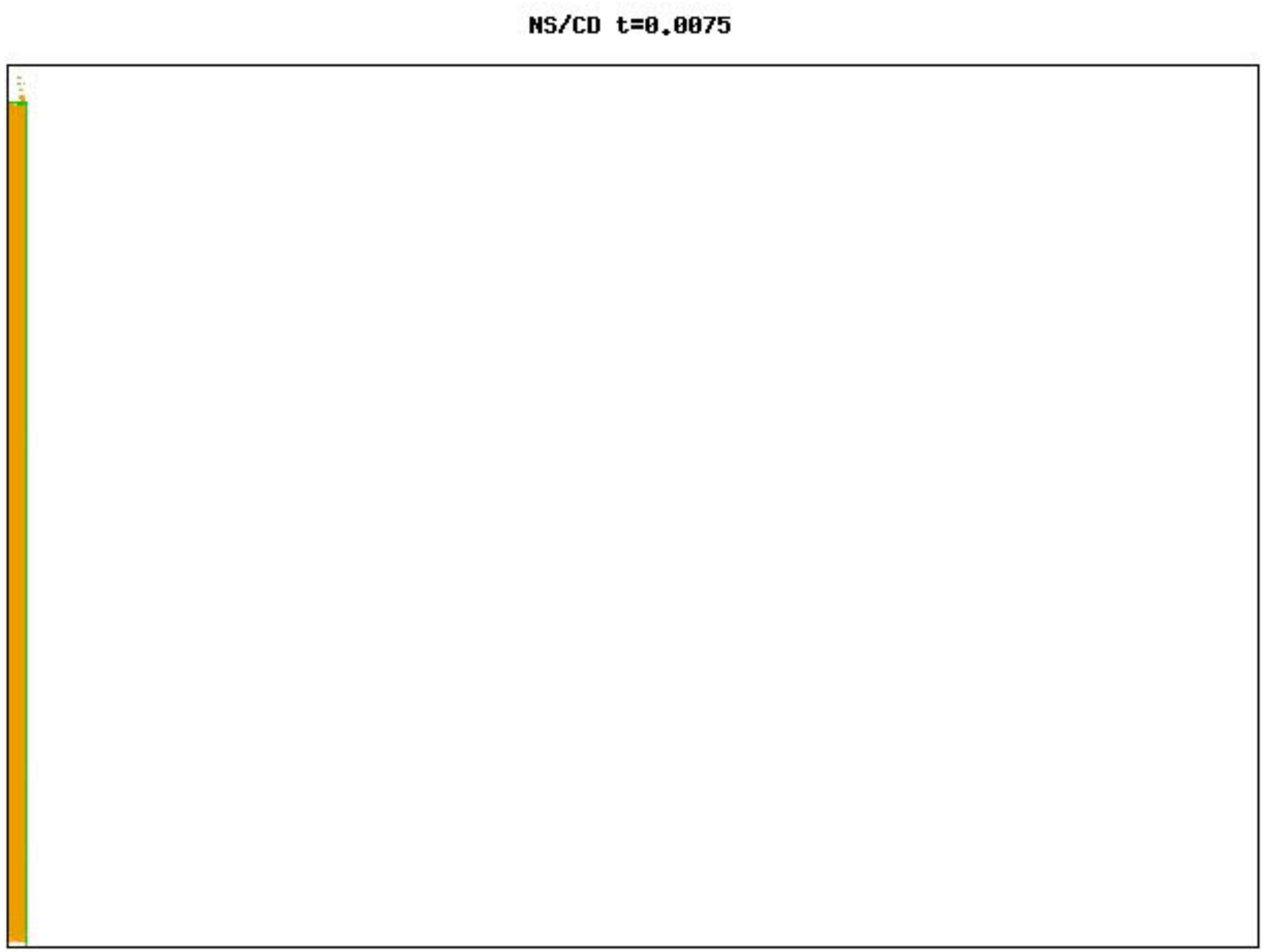

DCM vs *Gerris* $\mu(I)$

Collapse of columns simulation $\mu(I)$

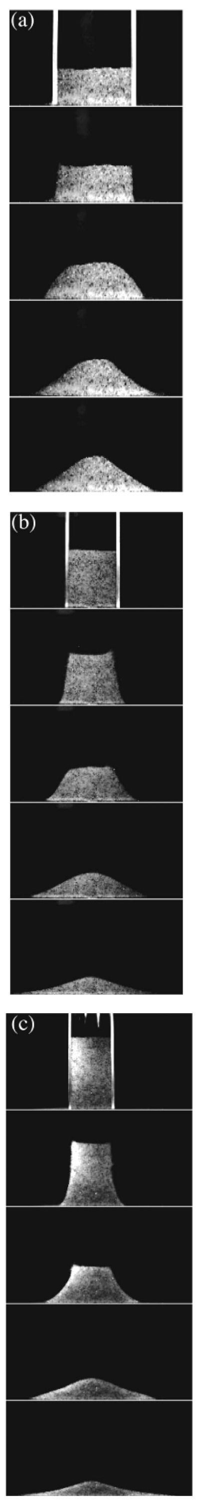

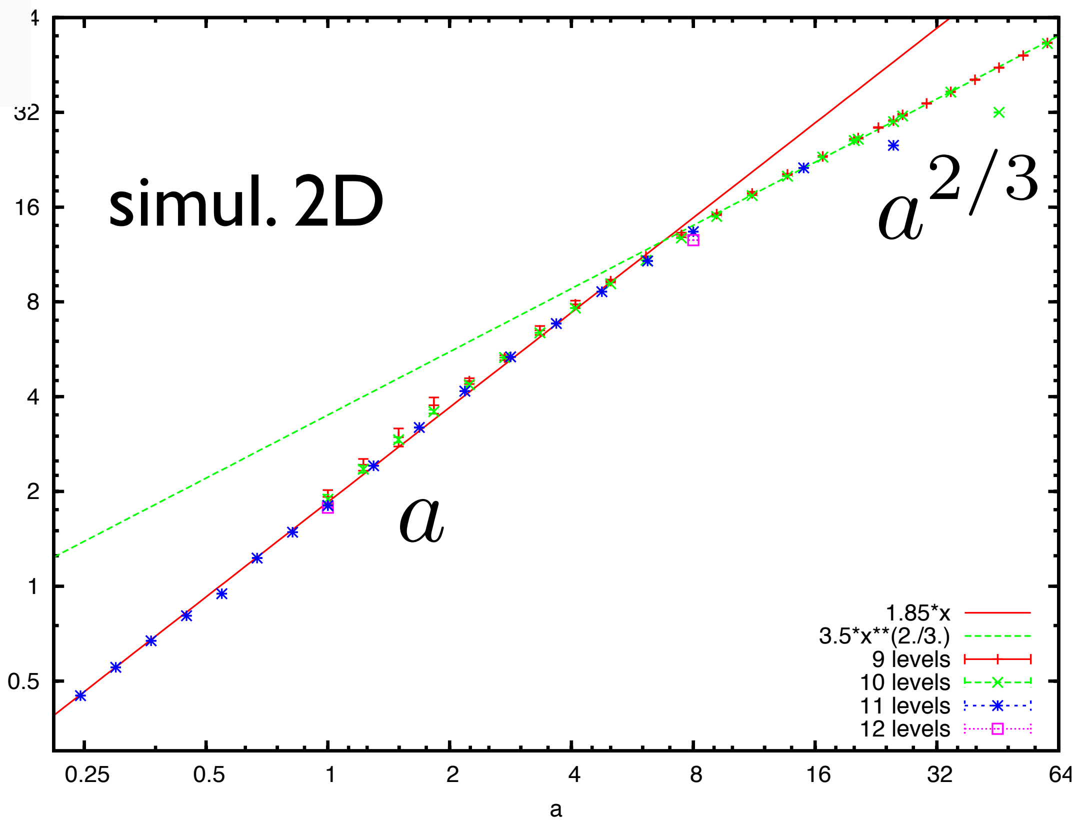

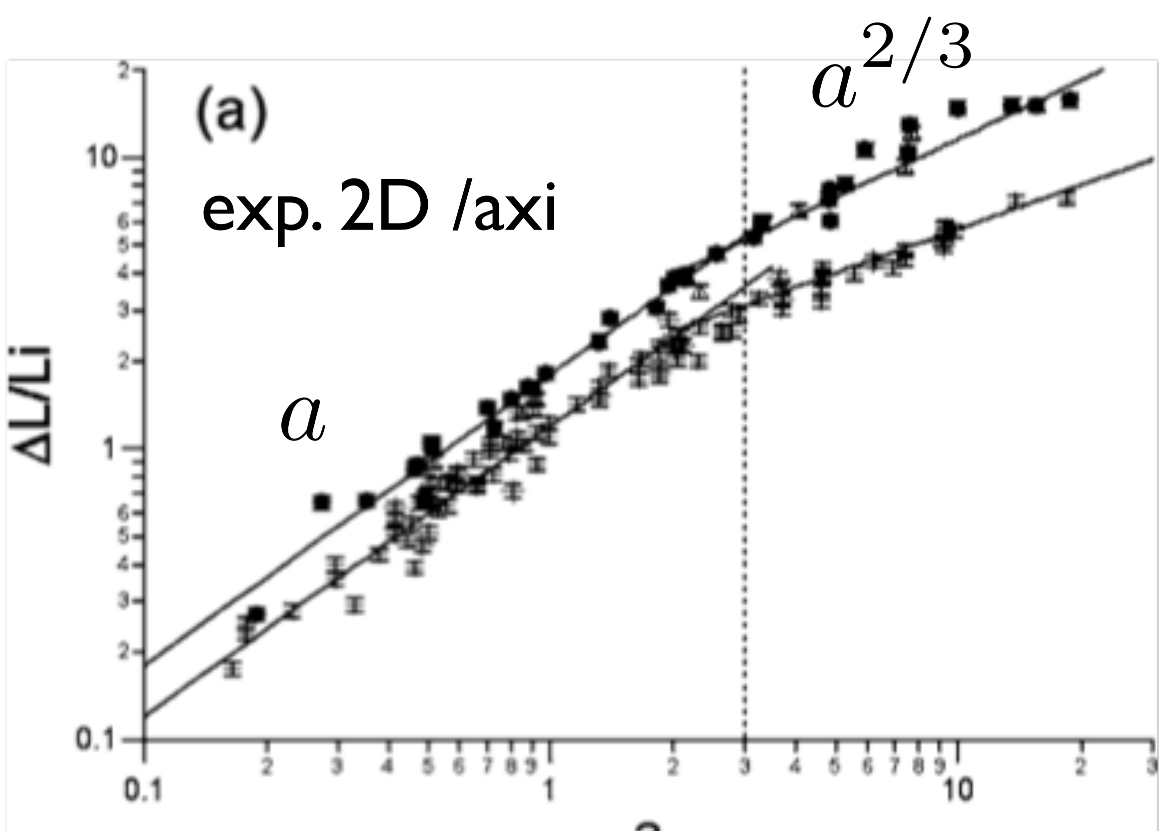

Normalised final deposit extent as a function of aspect ratio a.
Well-defined power law dependencies with exponents of 1 and 2/3 respectively.

$$\frac{\Delta L}{L_i} \propto \begin{cases} a & a \lesssim 3, \\ a^{2/3} & a \gtrsim 3. \end{cases}$$

We recover the experimental scaling [Lajeunesse et al. 04] and [Staron et al. 05].
Differences in the prefactors are due to the difficulties to obtain the run out length (discrete simulation shows that the tip is very gazeous, it can no longer explained by a continuum description).

Collapse of columns

under work
with Sylvain Viroulet IMFT, Anne Mangeney IPGP

discussion of BC

Solids are with friction at the wall

$$\tau = \mu_s p$$

implement solid friction at the wall
instead of no slip

Neumann condition, instead of no slip

$$\frac{\partial u}{\partial y}|_0 = \frac{\mu_s p}{\eta}$$

Results identical, good fit with experiment,
better than Ionescu 2015

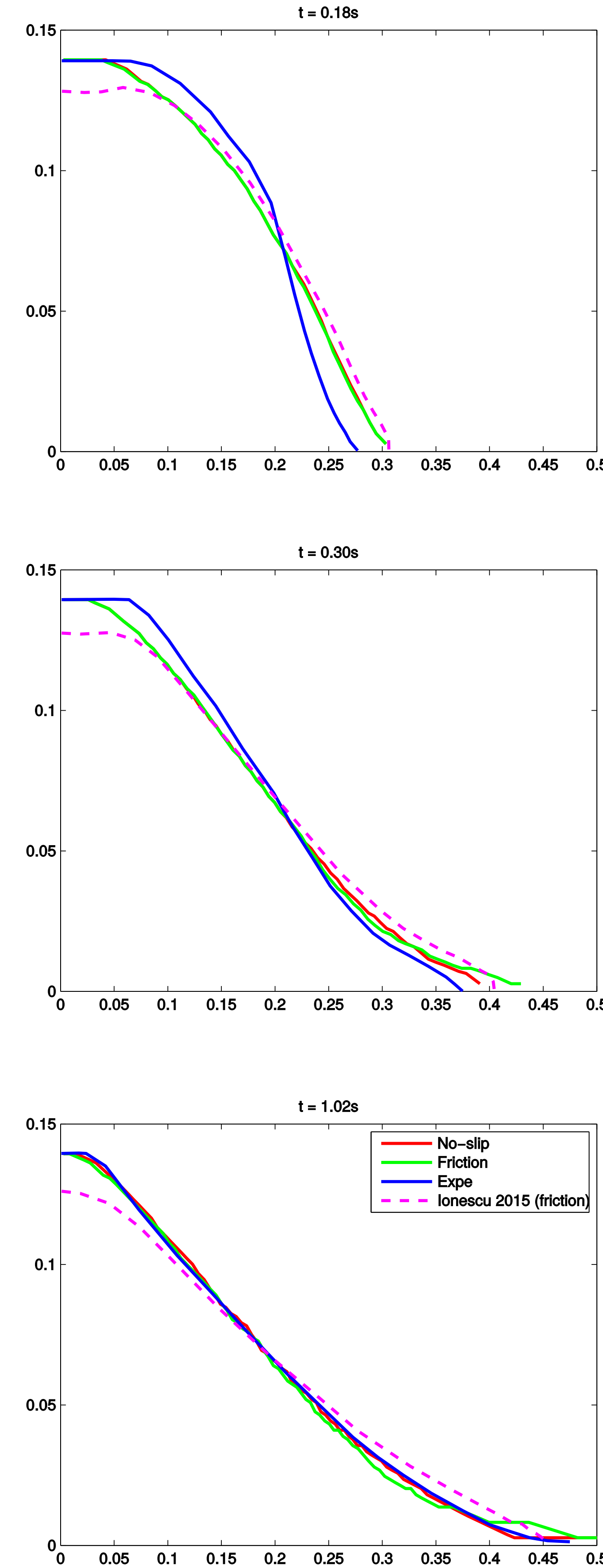

http://basilisk.fr/sandbox/M1EMN/Exemples/granular_column_muw.c

Collapse of columns

under work
with Sylvain Viroulet IMFT, Anne Mangeney IPGP

comparison Exp., Discrete, NS & SVSH

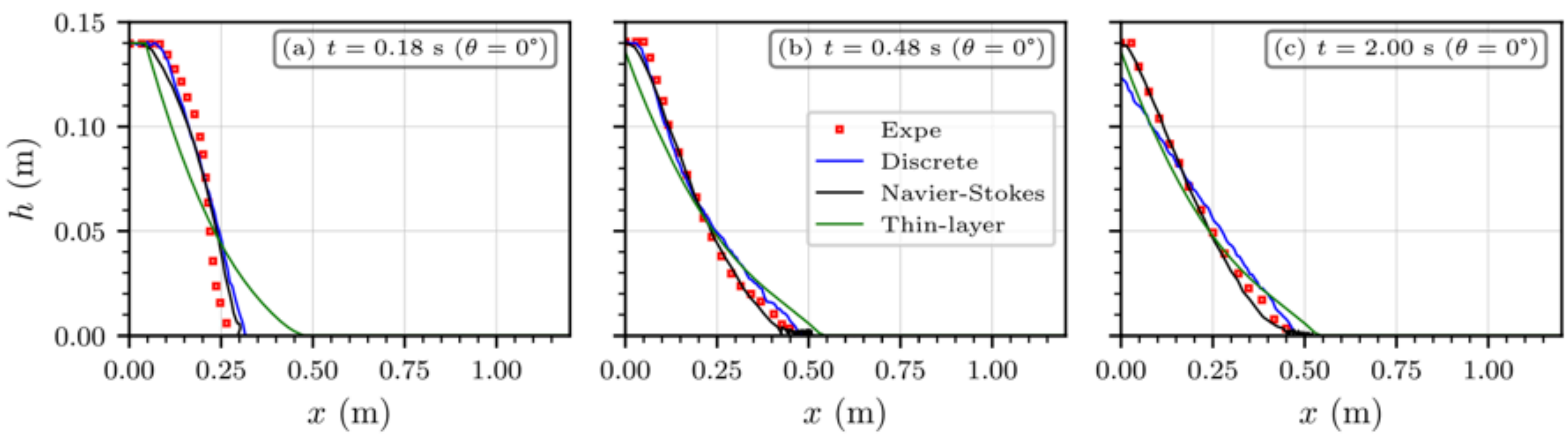

(Exp. ~ Discrete ~ NS) > SVSH

http://basilisk.fr/sandbox/M1EMN/Exemples/savagestaron.c

Gotthilf Hagen
1797-1884

- Problem:

  Simulate the hour glass with discrete and continuum theories

- try to recover the well know experimental result:
  Beverloo 1961 Hagen 1852 law from <u>discrete</u> and <u>continuum</u> simulations

- Flow in a Hourglass Discharge from Hoppers

simulation DCM

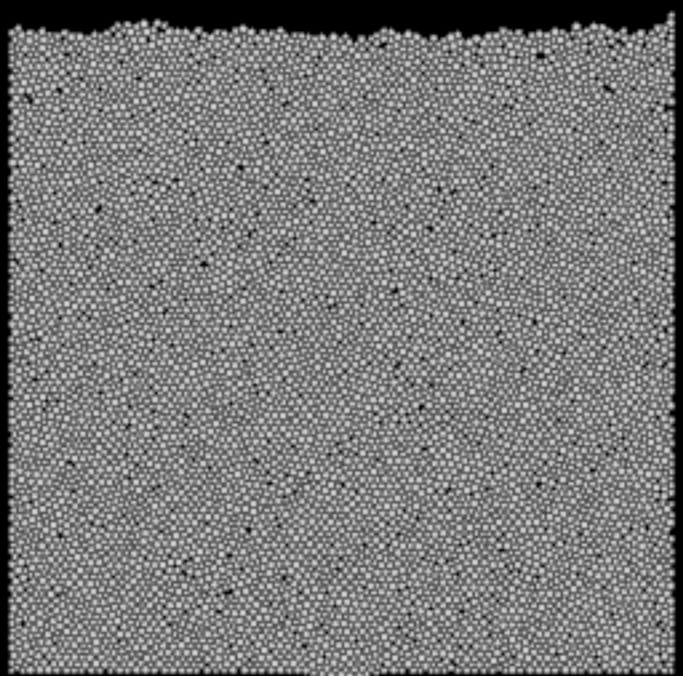

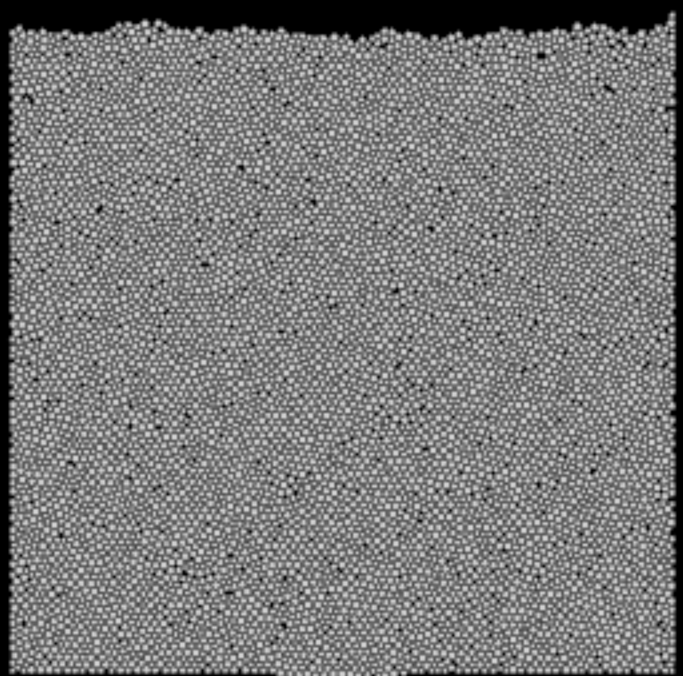

- **Flow in a Hourglass Discharge from Hoppers**

simulation Navier Stokes *μ(I)*

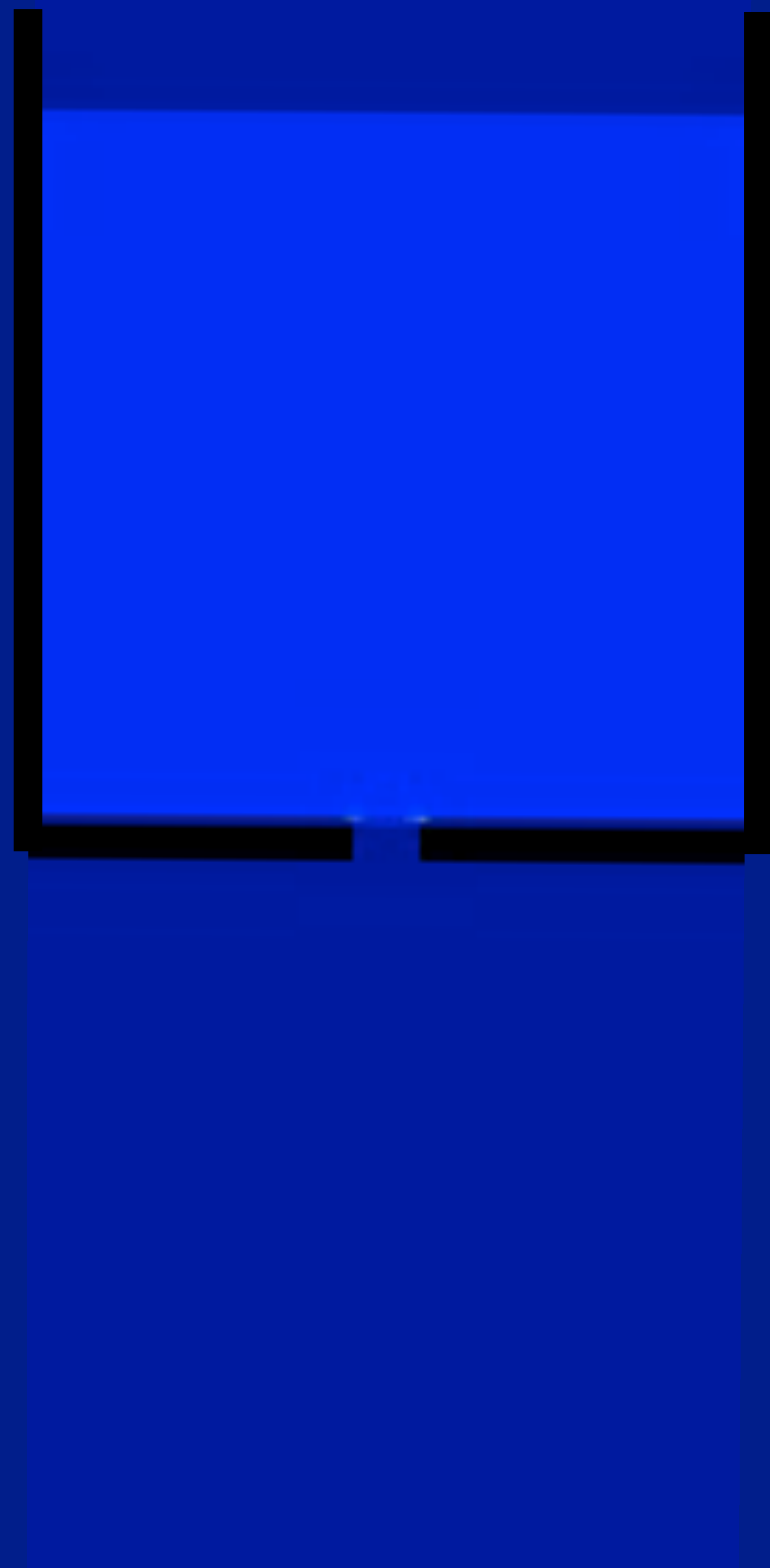

Gotthilf Hagen 1797-1884

- Hagen 1852 Beverloo 1961 constant discharge law

  mass flow rate

Π-theorem

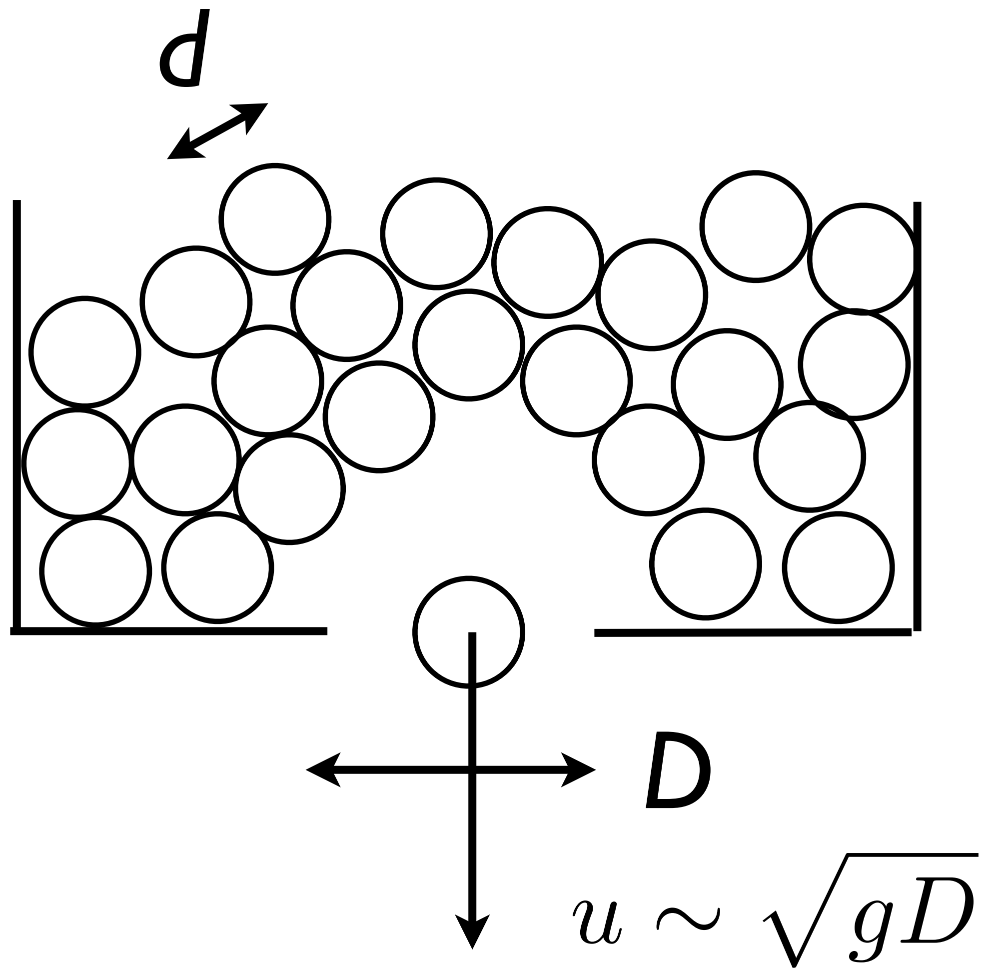

no influence of the hight
nor the width
influence of *D, d* and ρ,
so by dimensional analysis:

$$Q_{3D} \sim \rho\sqrt{gD}D^2$$

$$Q_{2D} \sim \rho\sqrt{gD}D$$

flow observed to be independent of depth
d << *D*

• Flow in a Hourglass Discharge from Hoppers

discrete *vs* continuum 2D

Gotthilf Hagen 1797-1884

Beverloo (1961)

Hagen (1852)

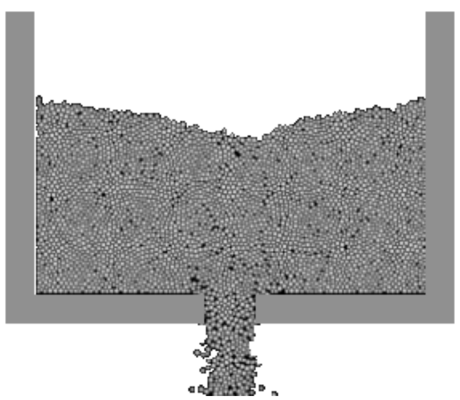

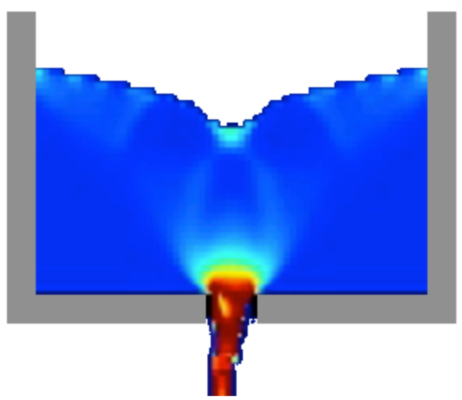

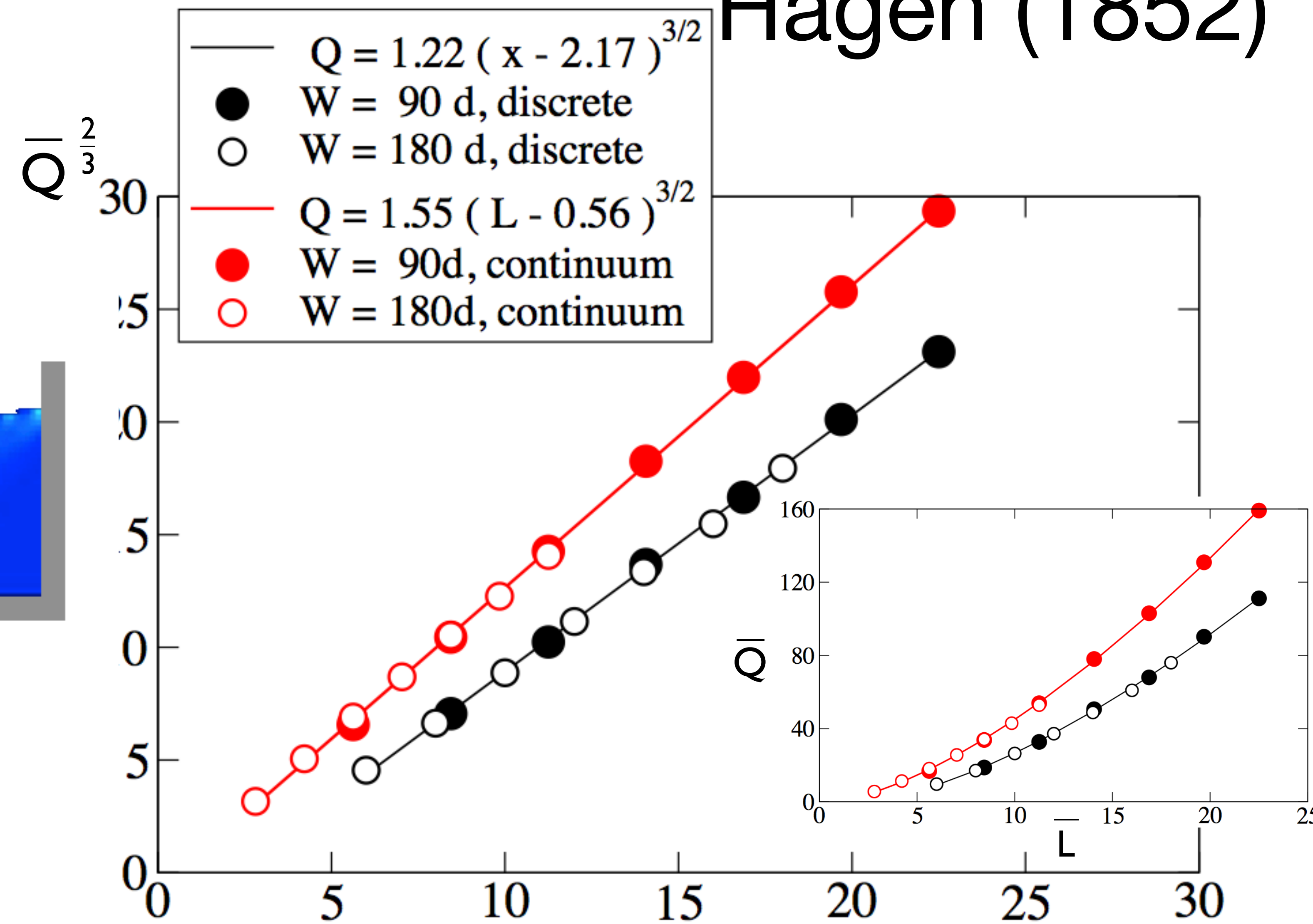

Width of the aperture

$$Q_{2D} \sim \rho\sqrt{gD^3}$$

http://basilisk.fr/sandbox/M1EMN/Exemples/granular_sandglass.c

• Flow in a Hourglass Discharge from Hoppers

continuum 3D

Gotthilf Hagen 1797-1884

The Hour Glass/ Marine Sandglass

Beverloo (1961)
Hagen (1852)

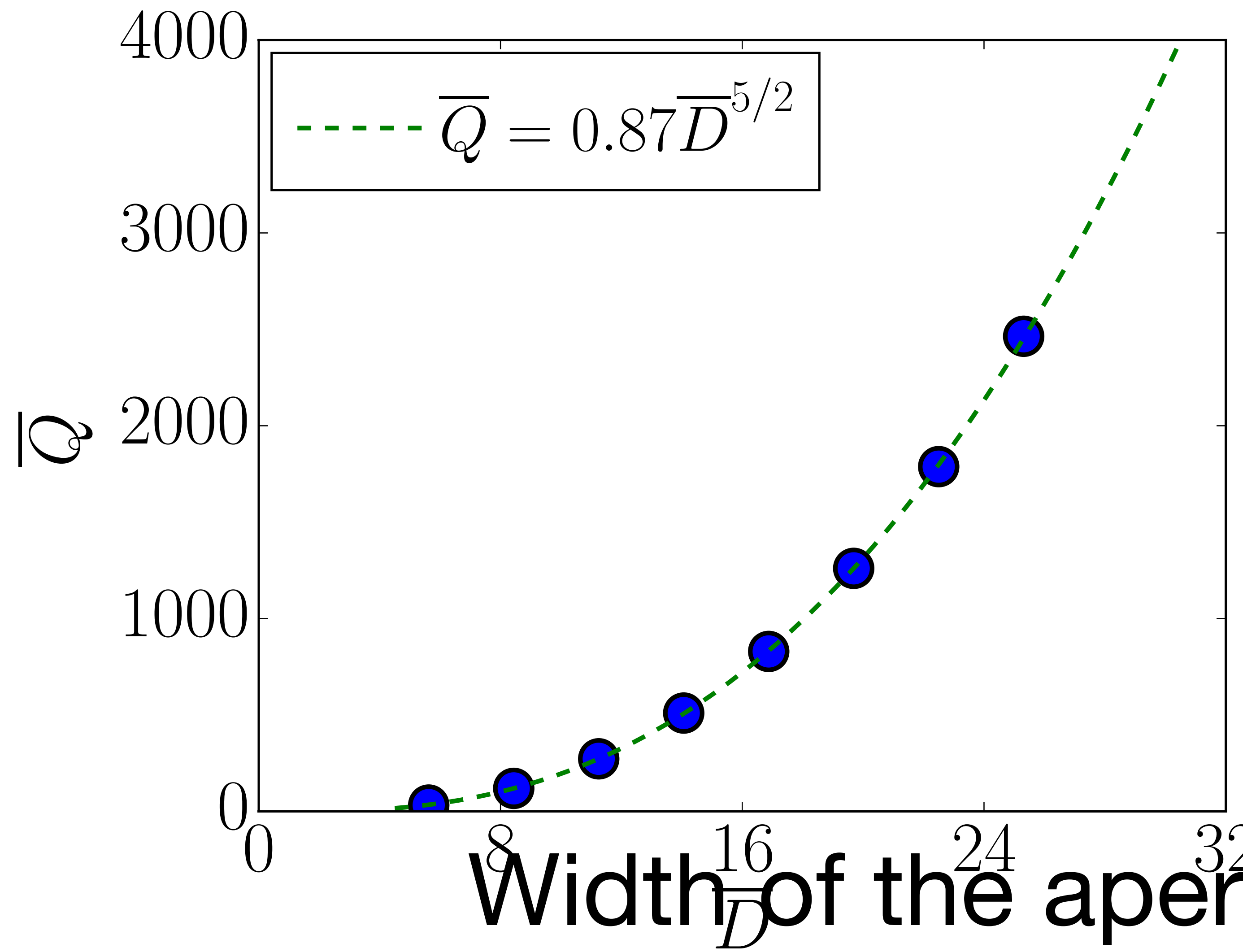

Width of the aperture

$$Q_{3D} \sim \rho\sqrt{gD^5}$$

Evangelista Torricelli 1608 1647

- **Flow in a Hourglass Discharge from Hoppers**

comparing Torricelli

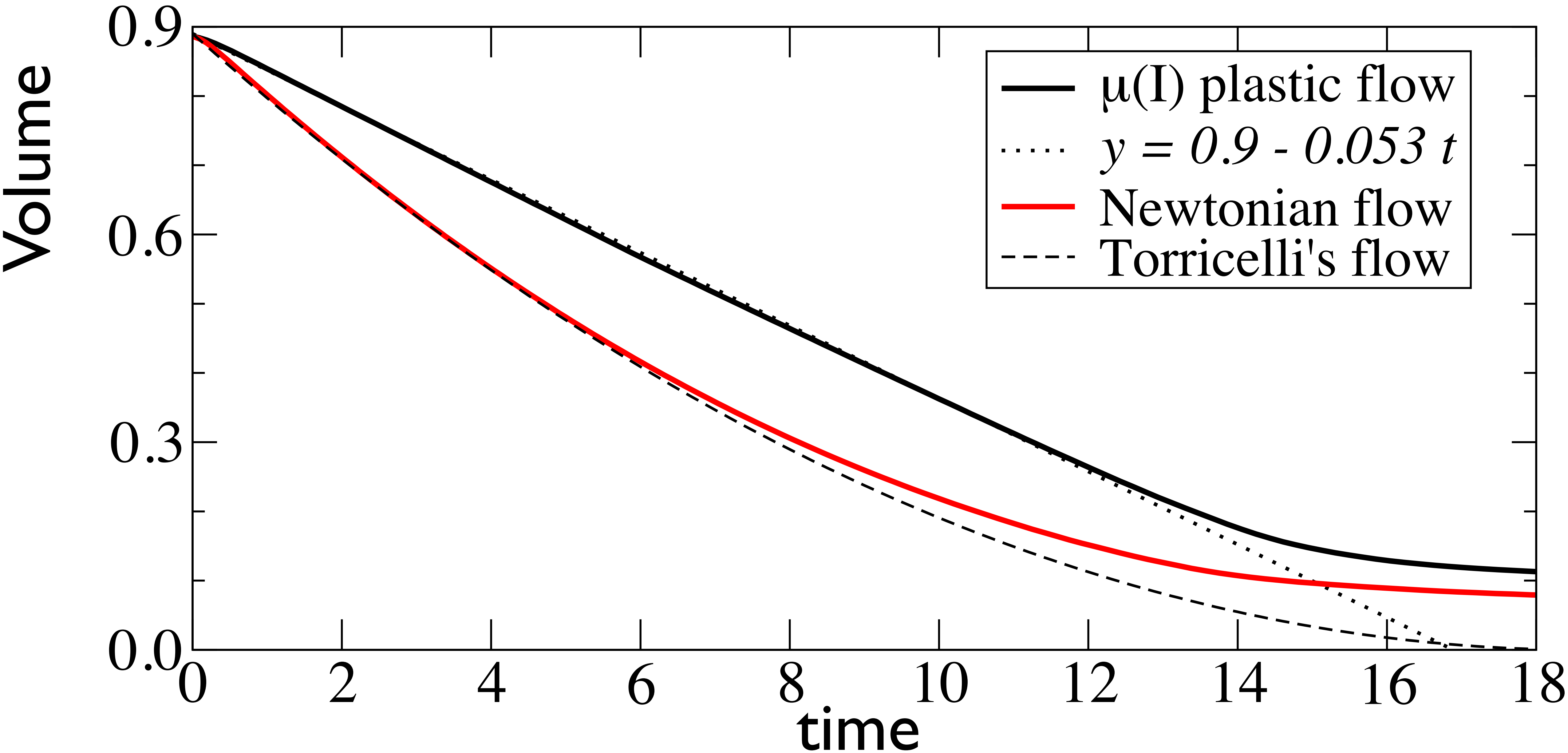

viscosity of the Newtonian flow extrapolated from the μ(I) near the orifice

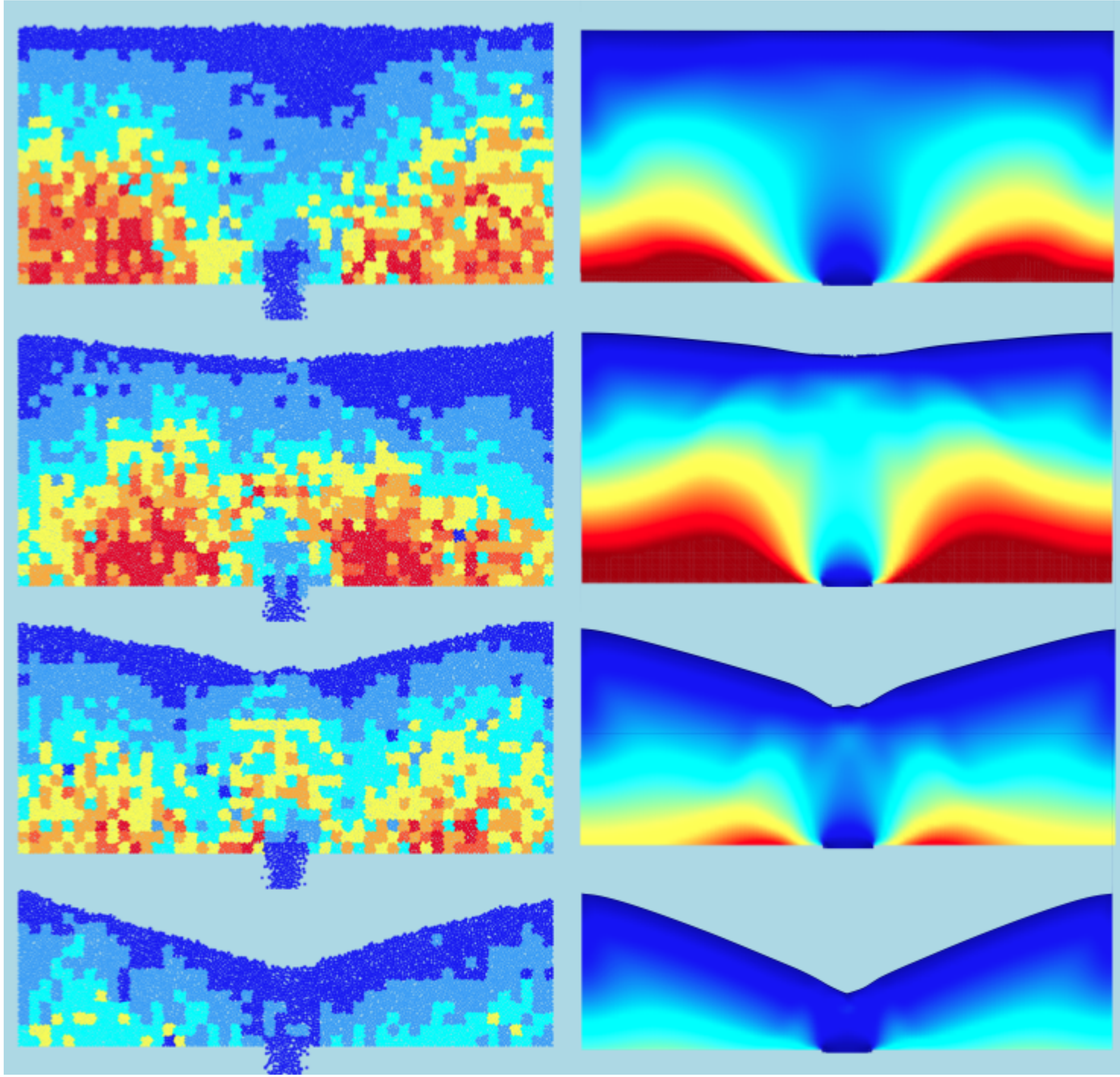

Staron Lagrée Popinet 2014

discrete *vs* continuum (at same rate)

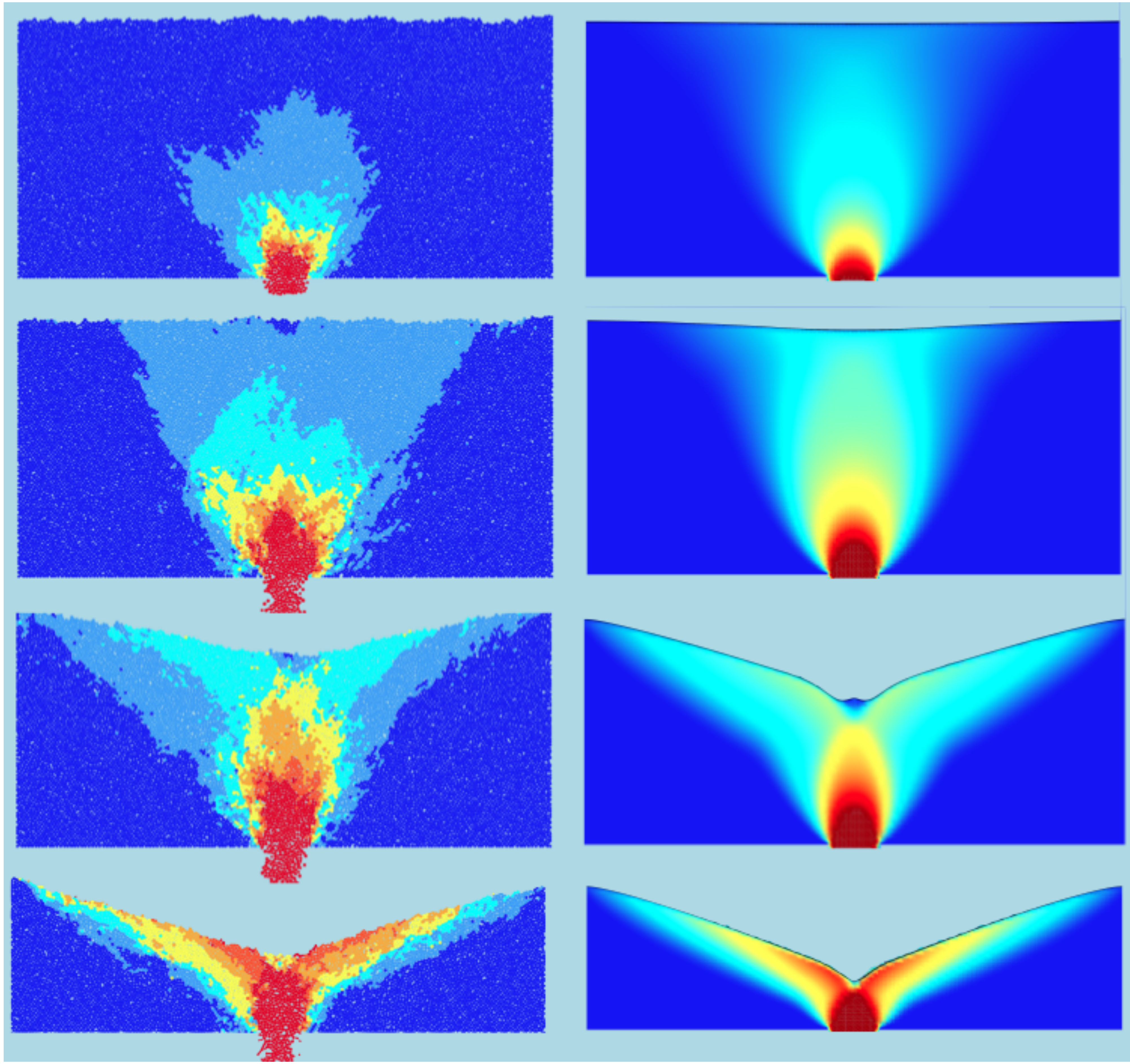

Staron Lagrée Popinet 2014

discrete *vs* continuum (at same rate)

3D as Hele-Shaw approximation

With Pascale Aussillous Pierre Ruyer and Yixian Zhou

The 3D equations are averaged across the cell of thickness W

$$\mathbf{u} = (u, v, w)$$

$$\nabla \cdot \mathbf{u} = 0, \quad \rho \left(\frac{\partial \mathbf{u}}{\partial t} + \mathbf{u} \cdot \nabla \mathbf{u} \right) = -\nabla p + \nabla \cdot (2\eta \mathbf{D}) + \rho \mathbf{g}$$

$$\int \cdot \, dz$$

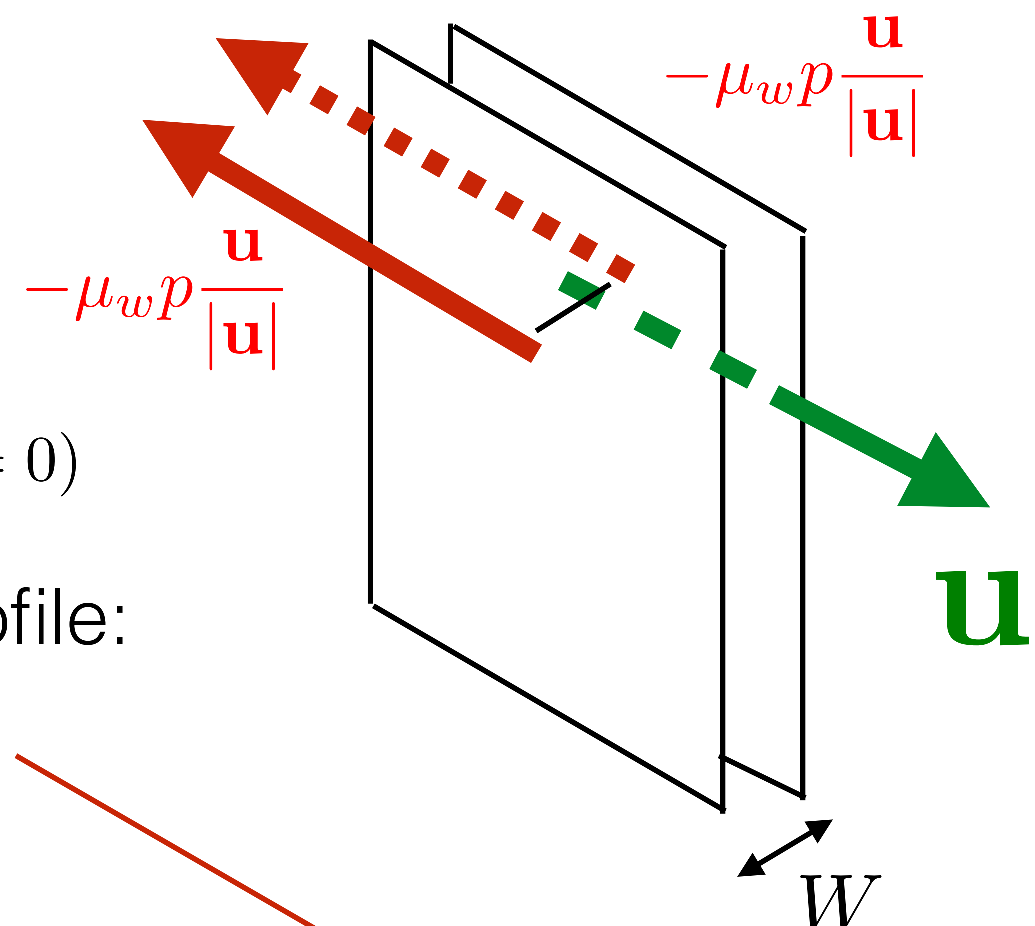

redefinition of velocity

$$\mathbf{u} = \left(\frac{1}{W}\int_{-W/2}^{W/2} u dz, \frac{1}{W}\int_{-W/2}^{W/2} v dz, w = 0\right)$$

suppose an almost transverse flat profile:
non linear closure coefficient is one
extra wall friction source term

2D width averaged Equations

$$\mathbf{u} = (u, v)$$

$$\nabla \cdot \mathbf{u} = 0, \quad \rho \left(\frac{\partial \mathbf{u}}{\partial t} + \mathbf{u} \cdot \nabla \mathbf{u} \right) = -\nabla p + \nabla \cdot (2\eta \mathbf{D}) + \rho \mathbf{g} - 2\mu_w \frac{p}{W} \frac{\mathbf{u}}{|\mathbf{u}|}$$

NS Hele-Shaw μ(I) vs Experiments

rescaling with: $$Q = \rho W^2 \sqrt{gW}\ \mathcal{F}(D/W)$$

large thickness $(D/W) \ll 1$

small thickness $(D/W) \gg 1$

plot as function of D/W

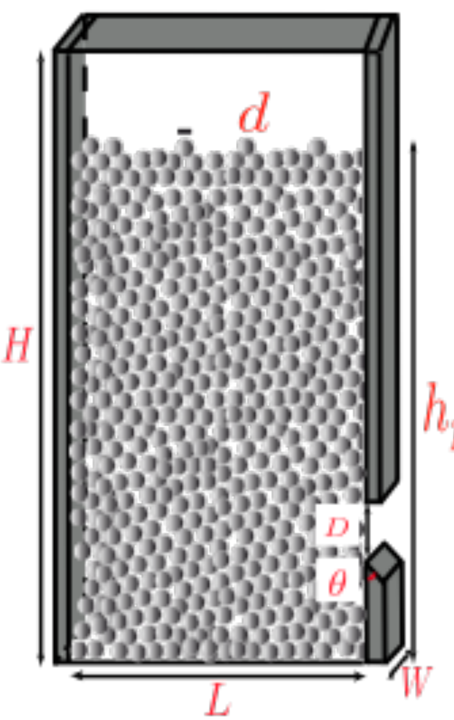

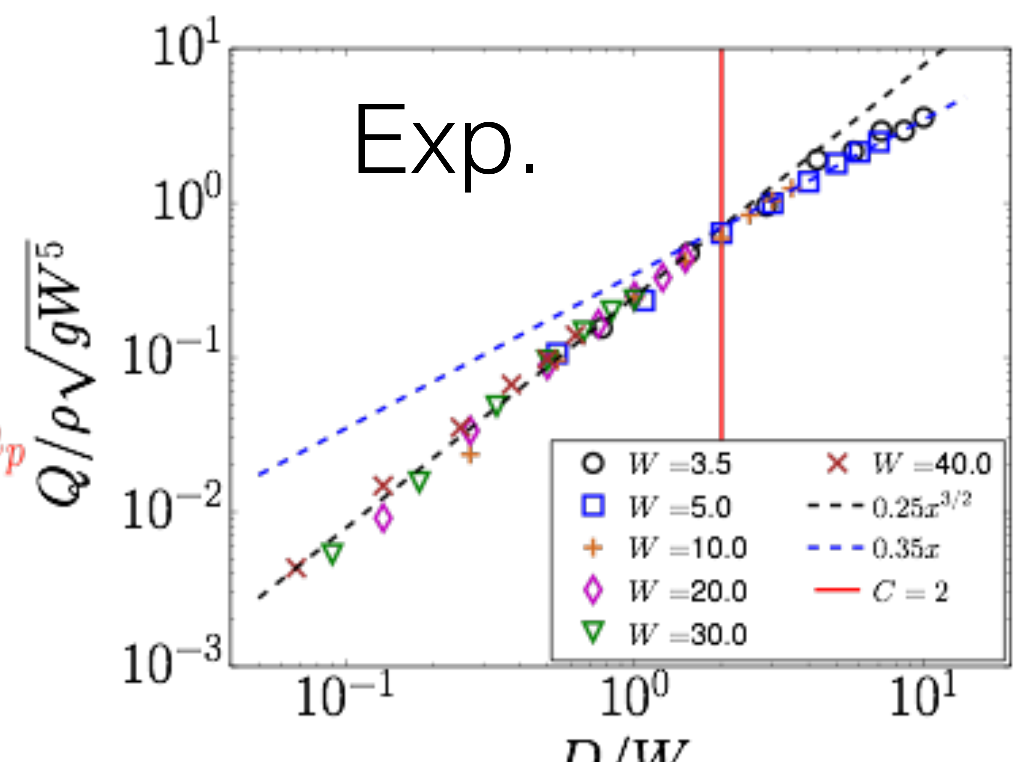

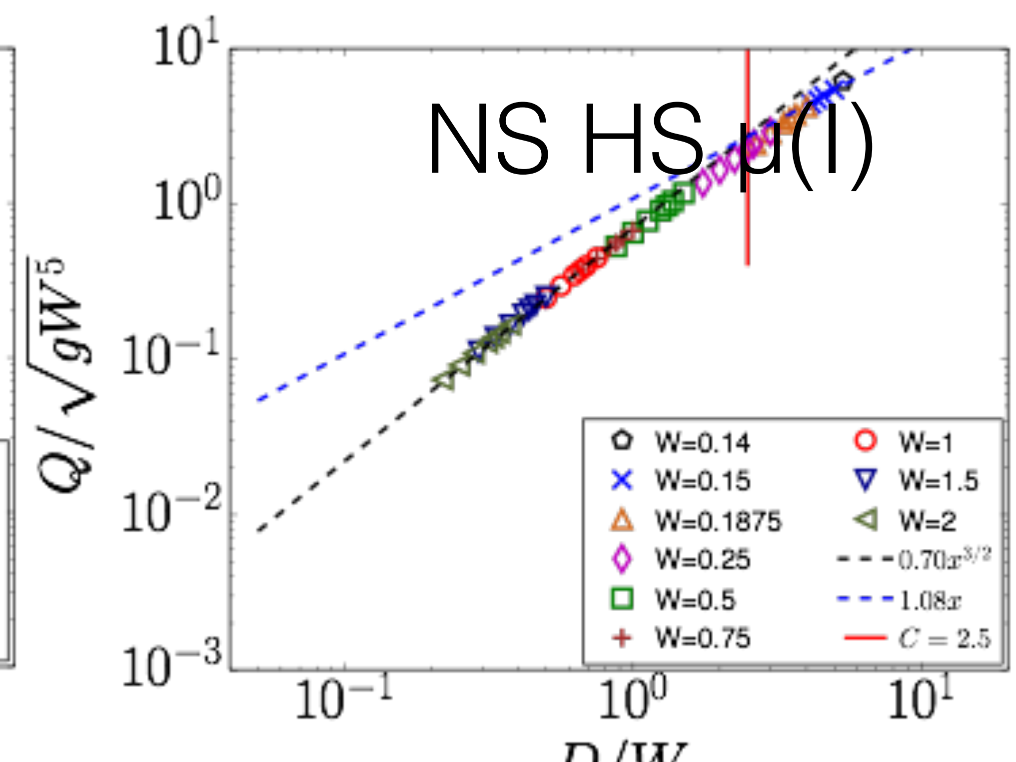

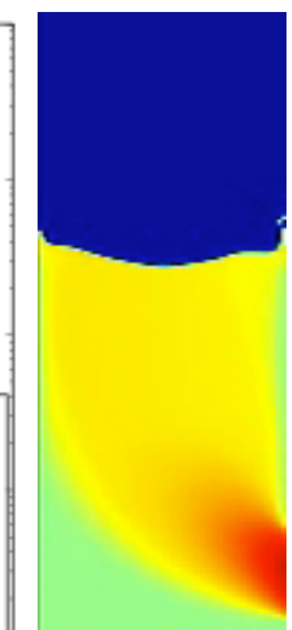

Hagen friction dominated Hagen friction dominated

$$(D/W) < 1, \quad Q \sim D^{3/2} W \qquad (D/W) > 1, \quad Q \sim W^{3/2} D$$

http://basilisk.fr/sandbox/M1EMN/Exemples/granular_sandglass_muw.c

Coupling granular with air: Darcy Forchheimer

With Pascale Aussillous Pierre Ruyer and Zhenhai Zou

Using simplified Jackson 00 two fluids equations model

Coupling unsteady Darcy Forchheimer (porous)

$$\nabla \cdot \mathbf{u}^f = 0$$

$$R^f \frac{\partial \mathbf{u}^f}{\partial t} = -\nabla p^f - B_l(\mathbf{u}^f - \mathbf{u}^p) - B_i|(\mathbf{u}^f - \mathbf{u}^p)|(\mathbf{u}^f - \mathbf{u}^p)$$

With granular flow

$$\nabla \cdot \mathbf{u}^p = 0$$

$$\rho^p \left(\frac{\partial \mathbf{u}^p}{\partial t} + \mathbf{u}^p \cdot \nabla \mathbf{u}^p \right) = -\nabla p^p + \nabla \cdot (2\eta \mathbf{D}) - \nabla p^f + \rho \mathbf{g}$$

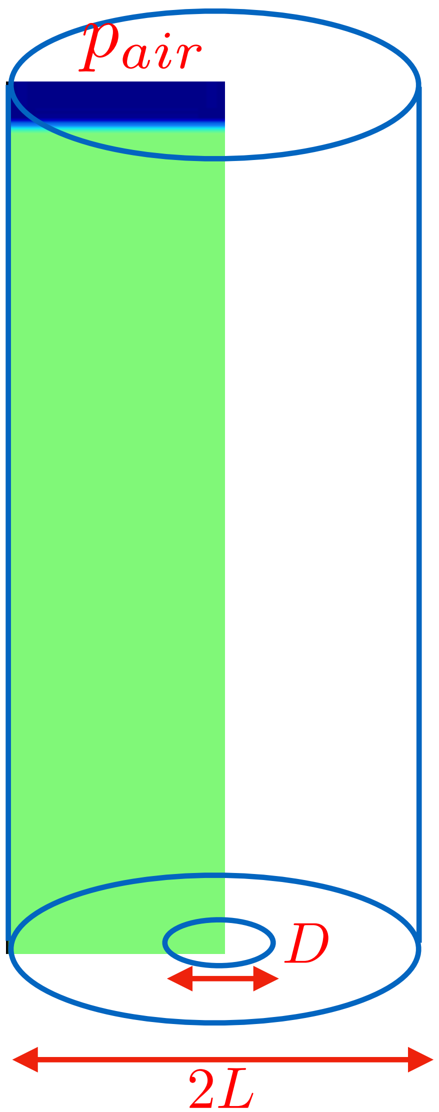

axi

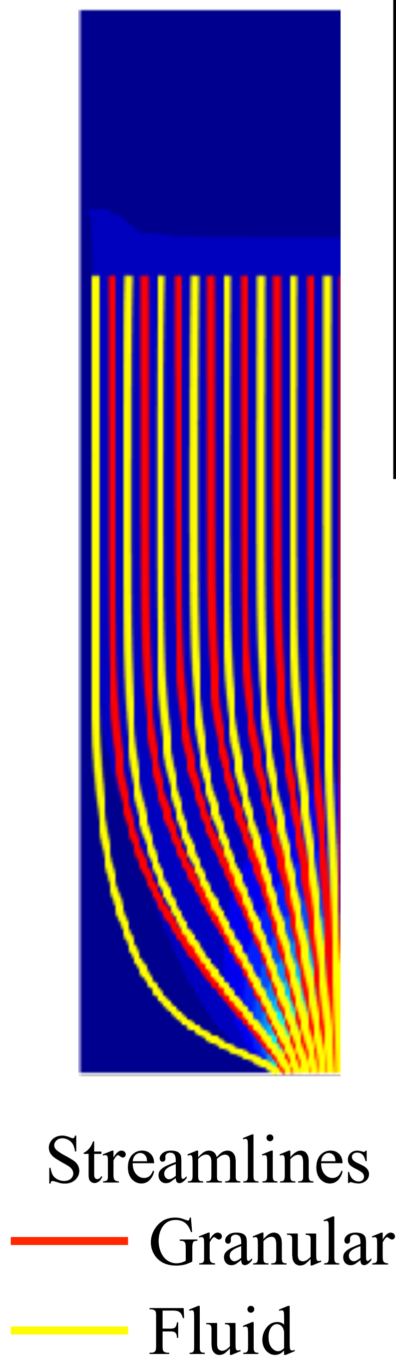

The flow rate is increased by the constant pressure drop

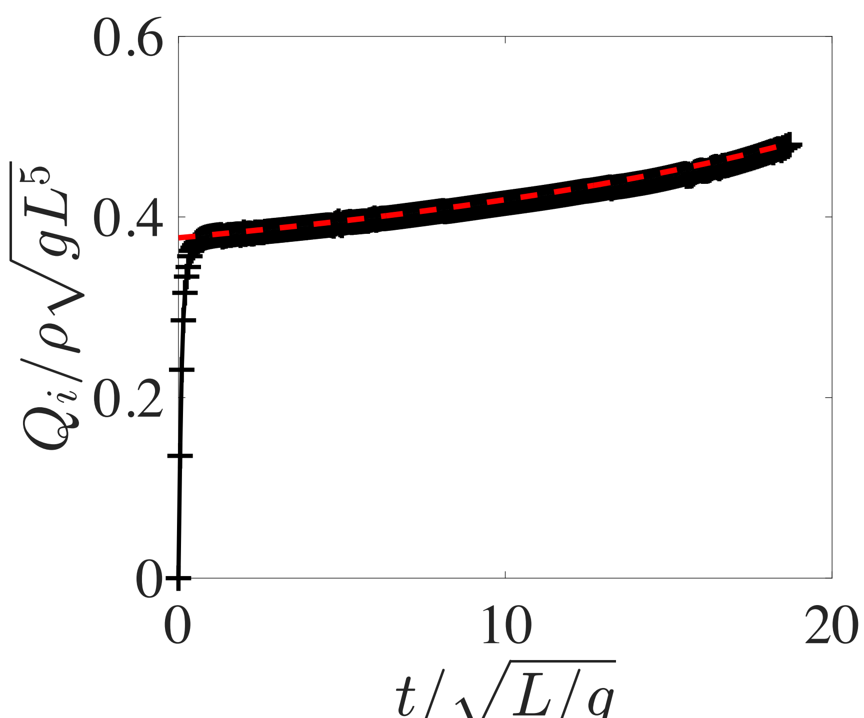

http://basilisk.fr/sandbox/M1EMN/Exemples/forchheimer.c

cohesive material vs experimental

With Anaïs Abramian, Lydie Staron, Adrien Gans ANR COPRINT

influence of cohesion: adds a threshold $\tau = \tau_c + \mu(I)P$

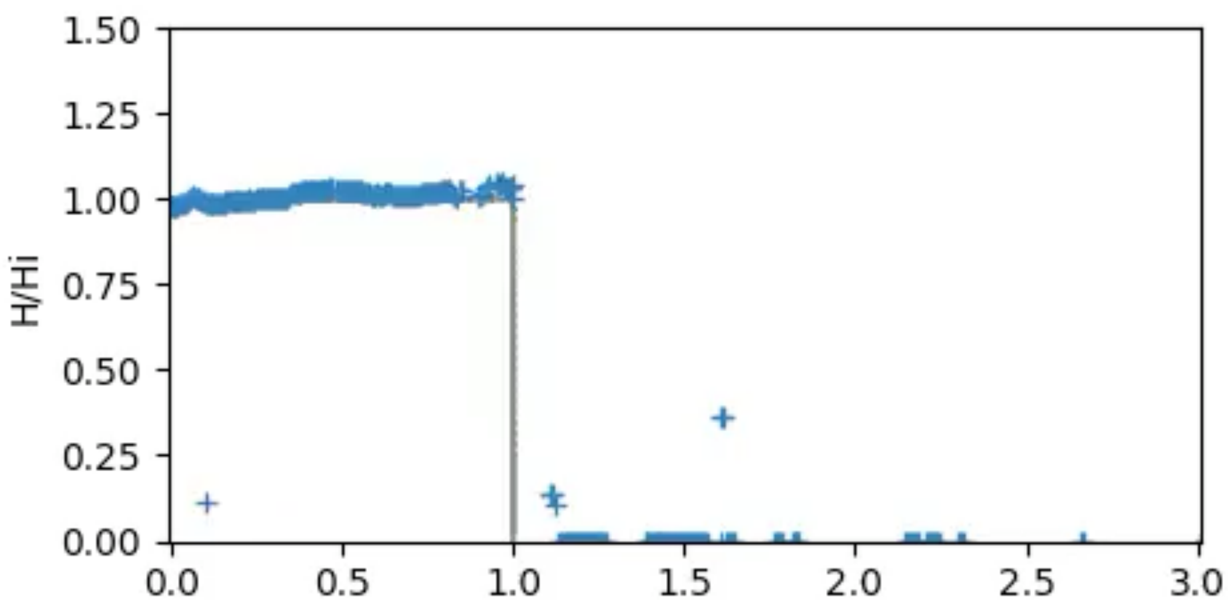

num/exp

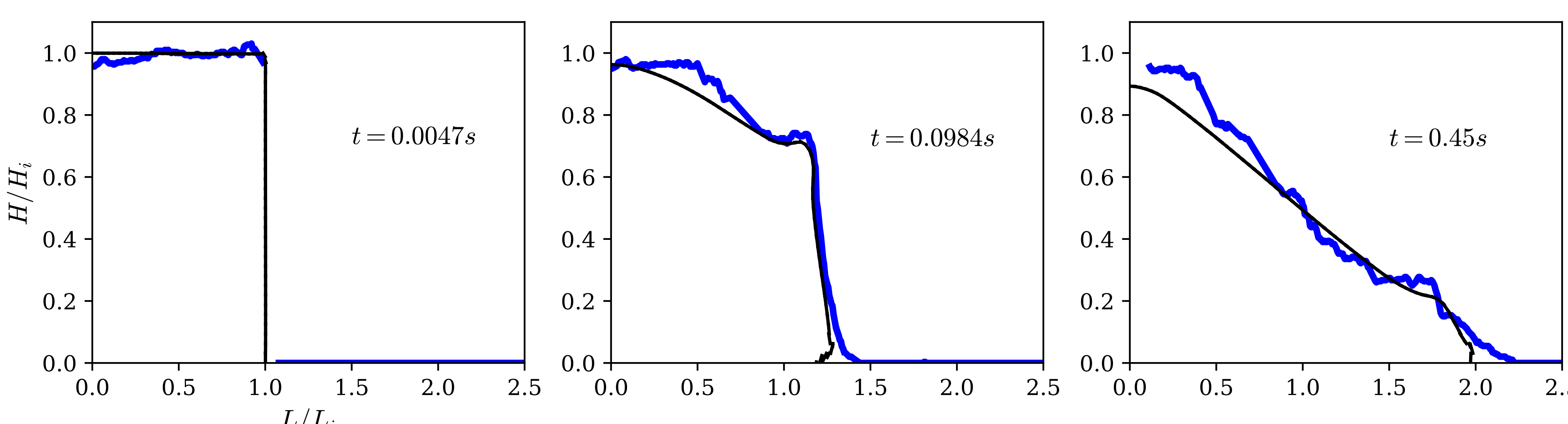

http://basilisk.fr/sandbox/M1EMN/Exemples/granular_column_cohesif.c

cohesive material continuum vs discrete

With Anaïs Abramian, Lydie Staron, Adrien Gans ANR COPRINT

DCIM

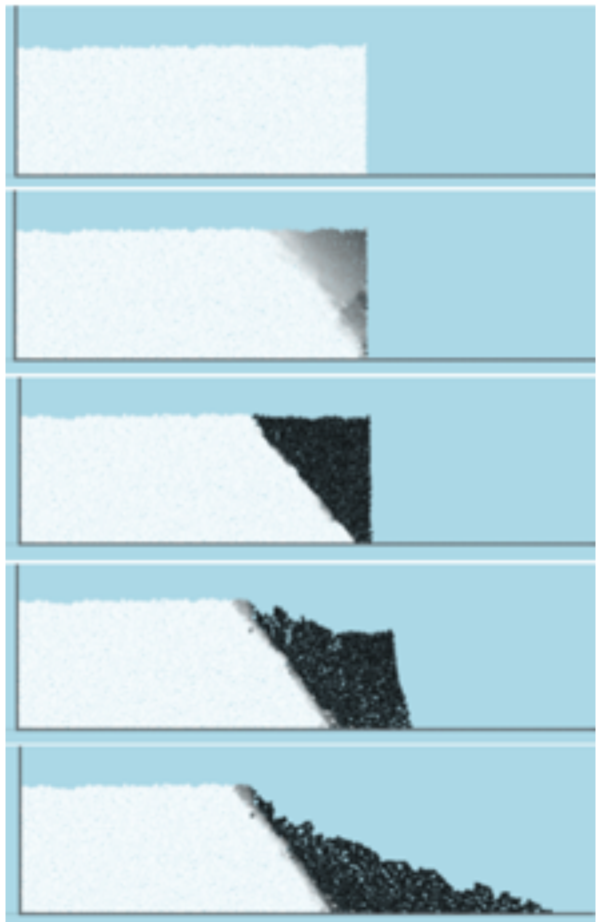

discrete adhesion on each grain $F_{adh} = -B_{ond}\, m_p g.$

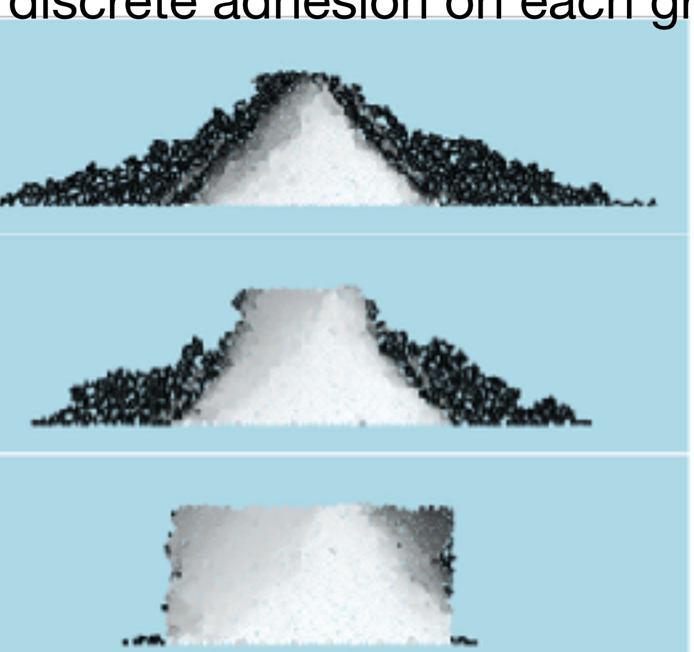

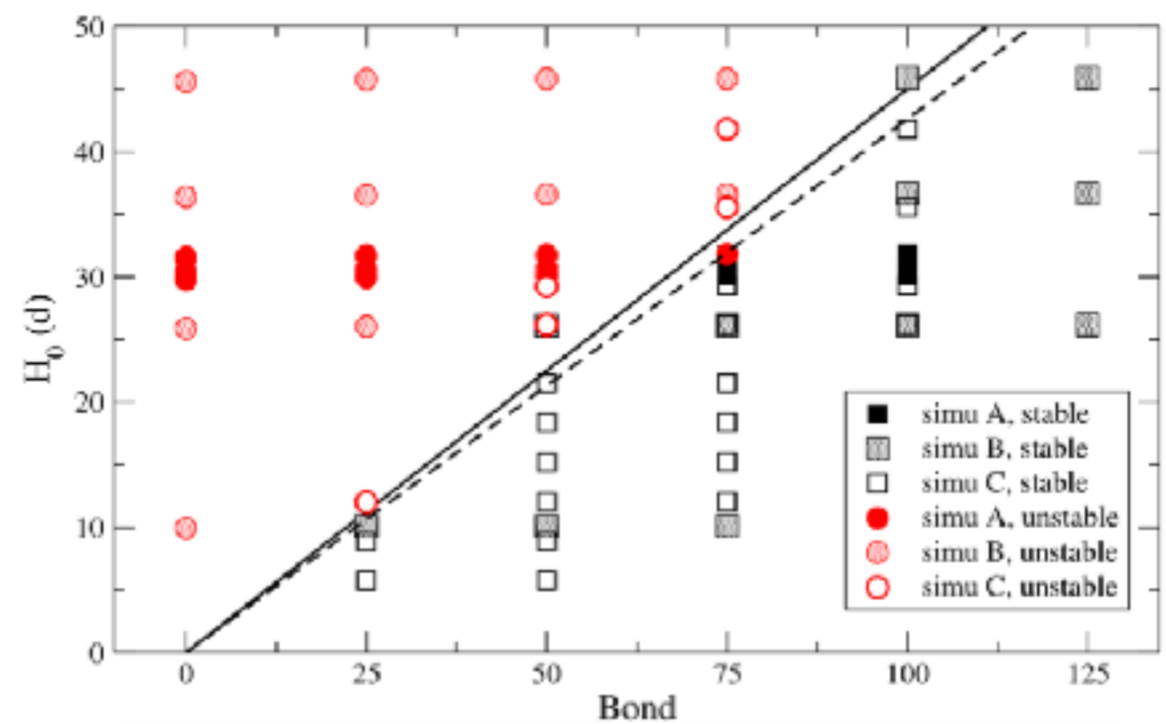

cohesive material continuum vs discrete

With Anaïs Abramian, Lydie Staron, Adrien Gans ANR COPRINT

DCIM

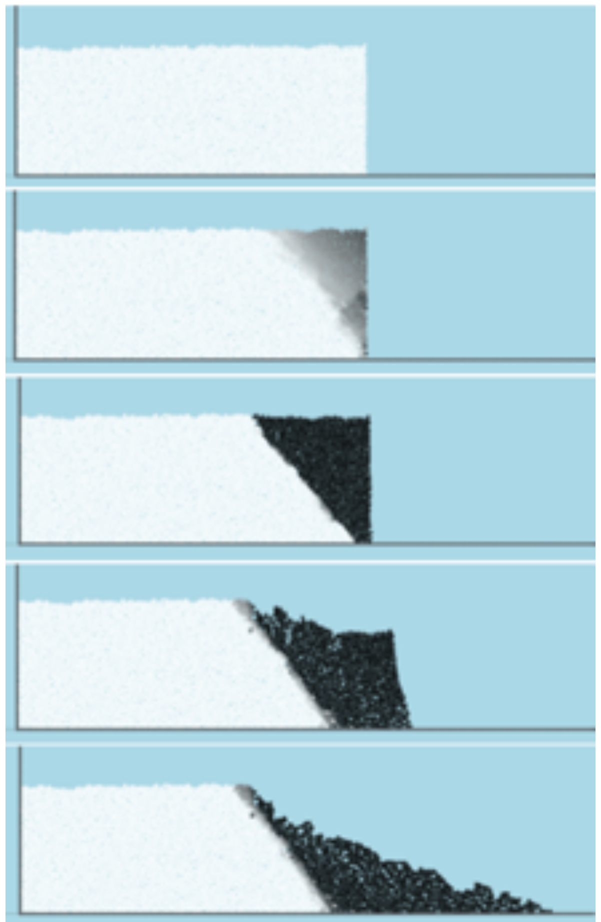

discrete adhesion on each grain $F_{adh} = -B_{ond}\, m_p g.$

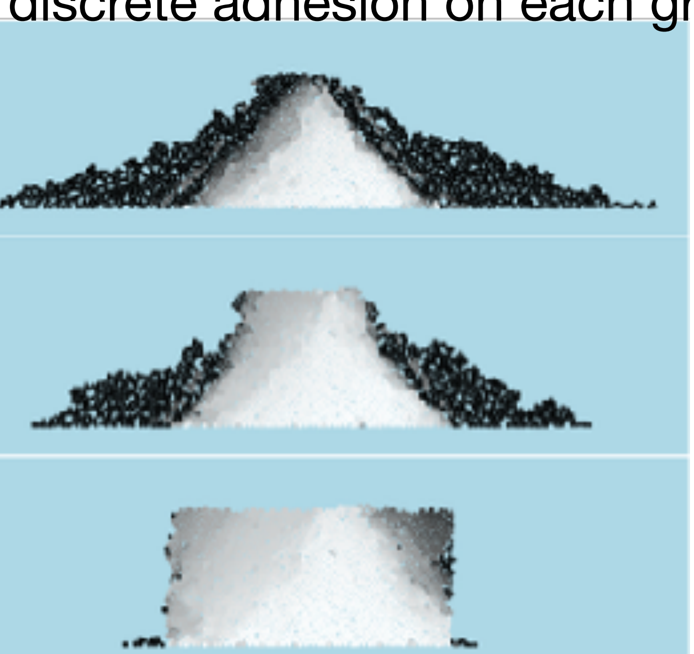

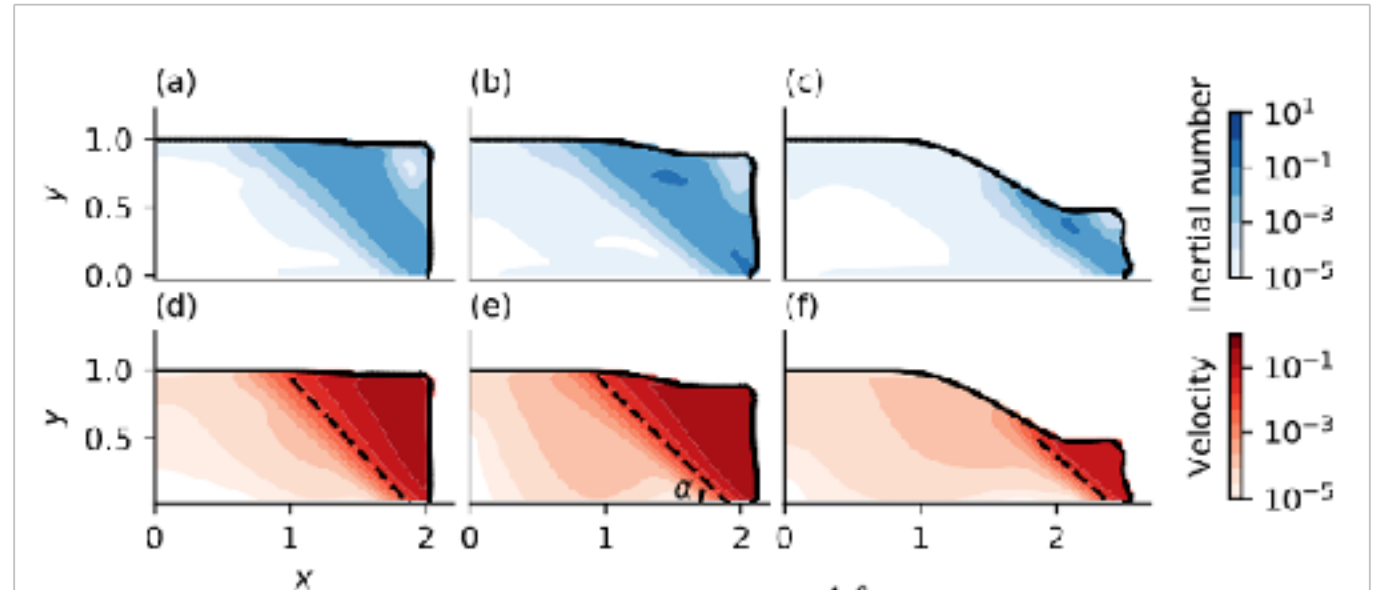

failure height: $H_y = \dfrac{4\ell_c}{\sqrt{\mu_s^2+1}-\mu_s},$

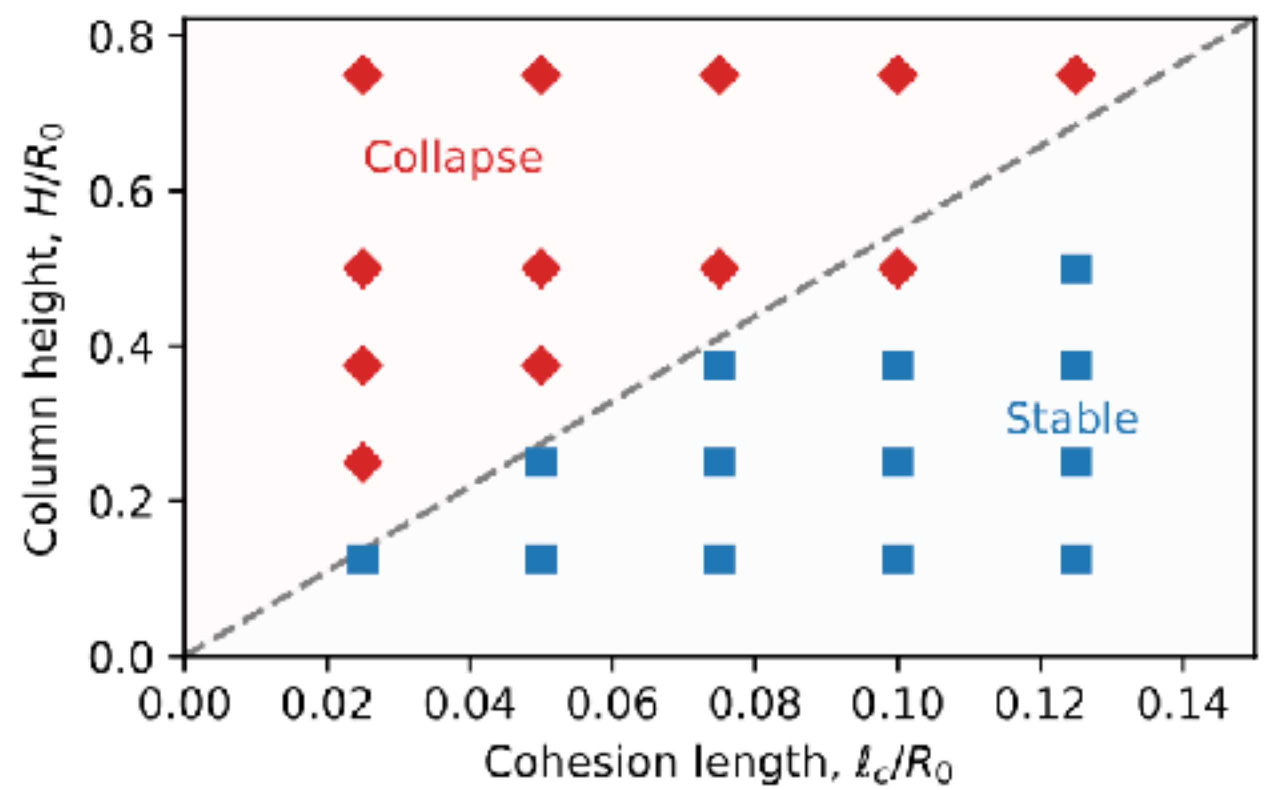

$$\ell_c = \frac{\tau_c}{\rho g},$$

cohesive material continuum vs discrete

With Anaïs Abramian, Lydie Staron, Adrien Gans ANR COPRINT

DCIM

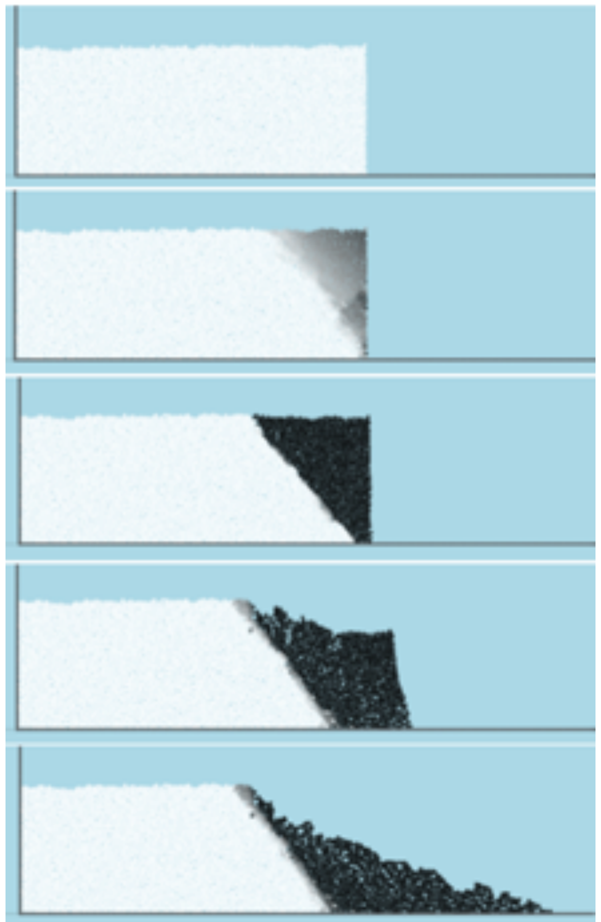

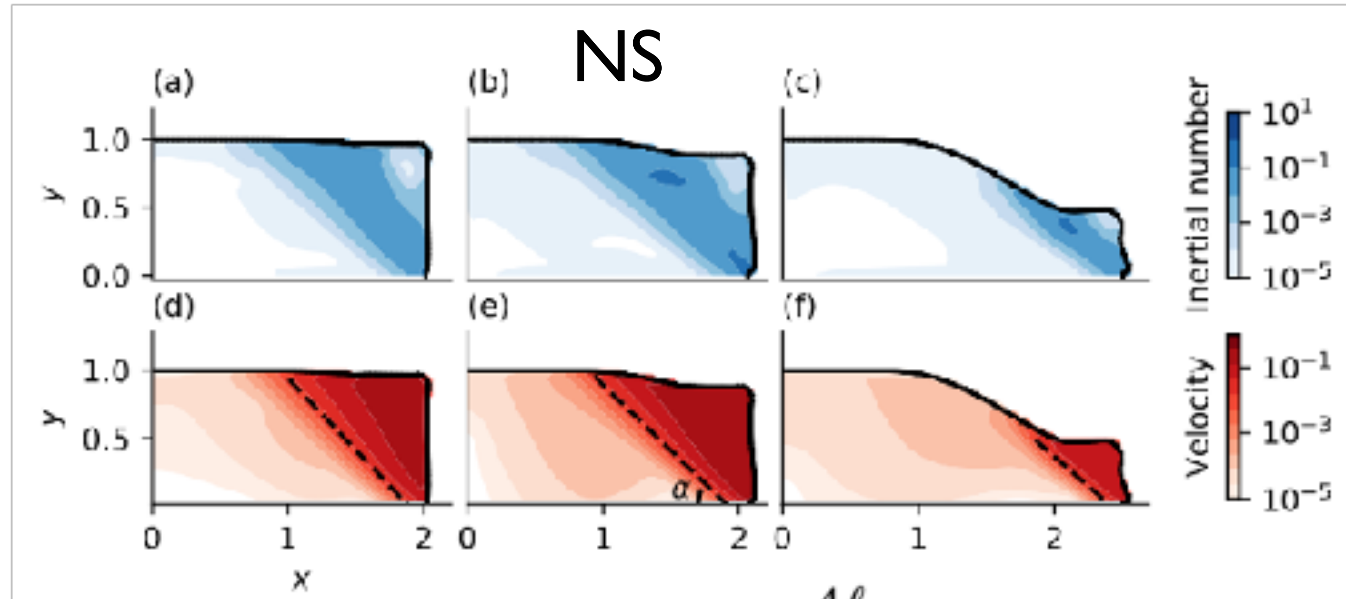

failure height: $H_y = \dfrac{4\ell_c}{\sqrt{\mu_s^2+1}-\mu_s}$,

discrete adhesion on each grain

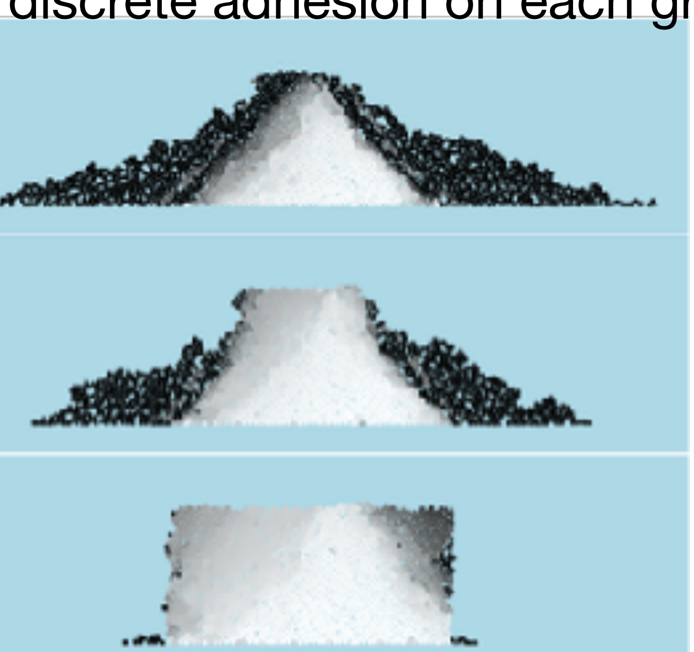

$$F_{adh} = -B_{ond}\, m_p g.$$

$$\frac{|F_{adh}|}{L} = \frac{B_{ond}}{L}\frac{\pi d^2}{4}\rho g,$$

$$\frac{\tau_c}{\rho g} = \frac{\pi d^2}{4L} \times B_{ond}.$$

$$L = 9d,$$

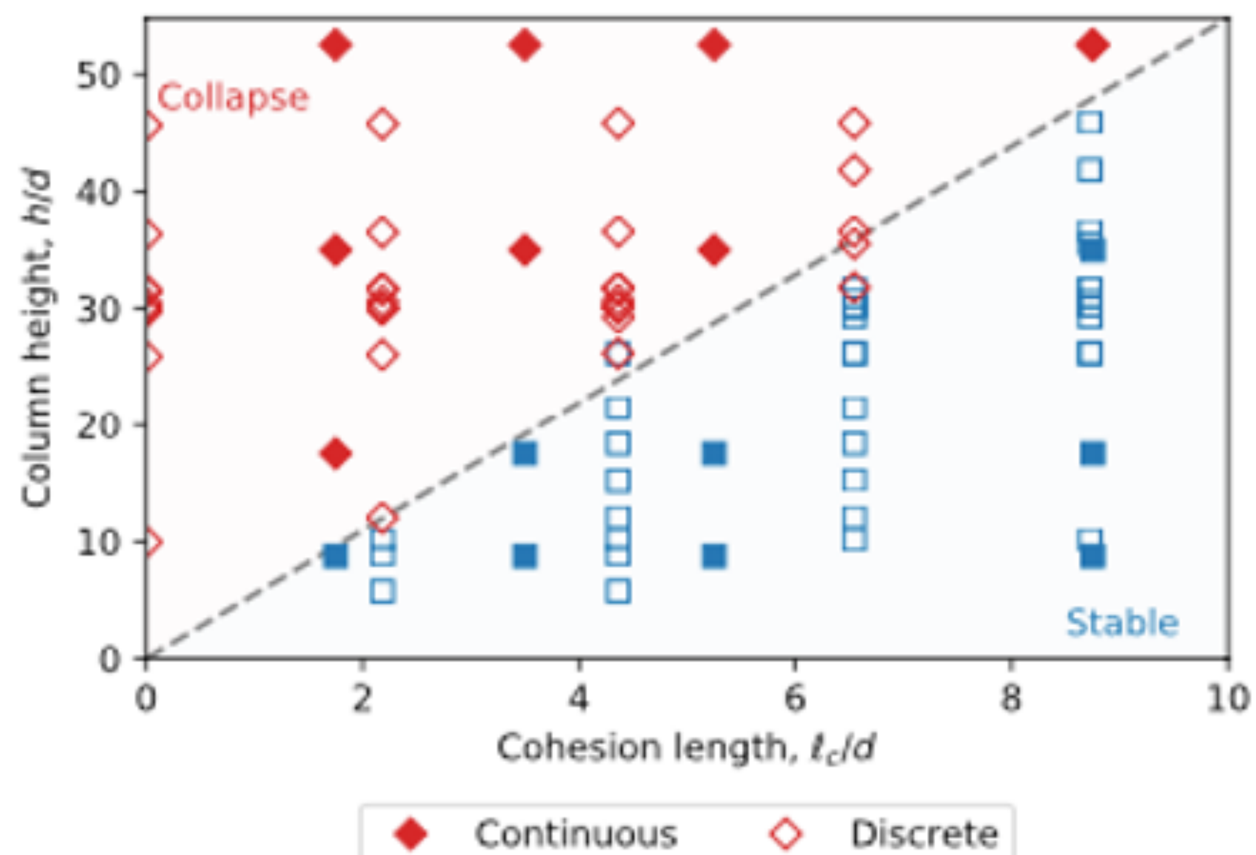

$$\ell_c = \frac{\tau_c}{\rho g},$$

Conclusion perspectives

Obvious societal problem

Experiment/ simulation/ modelisation

Granular μ(I) rheology shows agreement with experiments at least qualitatively

Method conserving exactly mass, fast code.

Problems here:
- it always flows (regularisation at small shear)
- no void formation (constant density)
- no steady flow
- no solid
- no "h stop"
- instabilities (ill posed)

Next:
- non locality,
- coupling with air/water

Jean Le Rond ∂'Alembert
1717 1783

Special Thanks to

Lydie Staron
Stéphanie Deboeuf
Pascale Aussillous
Pierre Ruyer
Anaïs Abramian
Yixian Zhou
Zhenhai Zou
Luke Fullard
Sylvain Viroulet
Guillaume Saingier
Thomas Aubry
Adrien Gans
…

& Stéphane Popinet

∂'Alembert par Félix LECOMTE. Avant 1786, Le Louvre Lens

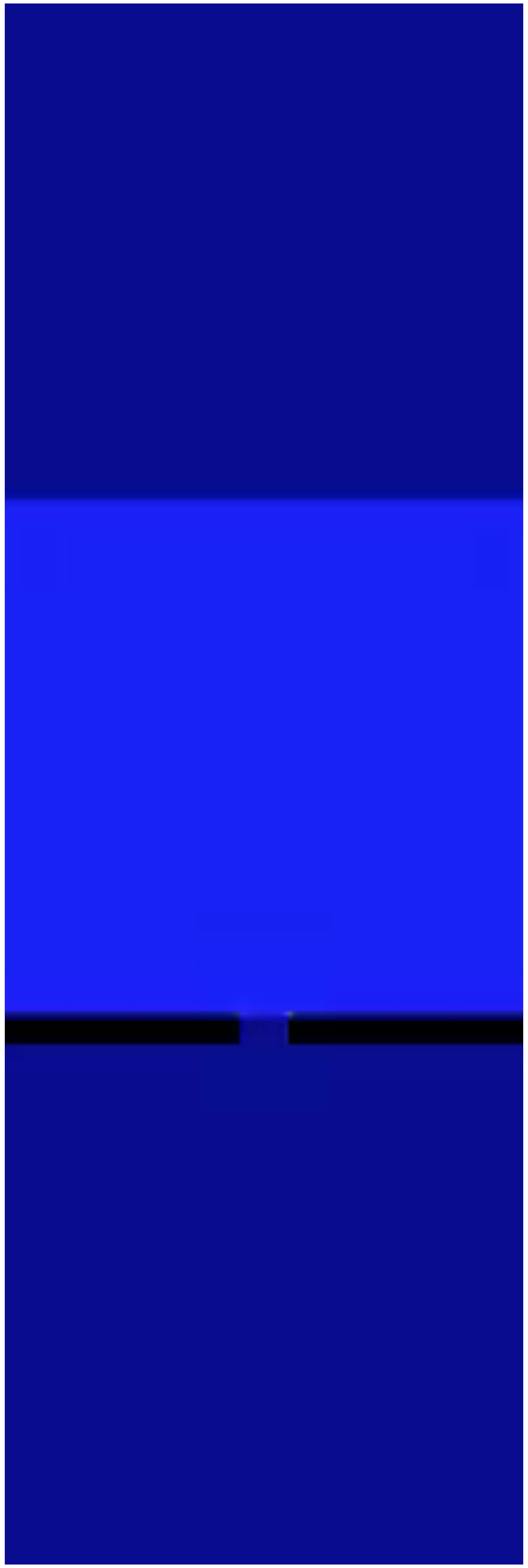

Time for questions?

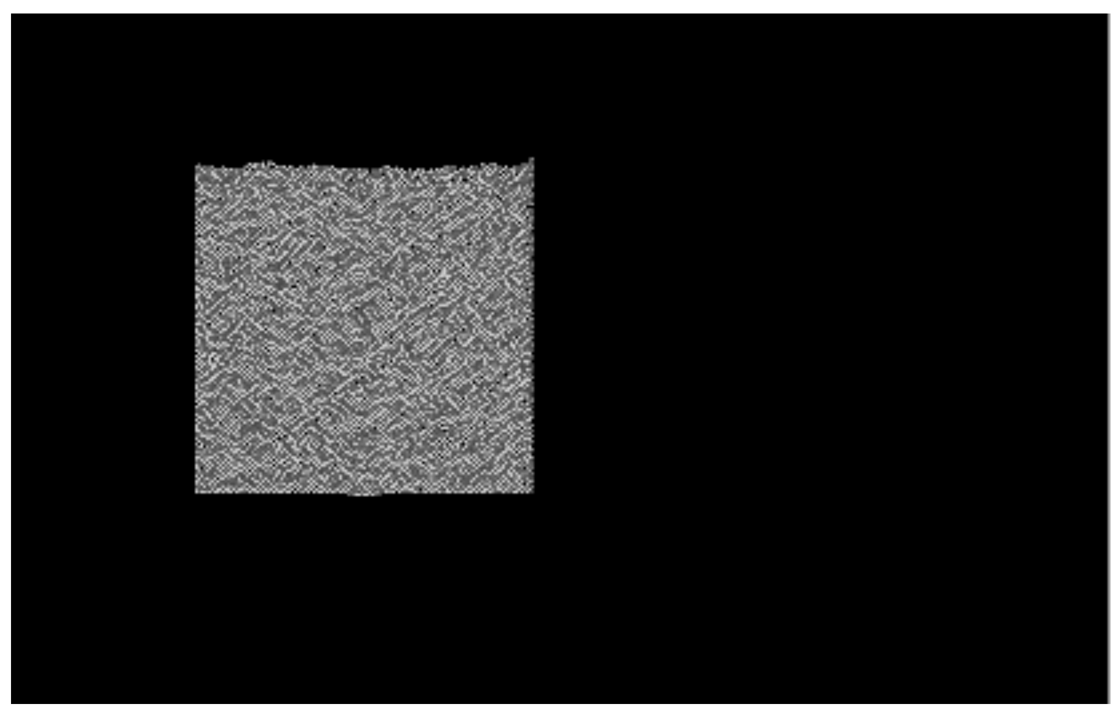

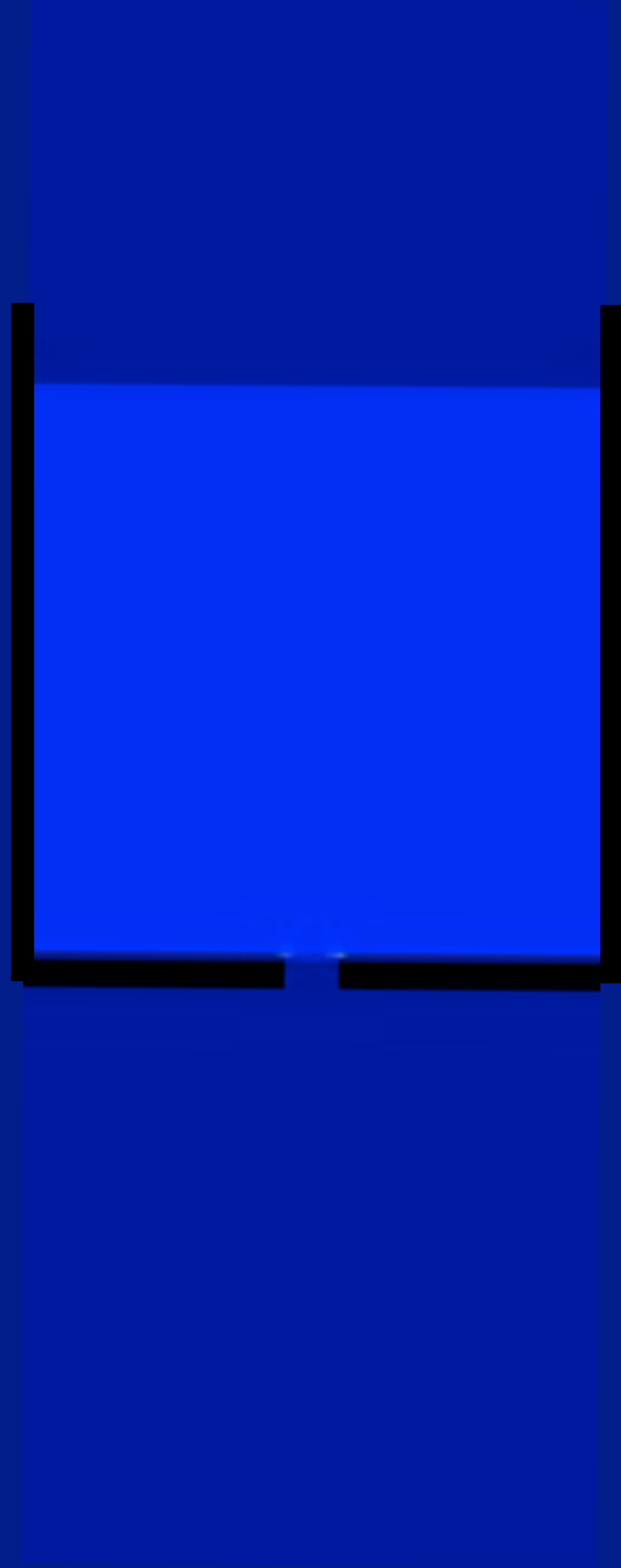

Time for questions?

μ(I) rheology for granular flows with *Gerris*

ENIT Tunis 29/10/12

tunis.key

- Newcastel
- ENSTA 250112
- ENS 9 septembre 13
- INRIA
- EPFL
- manchester
- Marnes 15/10/15
- Poitiers 26/02/2015
- Bristol 03/20/15
- Bordeaux16/11/15
- Piriac 24/05/16
- Gainesville 2015

Félix Lecomte (1737-1817)
D'Alembert (1717-1783), auteur de l'Encyclopédie
Avant 1786 Sculpture Marbre
H. 1,50 m ; l. 0,95 m ; pr. 0,92 m
Don de Napoléon Ier à l'Institut de France, 1807

Conclusion: a simple class of non newtonian flows solved with *Basilisk*

compared experiments, discrete and continuum simulations

http://basilisk.fr/sandbox/M1EMN/Exemples/column_SCC.c
http://basilisk.fr/sandbox/M1EMN/Exemples/granular_column_muw.c
http://basilisk.fr/sandbox/M1EMN/Exemples/granular_sandglass.c
http://basilisk.fr/sandbox/M1EMN/Exemples/granular_sandglass_muw.c

+ shallow water Savage Hutter on the web

http://basilisk.fr/sandbox/M1EMN/Exemples/front_poul_ed.c

comparisons
-2D
-RNSP Multilayer/
-1D (integral)

http://basilisk.fr/sandbox/M1EMN/Exemples/bingham_collapse_noSV.c
http://basilisk.fr/sandbox/M1EMN/Exemples/viscous_collapse_ML.c
http://basilisk.fr/sandbox/M1EMN/Exemples/bingham_collapse_ML.c

the model for the pertinent level of simplification

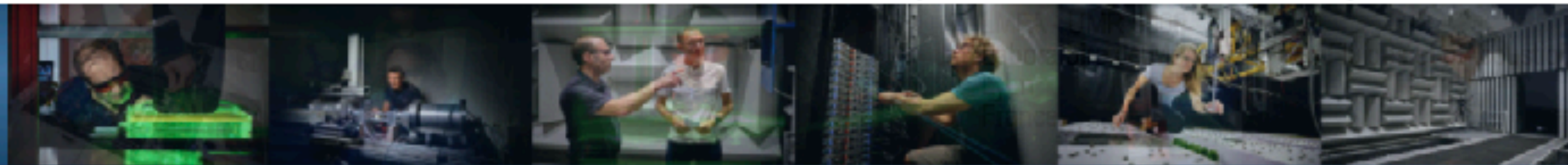

Pierre-Yves Lagrée - Institut Jean Le Rond d'Alembert

Écoulements granulaires

Vendredi 17 juin 2022, 14h30, Amphi 3, bât W, École Centrale de Lyon

Le sable, le gravier, les roches, mais aussi les céréales, le sucre... sont des exemples de matériaux granulaires de la vie de tous les jours. Constitués de millions de grains de forme quasi identique, les matériaux granulaires ont la particularité d'exister en "tas" ayant un comportement "solide" (tas de sable, tas de gravier, tas de blé, tas de patates, tas de billes, terril...). Ils ont aussi la particularité de "couler" comme un "fluide" : c'est ce qui arrive lors d'une avalanche de cailloux et roches sur le flan d'une montagne, lors d'un effondrement de pâté de sable sur la plage, de l'éboulement d'un fossé, d'une tranchée, de l'écoulement dans un sablier, ou dans un silo de céréales.

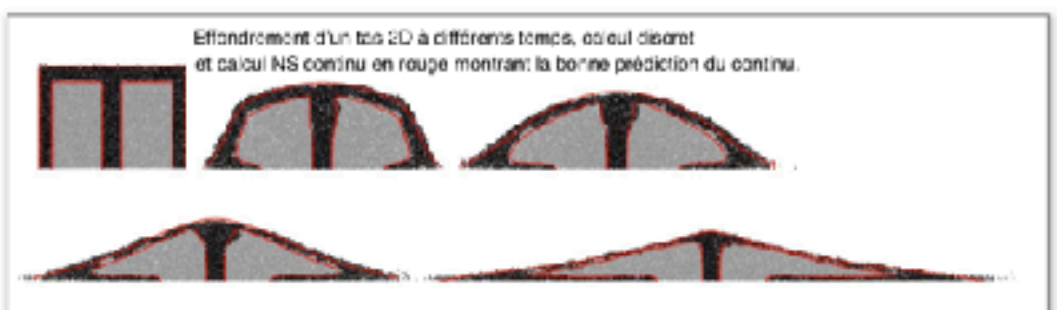

Pour résoudre ce type de problèmes, dans le cadre d'une modélisation de milieux continus, on présentera la rhéologie du μ(I) introduite par le GDR Midi qui décrit les granulaires secs comme un fluide non newtonien. Le cas des granulaires cohésifs sera aussi abordé. On montrera des exemples de résolution des équations de Navier Stokes d'archétypes d'écoulements (effondrements massifs, effondrements en couche mince, écoulements dans le sablier) en comparant à des données expérimentales ou des données numériques de simulations discrètes. Les limites de l'approche seront discutées.

Séminaires

Présentations en ligne
Archives 2020
Archives 2019
Archives 2018
Archives 2017
Archives 2016

Agenda

Avec résumé | Sans résumé
Archives | À venir

séminaire

Vendredi 17 juin 14:30-15:30 - Séminaire : Pierre-Yves Lagrée

iCal